PALMIET WETLAND SUSTAINABILITY: A HYDROLOGICAL AND GEOMORPHOLOGICAL PERSPECTIVE ON SYSTEM FUNCTIONING

Report to the

Water Research Commission

by

JL Tanner, C Smith, W Ellery and P Schlegel

Institute for Water Research, Rhodes University

March 2019

Obtainable from

Water Research Commission
Private Bag X03
Gezina, 0031

orders@wrc.org.za or download from www.wrc.org.za

EXECUTIVE SUMMARY

Prionium serratum (palmiet) is a robust plant with stems up to 2 m tall (Boucher & Withers, 2004). Palmiet is endemic to the nutrient-poor Table Mountain Group (TMG) sandstones and the Natal Group sandstones. The plant grows in dense stands that impede river flow, forming wetlands. Palmiet is thus known as an ecosystem engineer (Sieben, 2016). Palmiet also assists in controlling floods and improving water quality of rivers (Munro & Linder, 1997).

Palmiet wetlands in the Eastern and Western Cape are particularly threatened wetlands. This situation has potentially serious consequences for water security in many towns in their catchments, including cities such as Port Elizabeth. Rebelo et al. (2017:220) attributed the decline in palmiet wetlands in South Africa to "*erosion, agriculture and alien plant invasion*". Although degradation implies all three mechanisms, this study primarily focused on the erosion of palmiet wetlands. Despite large investments by the State in wetland restoration, serious knowledge gaps in our understanding of wetland structure and function remain, particularly regarding the hydrological functioning of these systems. This lack of understanding means that many restoration initiatives might be designed poorly, are not efficient, or may even be harmful.

This study aimed to reduce uncertainty around palmiet systems by improving the understanding of the hydrological and geomorphological functioning of these wetlands. The specific aims of the project included:

- Determining the surface and groundwater dynamics of the Krom River upper catchment (K90A).
- Identifying the relationship between wetlands and hydrological functioning of the catchment.
- Determining whether wetland degradation affects the hydrological integrity and water security of the river.

The study site was located in quaternary catchment K90A, the upper catchment of the Krom River, which enters the Indian Ocean at St Francis Bay. This investigation investigated palmiet wetlands in detail to improve understanding of small-scale wetland dynamics. Two palmiet wetlands formed the focus of this study. These wetlands are located along the Krom River in a valley bottom with an elevation ranging from ±400 masl to ±350 masl. The drainage area of these wetlands is 56 km^2, which is about 26% of the K90A quaternary catchment.

The study area has been subjected to significant drought throughout most of the study period, which affected data collection. Significantly, there was no useful flow data measured during this time as much of the riverbed was dry. As a result, the hydrological modelling that was originally envisaged could not be validated (particularly the way the wetlands absorb and modify high flows, and subsequent water retention in the wetland). Consequently, the study team decided to run a mixing cell model that used chemistry and isotope data to trace sources of water moving into and through the wetland. This model used flow data. Therefore, a Pitman model was set up (with a wetland submodel) to provide flow data to the best of our knowledge. In the absence of observed flow data, available information such as expected evapotranspiration from the wetland was used where possible to constrain the Pitman model outputs.

Floods are common in the Krom River catchment (which is expected in a steep mountainous Cape Fold Belt environment). Significant floods were recorded in 1931, 1965, 1981, 1996, 2001, 2006, 2007 and 2012 (McNamara, 2018). Alluvial fans occur at the end of a number of tributaries, curbing the extent of the palmiet wetlands. These fans can be considered to play a significant role in the structure of the

wetlands. Water tends to flow diffusely through the palmiet wetlands, with very small channels forming along the perimeter of the wetlands.

Gully erosion is a major concern along the Krom River, which has largely been attributed to land use change (in particular poor farming practices), buildings of roads and railway lines, and black wattle infestation (Haigh et al., 2009; Rebelo, 2012). Working for Wetlands has undertaken various rehabilitation interventions along the Krom River, including the placement of erosion-control structures (gabions) within the river. One of these structures is located at the lower end of the Kompanjiesdrif wetland.

One of the bigger questions around palmiet system functioning is why the wetlands are found pre-dominantly in the Cape Fold Belt (Eastern and Western Cape). Several palmiet characteristics make it ideally suited to this type of environment:

- Palmiet has a thick systems of roots that enable it to withstand high floods.
- Palmiet traps significant amounts of sediment. The long stem can withstand being buried in metres of sediment as the crown of the plant emerges.
- Palmiet grows relatively fast and has a seedling grown (already a small replica of an adult plant) within four weeks of germination (Munro & Linder, 1997); therefore, it can establish before the variable flow regime washes it away.
- Palmiet does not grow in saline conditions and does not thrive in shaded areas, but grows well in areas with direct sunshine (Boucher & Withers, 2004).
- Palmiet survives fires, which actually seem to boost flowering and sprouting of the plant (Boucher & Withers, 2004).
- Palmiet plays a role in naturally restoring eroded gullies and occupies three main habitats; namely, near-flat valley bottoms filled with organic and clastic sediment, bottom of gullies (recently infilled by sediment), and open water (Barclay, 2016).

It has been suggested that palmiet grows in acidic environments, which are typical of TMG rocks (Boucher & Withers, 2004; Sieben, 2016). However, Munyai (2013) investigated the soil nutritional levels of various sites across South Africa where palmiet is known to grow as well as sites (in the same geographic region) where palmiet does not grow. Munyai (2013) found that the soil nutritional values of the palmiet sites and non-palmiet sites were similar. This indicates that the distribution of palmiet is not necessarily linked to edaphic factors but that other parameters (for example, hydrological regime) may, in fact, be responsible for its occurrence.

The outcome of this study was that the hydrological functioning of palmiet wetlands is closely linked with high subsurface discharges typically found within TMG aquifers. The palmiet wetlands appear to be sustained by significant amounts of subsurface water (both groundwater and interflow) moving through preferential flow paths in the alluvial fans. In turn, these are sustained by groundwater discharge from the surrounding sandstones and quartzites of the Nardouw Subgroup and Peninsula Formation. This conceptual model indicates that a consistent water supply is a palmiet system driver and a key component of palmiet wetland formation. The wetlands clearly retain a significant amount of water, leading to the maintenance of prolonged flows and a larger baseflow. However, we suggest that the occurrence of palmiet as the dominant species in this wetland is due to the sustained low flows. The low flows are related to the catchment geology and high hydrological connectivity between the catchment and the wetland. This is enabled by flow paths that allow the free flow of water from the catchment to the wetland.

There is a strong relationship between the hydrological and geomorphological functioning of palmiet wetlands, and geomorphology is another clear system driver. The geomorphological aspect of the study showed that gully erosion leads to longitudinal slope reduction and valley widening in ways that can lead to wetland formation. The regional slope along the Krom River is 0.35%; however, the longitudinal slope of the Kompanjiesdrif wetland is 1.02%, which illustrates the localised steepness of this erosional reach compared with the regional slope. Extrinsic factors such as poor land management may accelerate natural gully formation, but erosion through gullying may also result from intrinsic factors.

The volume of sediment found within the wetlands (numerous sand lenses and filled gullies) indicates that palmiet traps sediment during high flow events, thereby creating deposits of sediment that have moved freshly from the catchment and are protected from dissolution diagenesis within the wetland (Pulley, Lagesse & Ellery, 2017). The study demonstrated that stream power (modelled using Caesar-Lisflood) in addition to localised longitudinal slope increases (due to sediment deposition by numerous alluvial fans) can result in the initiation of natural erosion gullies. Pulley et al. (2017) dated sediment from these gullies at between 470 BP and 7060 BP, thereby indicating that these gullies were part of a system functioning prior to the introduction of European farming. Pulley et al. (2018) also identified that palmiet wetland erosion is key to re-establishing wetland habitats downstream of the eroded wetland reach by reducing the longitudinal slope of the river. A large portion of the eroded sediment is thus deposited just downstream of the original erosion knickpoint and does not travel far downstream. Therefore, it is unlikely to be a significant risk to infrastructure downstream, such as Churchill Dam. However, should all wetlands be removed, this sediment would be more likely to travel downstream in large flood events, eventually affecting downstream infrastructure.

McNamara (2018:66) states that "*ongoing cut-and-fill cycles are the Krom Rivers' natural response to variation in water and sediment supply, and are therefore important longitudinal self-recovery processes within the system*". The structures in the Krom River are inhibiting the loss of existing palmiet wetlands, but are preventing periods of natural cutting (upstream of the structure) and filling (downstream of the structure) that reduce longitudinal slope and valley widening; the conditions that are linked to the long-term re-establishment of palmiet wetlands in a more geomorphologically stable setting.

This continuous cycle of erosion and re-establishment results in little nett hydrological loss from the catchment. The local lowering of the water table in response to erosion gullies would not likely result in excessive drainage of water from the system in the longer term due to wetland re-establishment just downstream of the erosion. Rebelo, Emsens, Meire and Esler (2018) also investigated the effect of channel erosion on palmiet wetlands in the Eastern and Western Cape and found no significant difference in relative groundwater depth between the degraded and pristine palmiet wetland sites.

Although this project proposes that gully erosion forms a natural part of palmiet system functioning, the loss of palmiet wetlands would have a significant impact on river systems. Palmiet wetlands provide essential sediment traps, and hydrological attenuation and retention services that would impact local water users and downstream infrastructure. Restoration initiatives should therefore focus on ensuring that downstream environments are kept suitable for the natural re-establishment of wetlands, and focus on softer protective infrastructures that do not completely inhibit the downstream movement of eroded sediment.

ACKNOWLEDGEMENTS

TABLE OF CONTENTS

LIST OF FIGURES

LIST OF TABLES

LIST OF ABBREVIATIONS

ACRU	Agricultural Catchments Research Unit
BH	Borehole
DGPS	Differential Global Positioning System
DTM	Digital Terrain Model
DWS	Department of Water and Sanitation
EC	Electrical Conductivity
EIA	Environmental Impact Assessment
ERT	Electrical Resistivity Tomography
ET	Evapotranspiration
ETa	Actual Evapotranspiration
GMWL	Global Meteoric Water Line
HEC-RAS	Hydrological Engineering Center River Analysis System
LMWL	Local Meteoric Water Line
MAE	Mean Annual Evaporation
MAP	Mean Annual Precipitation
MAR	Mean Annual Runoff
masl	Metres Above Sea Level
MCM	Mixing Cell Model
MODIS	Moderate Resolution Imaging Spectrometer
mya	Million Years Ago
NRF	National Research Foundation
PET	Potential evapotranspiration
PZ	Piezometer
SS	Surface Water Sample
TMG	Table Mountain Group
WULA	Water Use Licence Application
YBP	Years Before Present

1   INTRODUCTION AND OBJECTIVES

Wetlands are considered to be vital ecosystems on Earth. They are known to regulate water supplies, prevent floods and droughts, clean polluted waters, recharge groundwater aquifers and provide important habitats for various flora and fauna (Mitsch & Gosselink, 2007). Despite their value, wetlands are one of the most vulnerable ecosystems in South Africa with 65% of wetland ecosystems regarded as threatened (Nel et al., 2011). Palmiet wetlands in the Eastern Cape and Western Cape of South Africa are particularly threatened, with possible serious consequences for water security in many towns in their catchments, including cities such as Port Elizabeth. This is because floods are more prevalent and base flows are less reliable where palmiet wetlands have been damaged or destroyed (Rebelo, 2012).

Despite large investments by the State in wetland restoration, serious knowledge gaps in our under-standing of wetland structure and function remain, particularly in the hydrological functioning of these systems. This lack of understanding means that many of these restoration initiatives might be poorly designed, are not efficient, or may even be harmful.

To understand the functioning of wetlands, it is important to have a multidisciplinary perspective of the geomorphological, hydrological and ecological factors that underpin and sustain wetland ecosystems. Scientists agree that the main driver of wetlands is their hydrological regime. This refers to the frequency, depth and duration of inundation. The hydrological regime results from interactions between rainfall and evapotranspiration (ET), surface inflows and outflows, and groundwater discharge and recharge (Fretwell, Williams & Redman, 1996; Mitsch & Gosselink, 2007; Ellery et al., 2009; Jackson, Thompson & Kolka, 2014).

Groundwater discharges to lowland wetlands, which are associated with the deep circulating Table Mountain Group (TMG) aquifer, have been reported (Roets, Xu & Brendonck, 2008). However, wetlands in TMG aquifers are varied in terms of hydrological functioning and are often misunderstood (Parsons, 2009) due to the complex and heterogeneous nature of the fractured rock aquifers. Roets et al. (2008) described the common hydrological properties of the TMG aquifers and mentioned "*real and perceived groundwater discharges*". The contribution of interflow and groundwater to the low flows that support rivers and wetlands in the TMG is often difficult to differentiate, but is very important in terms of the effect that groundwater abstractions can have on the flow regime and therefore on wetland distribution, structure and functioning.

Prionium serratum (palmiet) is a robust plant with stems up to 2 m tall (Boucher & Withers, 2004). Palmiet is endemic to the nutrient-poor TMG sandstones and grows in dense stands that impede river flow, forming wetlands. It is thus known as an ecosystem engineer (Sieben, 2016). Palmiet also assists in controlling floods and improving water quality of rivers (Munro & Linder, 1997).

This study focused on an area located in the upper Krom River catchment (K90A) (Figure 1). Two largely intact and pristine palmiet wetlands were investigated. Working for Wetlands built structures to protect these wetlands. The Krom River is a main water source for the city of Port Elizabeth via Churchill Dam. Wetland loss could potentially affect the river and dam through increased sedimentation and decreased flood control. Also, a loss of baseflow or increased floods could impact biodiversity and ecosystem services of the river.

The investigation used an integrated approach as surface water and groundwater were thought to be significant within the upper Krom River catchment. There was a strong possibility that the wetlands are groundwater dependent. This project aimed to improve the understanding of the hydrological

functioning of palmiet wetlands endemic to the Eastern Cape and Western Cape, largely by attempting to understand the small-scale dynamics of a palmiet wetland system located in the headwaters of the Krom River.
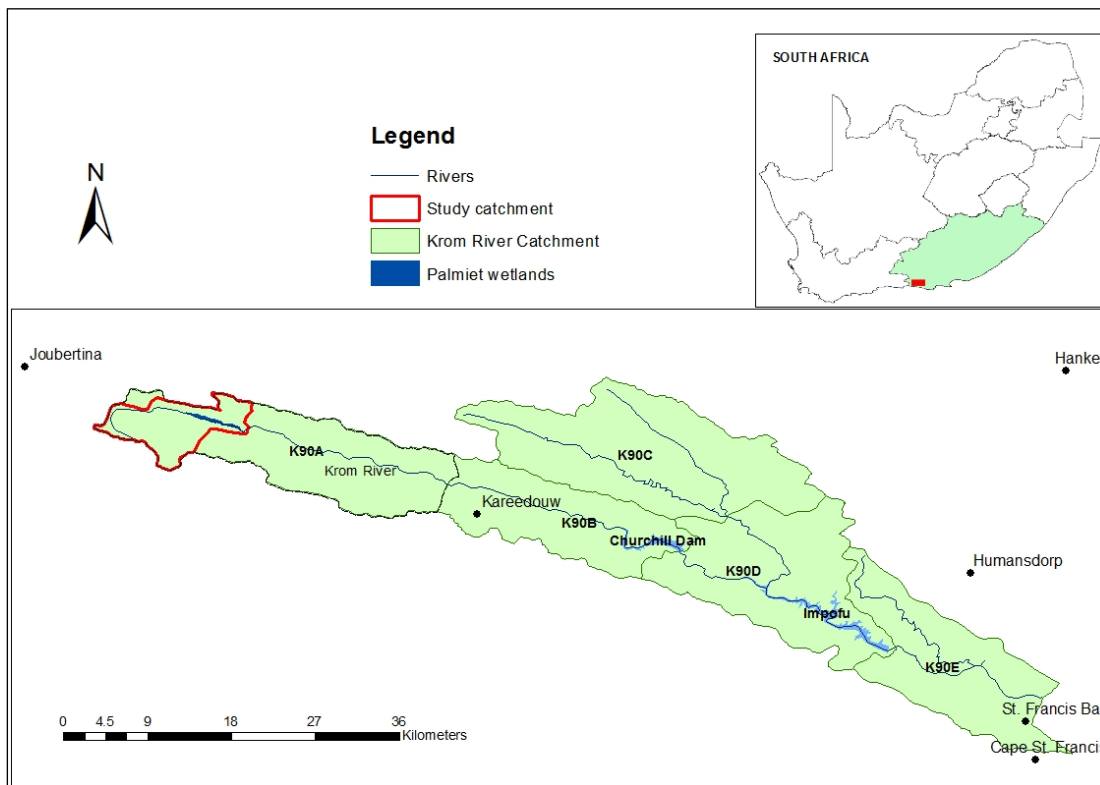
Figure 1: Locality map of the study area

The specific aims of the project included:

- Determining the surface and groundwater dynamics of the Krom River upper catchment (K90A).
- Identifying the relationship between wetlands and hydrological functioning of the catchment.
- Determining whether wetland degradation affects the hydrological integrity and water security of the river.

The project included a field investigation along with appropriate modelling to explore various hypotheses of system functioning. The project significantly overlapped with a National Research Foundation (NRF) project 40348 (NRF Krom River Study). The NRF project examined the geomorphological functioning of the upper Krom River palmiet wetlands

The study area has been subjected to a significant drought throughout most of the study period, and data collection was affected. Significantly, there was no useful flow data measured during this time as much of the riverbed was dry. As a result, the hydrological modelling originally envisaged could not be validated (particularly the way the wetlands handle/affect high flows, and subsequent water retention on the wetland). Consequently, the study team decided to run a mixing cell model (MCM) that used chemistry and isotope data to trace sources of water moving into and through the wetland. This model used flow data. Therefore, a Pitman model was set up (using a wetland submodel) to provide flow data to the best of our knowledge. In the absence of observed flow data, available information such as expected ET from the wetland was used where possible to constrain the Pitman model outputs.

2   GENERAL CHARACTERISTICS OF PALMIET WETLANDS IN SOUTH AFRICA

2.1   Description of Palmiet

Palmiet (*Prionium serratum*) is a hardy palm-like plant that grows in riverbeds and within wetlands. Its stem grows up to 3 m high. It has flat, narrow serrated leaves up to 1.2 m long (Figure 2 and Figure 3). *Prionium serratum* was previously included in the family *Juncaceae* but due to its strange growth form, it was regrouped in the family *Prioniaceae*. Palmiet is endemic to nutrient-poor rivers (usually on sandstone, most commonly TMG sandstone) in the Eastern Cape, KwaZulu-Natal (Natal Group sandstones) and the south Western Cape of South Africa (Munro, Kirschner & Linder, 2001; Boucher & Withers, 2004; Van Ginkel et al., 2011; Munyai, 2013).

Palmiet has a thick system of fibrous roots that grow significantly deeper (sometimes up to 5 m deep) than other similar wetland plants. Its deep rooting system appears to play an important role in the ecosystem functioning of the plant and its ability to withstand heavy floods, which are characteristic of the TMG (Munro & Linder, 1997; Sieben, 2016). Palmiet grows relatively fast, with a seedling grown (already a small replica of an adult plant) within four weeks of germination (Munro & Linder, 1997).

According to Boucher and Withers (2004), palmiet does not grow in saline conditions and does not thrive in shaded areas, but it grows well in areas with direct sunshine. The plant survives fires, which actually seems to boost flowering and sprouting of the plant (Boucher & Withers, 2004). Pulley et al. (2017) studied the mineral magnetic properties of sediment within the Krom River palmiet wetlands and found that these wetlands have been subjected to (and survived) various fire events in the past.

Figure 2: Palmiet growing in the Krom River, Eastern Cape
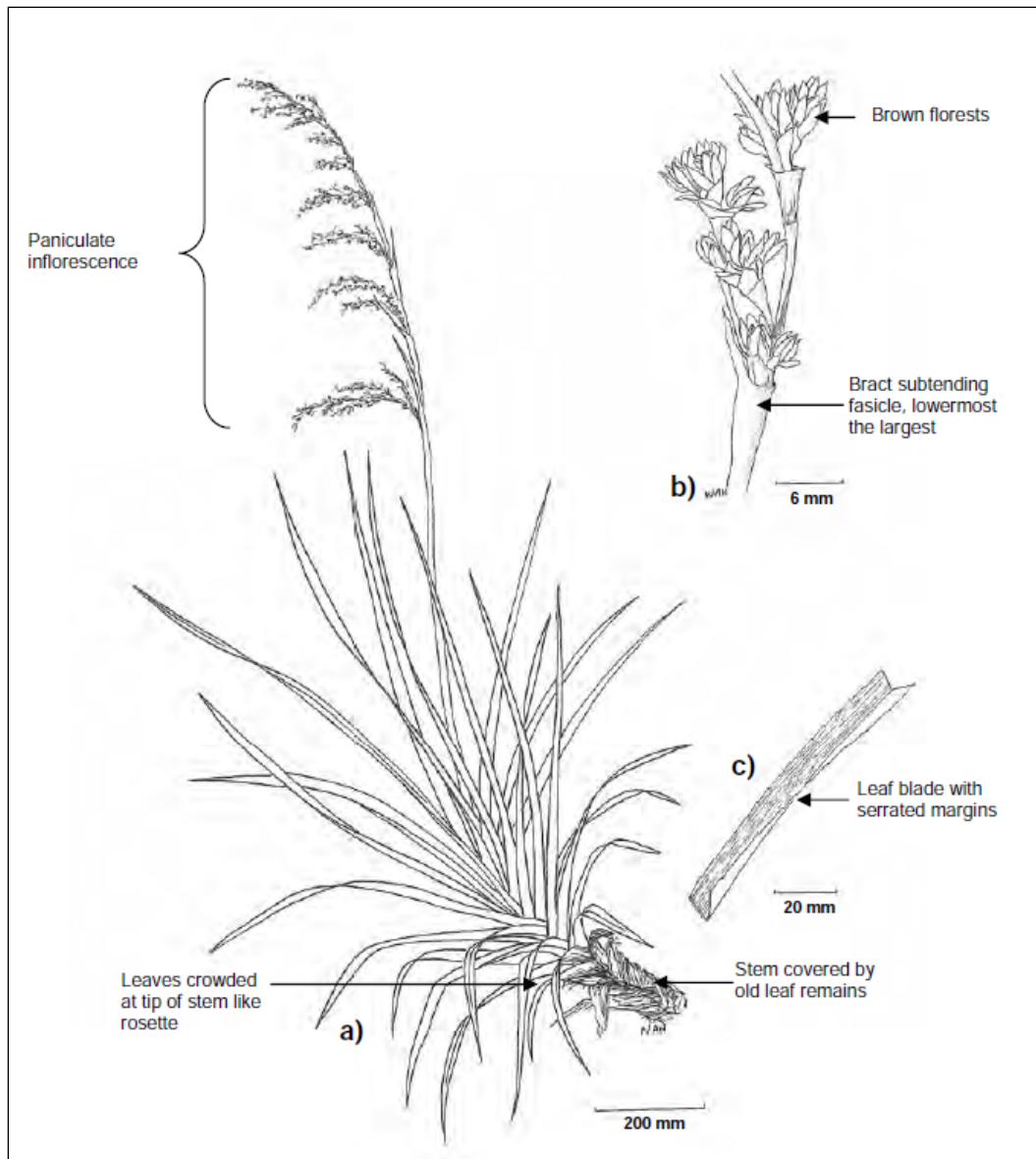
Figure 3: Illustration of the typical palmiet plant (a), palmiet inflorescence (b) and palmiet leaf (c) (Van Ginkel et al., 2011)

Palmiet wetlands are commonly underlain by thick peat beds (Rebelo, 2012; Job, 2014; Bekker, 2016; Pulley et al., 2018). These wetlands provide important ecosystem services such as carbon sequestration, flood attenuation and water purification (Rebelo, 2017). Rebelo, Emsen, Esler and Meire, 2018 illustrated that palmiet wetlands (in a pristine ecological condition) play an important role in purifying water by acting as a sink for pollutants derived from nearby agricultural activities.

Rebelo et al. (2017) examined four palmiet wetlands within the Cape Floristic Region of South Africa using multispectral imagery, aerial photographs, and the Maxent model to determine the extent of land cover changes within these wetlands over time. These palmiet wetlands have decreased in size by about 31% over the last 60–70 years. Rebelo et al. (2017:220) attributed the decline in palmiet wetlands in South Africa to "*erosion, agriculture and alien plant invasion*".

2.2   Palmiet and Gully Erosion

Intensive gully erosion is common in palmiet wetlands of the Western Cape (Job, 2014). While various authors attributed gully erosion in palmiet wetlands to human impacts, recent studies of the Krom River palmiet wetlands in the Eastern Cape by Lagesse (2017), Schlegel (2017) and Pulley et al. (2018) indicated that gully erosion may be a natural part of palmiet wetland functioning, and that human impacts only speed up this natural process. According to Pulley et al. (2018), gullying forms an essential function in terms of removing excess sediment that builds up within the wetlands, particularly due to commonly found alluvial fans constricting wetland extent in the Cape Fold Belt region. This erosion is deposited downstream, laterally flattening the valley bottom and decreasing the longitudinal slope, forming an environment fit for wetland formation downstream of the erosion point.

2.3   Palmiet as an Ecosystem Engineer and its Effect on the Hydrology of Rivers

Sieben (2012) and Barclay (2016) described palmiet as an ecosystem engineer since it alters its environment to support its own growth and it appears to play a significant role in the formation of valley-bottom wetlands. According to Jones, Lawton and Shackak (1994:374), ecosystem engineers "*are organisms that directly or indirectly modulate the availability of resources (other than themselves) to other species, by causing physical state changes in biotic or abiotic materials. In so doing, they modify, maintain and/or create habitats*". Wetland plants generally affect the hydrology of their environment by binding and trapping sediments, altering water flow, and creating peat (Mitsch & Gosselink, 2007). As palmiet grows in foothill streams, it traps sediment and leads to peat formation, expanding until the entire river is colonised by the plant resulting in a unchannelled valley-bottom wetland. "*The deep and extensive rooting system together with its clonal growth and ability to withstand strong flood events provide the key traits that help the plant to transform its own environment*" (Sieben, 2012:816–817).

Job (2014:66) suggested that the distribution of the peatland in the Goukou River (Western Cape) is linked to the occurrence of palmiet and that the palmiet forms "*a local base level and water ponding*" in the river. The higher base level created by the palmiet results in a relatively constant water table and allows organic matter to accumulate (and exceed decomposition). Palmiet grows throughout the Goukou wetland and it is effective at collecting clastic sediment. During continued low flows in the Goukou River, palmiet spreads out and "*the plant can extend well into river channel open water, narrowing channel width, such that palmiet may densely fill a river channel*". By extending across the valley floor, palmiet colonises the river, traps sediment, and reduces flow. This process alters the flow in the river to a diffuse flow, allowing organic material to accumulate and a deep peat basin to form (Job, 2014:68). A similar process was also noted by Czegledi (2013) in a study of the Hudsonvale palmiet wetland in the Krom River and by Bekker (2016) in a study of the Tierkloof palmiet wetland along the Tierkloof River.

A study of a palmiet wetland in the upper Krom River, namely, Kompanjiesdrif wetland, indicated that palmiet may have converted the braided to anastomosing stream at this site to an unchannelled valley-bottom wetland with diffuse flow by colonising gully beds and areas of open water. Barclay (2016) found that palmiet plays a role in naturally restoring eroded gullies along this river. In her investigation of this wetland, it was clear that palmiet occupied three main habitats; namely, near-flat valley bottoms filled with organic and clastic sediment, the bottom of gullies (recently infilled by sediment), and open water.

The Kompanjiesdrif wetland has been subjected to various episodes of gully formation and infilling. Barclay (2016) indicated that palmiet affects these gullies by filling them (trapping sediment in the gullies), colonising gullies that have been filled by alluvial fan sediment, and encroaching into former gullies filled with water ('dammed' or 'ponded up') and are obstructed downstream by alluvial fan sediment. Palmiet forms a tangled mat over the open water surface of these former gullies. After an

erosional gully develops, sediment (formed through headward erosion) accumulates as sand bars in the gully. These bars are colonised by palmiet, which also traps clastic sediment and forms peat. The sand bars keep forming and are colonised by palmiet until the gully is ultimately filled (Figure 4).
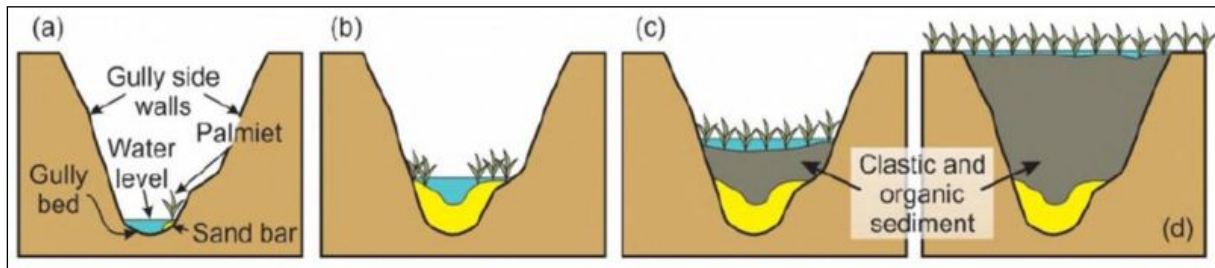
Figure 4: Illustration of palmiet inhabiting sedimentary bars, trapping sediment and forming peat in a gully (Barclay, 2016)

2.4   The Water Use of Palmiet

According to Rebelo (2012), many riparian landowners consider palmiet to be a high water user. Using the Jonkershoek wetland (33°58'38" S, 18°56'48" E) as her study area, Rebelo (2012) investigated the stomatal conductance of palmiet plants using porometer measurements. The measurements revealed that *Prionium serratum* has a low stomatal conductance (18–112 mmol.m^{-2}.s^{-1}) and was a relatively low water user. The acquired stomatal conductance was similar to that of the Cederberg area restioid vegetation, which was shown to be 89–139 mmol.m^{-2}.s^{-1}. This vegetation type matched the riverine wetland plant community in Jonkershoek, which was indicated to have an actual evapotranspiration (Eta) of close to 1332 mm per annum. Based on the similarities between the two vegetation types, ETa of palmiet plants in Jonkershoek can be expected to be close to 1332 mm per annum.

Rebelo (2012) also studied a palmiet wetland at Franschhoek and obtained annual ET estimates of 1526 mm (scintillometry), 1042 mm (MODIS[1]) and 1623 mm (Landsat) for the plant. The ET estimates modelled by the Agricultural Catchments Research Unit (ACRU) for palmiet in the Krom River are lower at 694.6 ± 21.46 mm per year, which is approximately 246.21 mm higher than natural fynbos, but approximately 200 mm lower than invasive *Acacia mearnsii* (black wattle) (Rebelo et al., 2015). However, ACRU model wetland ET estimates are known to be low. This is due to the ACRU wetland model structure that does not allow wetland plants to access channel water recharging a wetland.

Additional information on the water use of palmiet was obtained through the following data sources:

- FruitLook (www.fruitlook.co.za) – FruitLook calculates ET using the ETLook algorithm (Pelgrum et al., 2012) and has a pixel size range of < 30 m to 250 m (Jarmain et al., 2014).

- Moderate resolution imaging spectroradiometer – MODIS (MOD16A2: https://search.earthdata.nasa.gov/search) with a pixel size of 500 m.

- Daily scintillometer data (unpublished), which was provided by Dr Jarmain for the Helderstroom palmiet wetland along Riviersonderend River in the Western Cape. Measurements were taken over a brief period in October 2008.

---

[1] Moderate Resolution Imaging Spectrometer

The ET rates from several different palmiet wetlands located in the E10J, G22F, H60B, H60D, H90A and H90C quaternary catchments were obtained through these data sources. The locations of these wetlands are given in Figure 5.
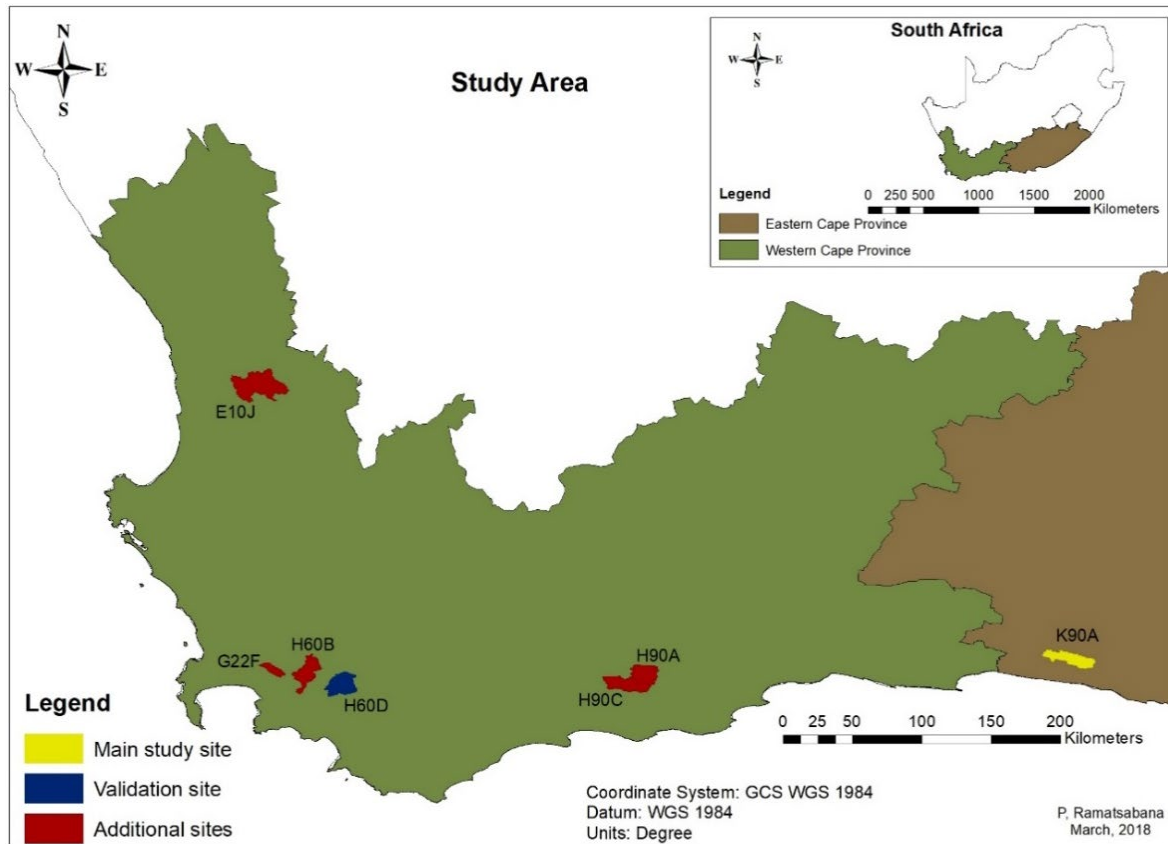
Figure 5: Locations of palmiet wetland study sites in the Western Cape, South Africa. The Krom River is shown in yellow, the site with scintillometer data shown in blue, and the remaining palmiet wetlands are shown in red

Although MODIS was investigated as a possible source of water use data for palmiet wetlands, it was found that MODIS underestimated ETa from wetlands (Table 1). This is probably due to the MODIS pixel size and the comparatively small size of the palmiet wetlands. MODIS is therefore probably not picking up the full wetland ET signal.

Table 1: Validation of MOD16 data using scintillometer-derived ETa data, October 2008. Shaded values are directly comparable (full set of data available for that period)

Date	Scintillometer ETa (mm/day)	Scintillometer ETa (mm/8day)	MOD16 ETa (mm/8day)
14-Oct	2.9		
15-Oct	3		15.50
16-Oct	2.8		
17-Oct	5.9		
18-Oct	6.1		
19-Oct	6.3		
20-Oct	3.8		
21-Oct	2.9		

Date	Scintillometer ETa (mm/day)	Scintillometer ETa (mm/8day)	MOD16 ETa (mm/8day)
22-Oct	2		
23-Oct		32.8	13.97
24-Oct			
25-Oct	6.5		
26-Oct			
27-Oct			
28-Oct	6		
29-Oct	5.5		

There were only two MODIS ETa values available that coincided with the acquired scintillometer data. Data was validated by upscaling scintillometer data to a cumulative eight-day value. Measurements starting from 16 October to 22 October were considered (Table 1) since only seven measurements were available for scintillometer ETa. The cumulative of these estimates (32 mm/7day) is at least twice more than the MODIS ETa cumulative value (13.97 mm/8day), which indicates that MODIS under-estimated ETa for this study. Figure 6 compares the ETa from the ETLook model (www.fruitlook.co.za) and MODIS (for the Krom River wetlands).
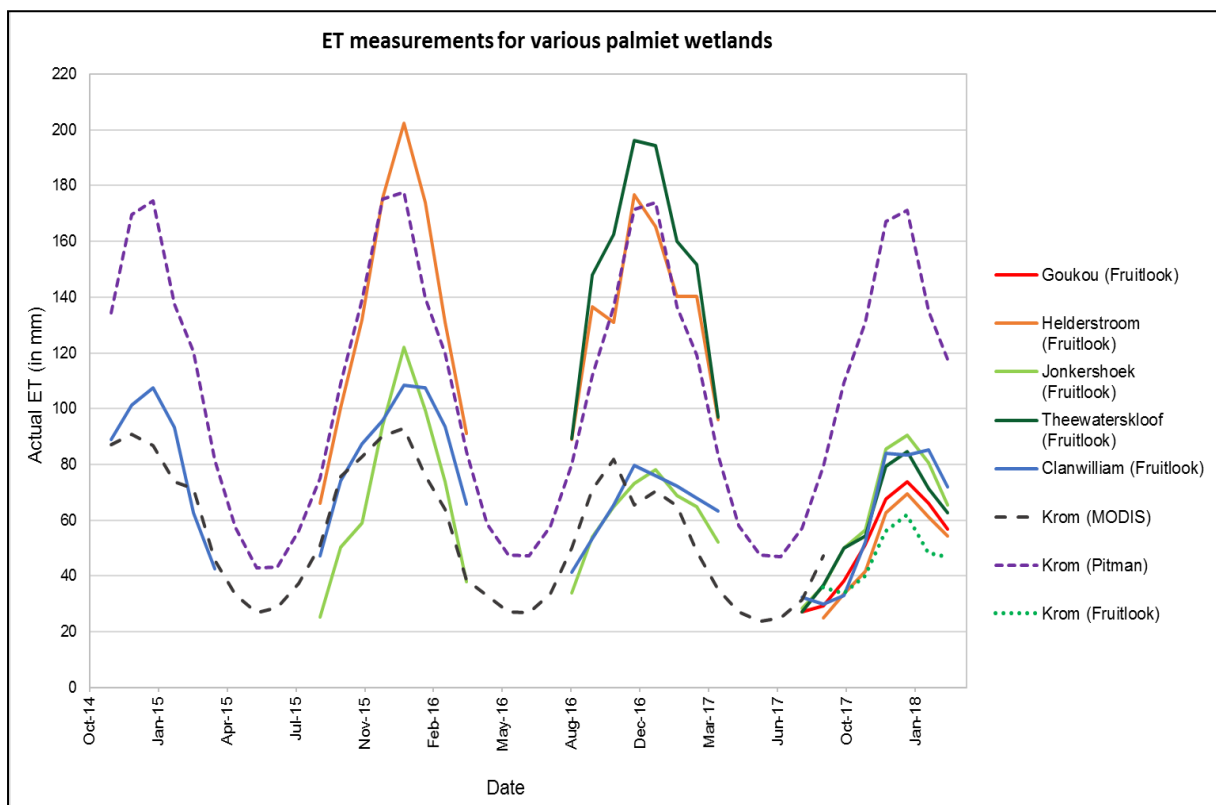
Figure 6: ET measurements for various palmiet wetlands. Fruitlook only reports data during the growing season

3 APPROACH: UNDERSTANDING SMALL-SCALE DYNAMICS OF SYSTEM FUNCTIONING

3.1 Introduction

The project resources were focused on understanding the small-scale processes behind the functioning of the wetlands to improve overall understanding and reduce the uncertainty surrounding wetland functioning. The project included a small-scale field investigation along with appropriate modelling to explore various hypothesis of system functioning.

3.2 Overview of the Study Site

3.2.1 Location, catchment boundaries, and topography

The study area is located within a subcatchment of the K90A upper Krom River catchment, approximately 20 km east of the town of Joubertina in the Eastern Cape Province of South Africa (33°52'41.04", 24°3'6.83") (Figure 7). The Krom River is approximately 100 km long from its upper reaches to its estuary at St Francis Bay. It is bounded by the Suuranys Mountains (±1050 masl) to the north and the Tsitsikamma Mountains (±1500 masl) to the south. The Krom River provides the Nelson Mandela Bay Municipality with about 24% of its water via the Churchill Dam and sustains peatlands dominated by palmiet (Rebelo, 2002; Haigh et al., 2009).
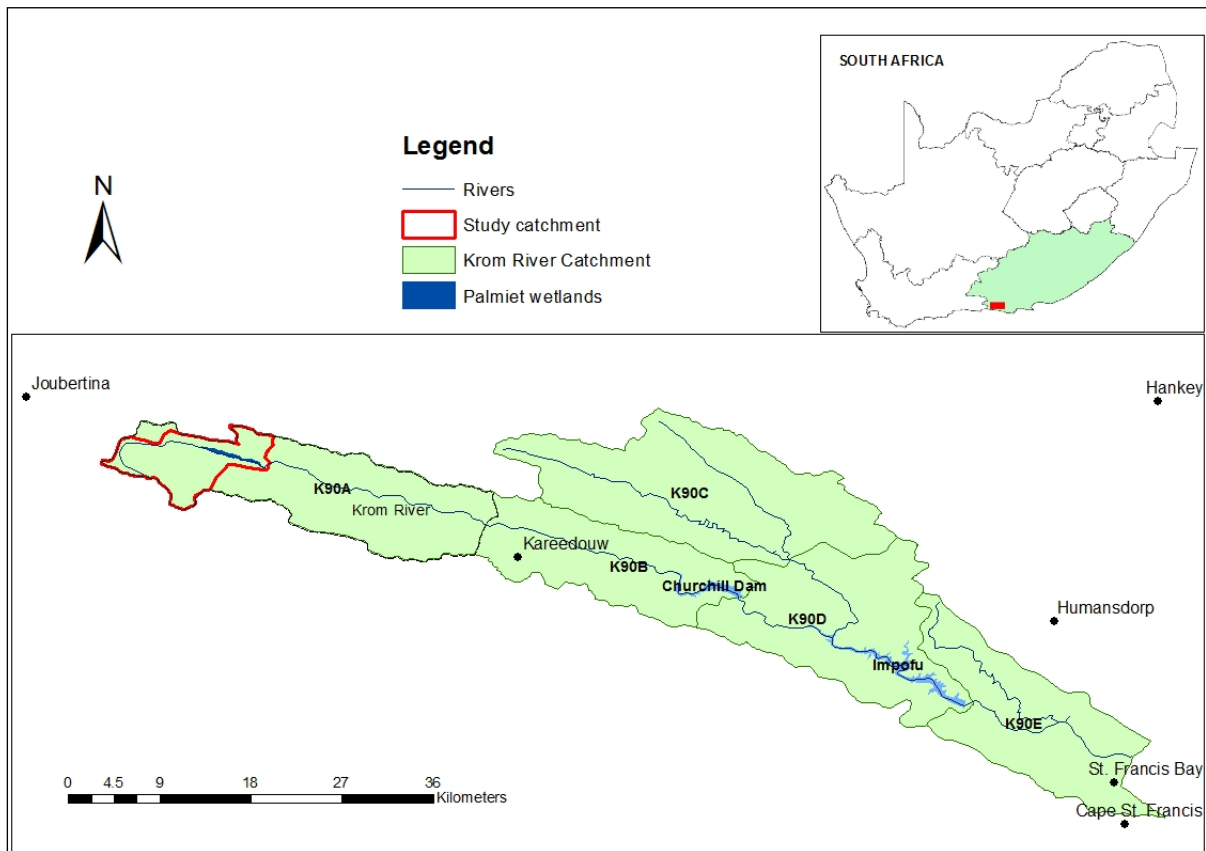
Figure 7: Locality map illustrating the study catchment (in red) within the K90A catchment

Two palmiet (*Prionium serratum*) wetlands form the focus of this study. The wetlands are located along the Krom River in a valley bottom with an elevation that ranges from ±400 masl to ±350 masl (Figure 8). The upstream catchment area feeding these wetlands is 56 km^2, which is about 26% of the K90A quaternary catchment.

Figure 8: Locality map illustrating the two palmiet wetlands

3.2.2   Land cover, land use, and vegetation

The floodplains of the Krom River formed and accumulated sediments over millennia. Pulley et al. (2017) dated sediments up to 7000 years old within the palmiet wetlands. The geomorphology of much of the Krom River has since been modified and the palmiet wetlands are threatened by erosion. According to Haigh et al. (2009), the palmiet wetlands in the K90A and K90B catchments have declined significantly in size since 1942.

According to Rebelo (2012), the land cover within the Krom River catchment has been transformed by orchard farming, overgrazing, road construction, and black wattle (*Acacia mearnsii)* infestation. Haigh et al. (2009), Rebelo (2012), and Nsor and Gambiza (2013) provided a detailed history of land use change in the Krom River catchment since the eighteenth century. Figure 9 illustrates the current land use in the study catchment. Rebelo et al. (2015) calculated that the palmiet wetlands declined by 84% and riparian vegetation by 92% in the Krom River catchment (K90A and K90B) over the last century.
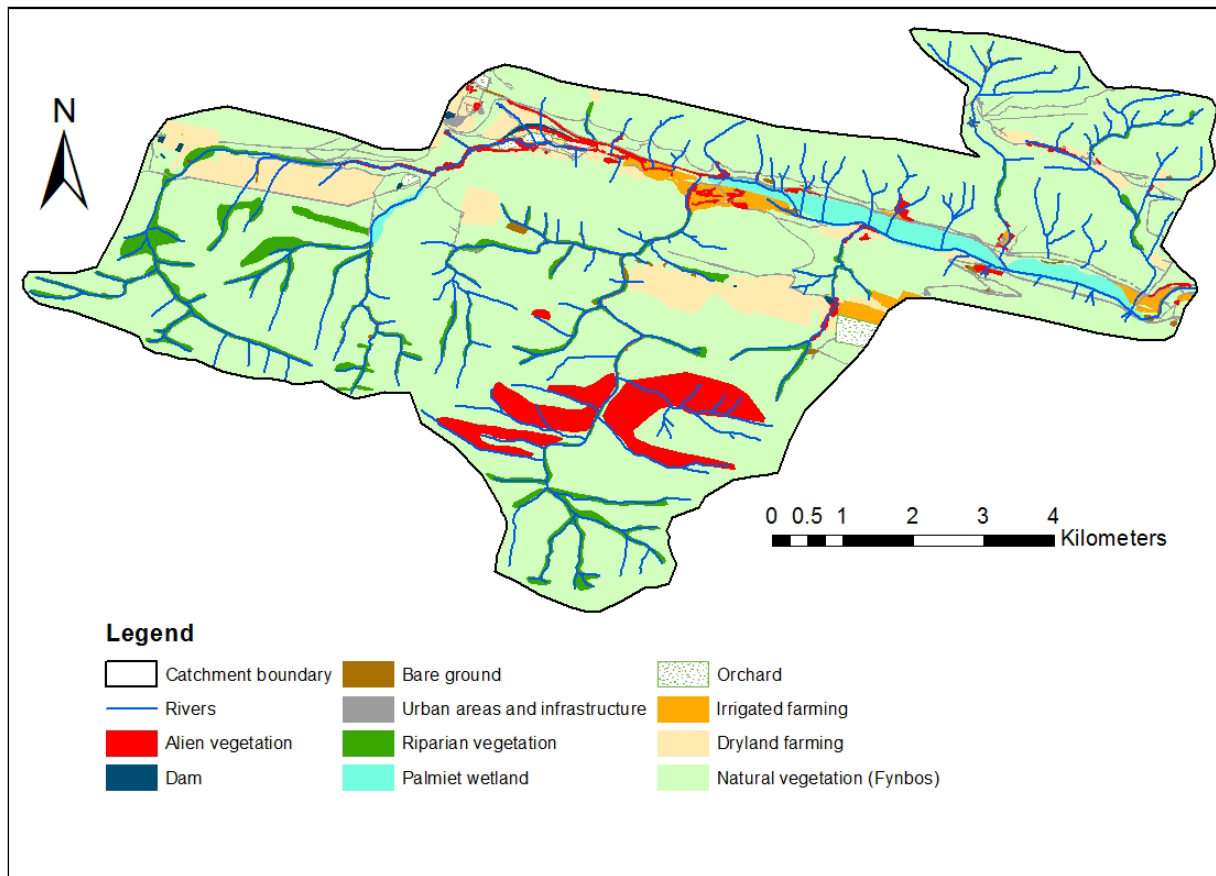
Figure 9: Land cover in the study catchment [land cover shapefiles edited from Rebelo (2012)]

The upper Krom River catchment is located within the fynbos biome. It is characterised by sandstone fynbos, shale band vegetation and shale renosterveld (Rebelo et al., 2006). The wetlands are dominated by palmiet (*Prionium serratum*) and also contain plant species such as *Miscanthus capensis, Juncus kraussii, Metalasia densa* and *Pennisetum clandestinum* (alien invasive grass) (Barclay, 2016). Alien vegetation (in particular black wattle) has invaded parts of the Krom River catchment and palmiet wetlands. Working for Water and Working for Wetlands have been clearing black wattle along the Krom River since 1996 (Rebelo & Cowling, 2013).

3.2.3 Climate

The Krom River catchment experiences a bimodal pattern of rainfall with spring (August to October) and autumn (February to April) receiving higher rainfall than the rest of the year (Nsor & Gambiza, 2013). Rainfall is unevenly distributed within the Krom River catchment, with higher rainfall occurring in the south and south-west of the catchment than the north and north-east (Haigh et al., 2009). Rainfall also tends to increase from inland towards the coast (Bailey & Pitman, 2016).

The Water Resources 2012 database (Bailey & Pitman, 2016) determined a mean annual precipitation (MAP) of 716 mm, a mean annual evaporation (MAE) of 1400 mm, and a mean annual run-off (MAR) of 27 million m^3 in the K90A Krom River catchment. A local weather station, which is located at Twee Riviere 13 km from the study site, recorded a MAP of 346 mm and a MAE of 1095 mm (based on seven years of data).

3.2.4   Geomorphology and hydrology

Floods are common in the Krom River catchment, which is expected in a steep mountainous Cape Fold Belt environment. Significant floods have been recorded in 1931, 1965, 1981, 1996, 2001, 2006, 2007 and 2012 (McNamara, 2018). The K90A catchment has a trellis drainage pattern with six large tributaries and five minor tributaries flowing into the Krom River from the south side. Seven large and numerous short tributaries flow in from the northern side of the river.

Alluvial fans occur at the end of several tributaries, which curb the extent of the palmiet wetlands. These fans can be considered to play a significant role in the structure of the wetlands (Figure 10). This is particularly evident at Kompanjiesdrif (Haigh et al., 2009). Water tends to flow diffusely through the palmiet wetlands with very small channels forming along the perimeter of the wetlands. Grundling et al. (2017) listed the main sources of water for the palmiet wetlands in the upper Krom River as river water, groundwater, side seepage, and shallow subsurface flow through alluvial fans.

Figure 10: Alluvial fans (stippled black line) impinging on the Kompanjiesdrif wetland, curbing the extent of the wetland

Gully erosion is a major concern along the Krom River, which has largely been attributed to land use change (in particular poor farming practices), building of roads and railway lines, and black wattle infestation (Haigh et al., 2009; Rebelo, 2012). Channels caused by the head cuts drain groundwater from the alluvium, which destroy the wetlands in the process (Rebelo, 2012). Working for Wetlands has undertaken various rehabilitation interventions along the Krom River, which include placing erosion-control structures (gabions) in the river. One of these structures is located at the end of the Kompanjiesdrif wetland.

3.2.5 Geology

The Krom River is located within quarzitic sandstones and shales of the Cape Supergroup, specifically the Bokkeveld Group (which tends to cover the valley bottom) and the TMG, which were deposited in a passive margin basin between 500 mya and 330 mya (Thamm & Johnson, 2006).

Approximately 330 mya, compression of these sedimentary rocks (due to a subduction zone along the southern boundary of Gondwana) resulted in the formation of the folded and faulted Cape Fold Belt (McCarthy & Rubidge, 2005). The 1:250 000 geological map of the area (Toerien, 1986) illustrates the intensely folded nature of the Krom River catchment with anticlines occurring in the south followed by synclines (along the Krom River valley) and anticlines again in the north. Figure 11 illustrates the geology of the study catchment.

Figure 11: The geology of the study catchment based on the 1:250 000 geological map (Toerien, 1986) with the location of the cross section (illustrated in Figure 12) indicated by the red line

The two wetlands that are the focus of this study are located in the centre (valley bottom) of an overturned syncline of the Cape Fold Belt rocks. As is evident in the geological cross section (Figure 12), the valley comprises less resistant shale material and the steeper valley sides tend to consist of more resistant quarzitic sandstone. Table 2 provides a more detailed lithological description of the rocks in the study catchment.
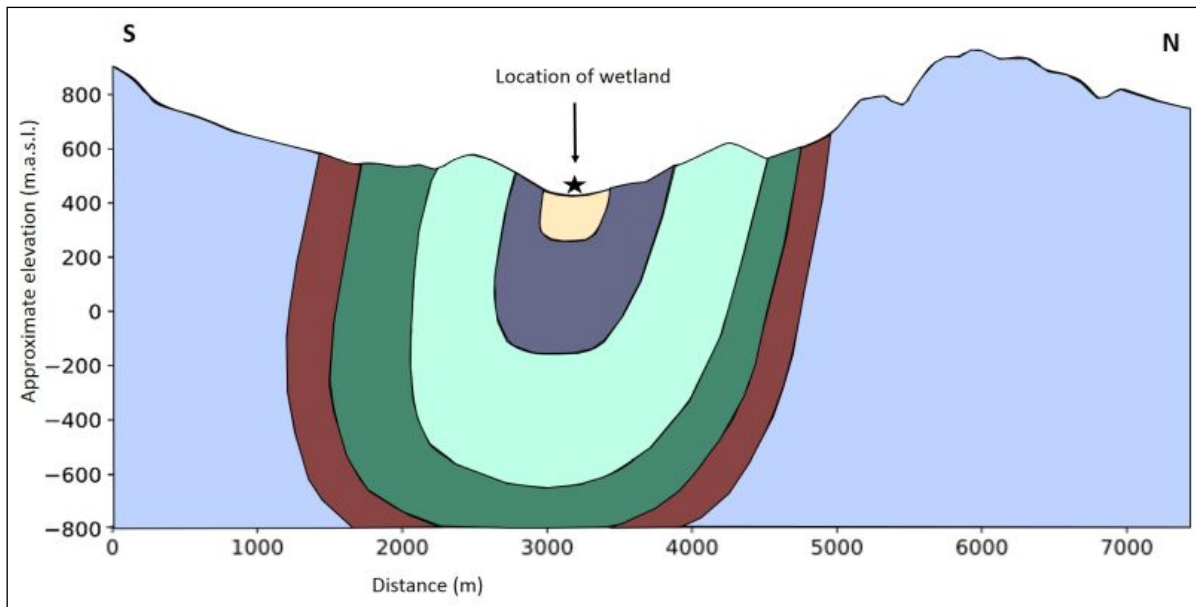
Figure 12: Simplified geological cross section illustrating the steeply dipping overturned synclinal rocks of the Cape Supergroup, with the wetland located in the centre of the valley bottom (vertical exaggeration = 2)

Table 2: Stratigraphy of study area (Toerien, 1971–1972; Toerien, 1972; Toerien, 1986; Thamm & Johnson, 2006; Toerien, n.d.)

	Group	Subgroup	Formation	Lithology
	n/a	n/a	n/a	Alluvium.
	n/a	n/a	Grahamstown	Terrace gravel, silcrete, and ferricrete.
	Bokkeveld	Ceres	Gydo	Black shale with minor siltstone, fossiliferous.
	Table Mountain	Nardouw	Baviaanskloof	Impure feldspathic sandstone (fine- to medium-grained), minor shale, fossiliferous.
			Skurweberg	White-weathering (medium to coarse-grained) quarzitic sandstone, feldspathic towards the top, cross-bedded.
			Goudini	Brownish-weathering quarzitic sandstone (fine to coarse-grained), minor siltstone and shale.
			Cederberg	Black shale, arenaceous towards to the top and can be fossiliferous.
			Peninsula (main unit of the Cape Supergroup)	Whitish-weathering quarzitic sandstone (medium to coarse-grained).

The wetland basins appear to be located on the Post Africa II erosion surface (formed approximately 5 mya), while the Post Africa I surface (formed approximately 20 mya) is above the wetland surface located on a break in slope in the northern Suuranys Mountains (Figure 13). The African erosion surface (formed before 60 mya) is located on the crest of the northern Suuranys Mountains (McCarthy & Rubidge, 2005; Lagesse, 2017).
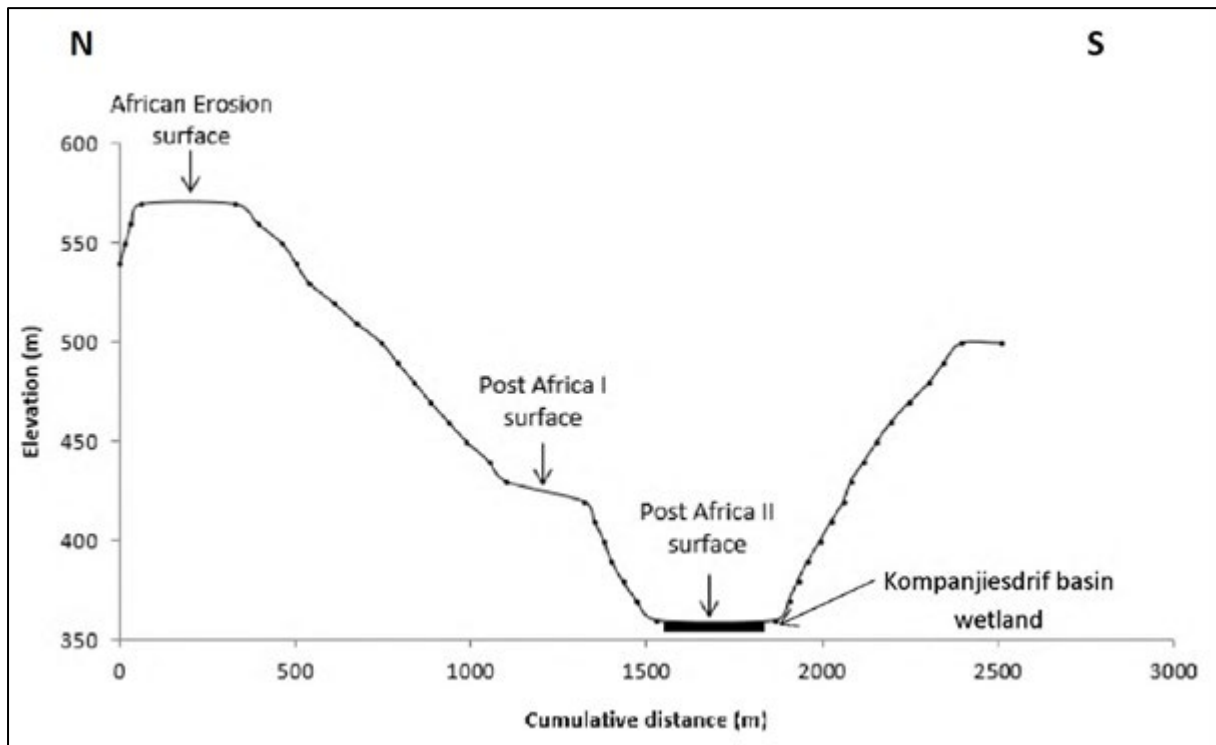
Figure 13: Position of the Kompanjiesdrif wetland basin in relation to the three erosion surfaces (Lagesse, 2017)

3.2.6   Geohydrology

The Cape Supergroup sandstones and quartzites can be a significant source of groundwater, but the volumes of water they yield are variable and generally depend on the occurrence of fractures, faults and folding to provide secondary porosity and flow paths (Xu, Lin & Jia, 2009). Dennis and Pretorius (2006) used a numerical flow model (MODFLOW) to estimate the groundwater contribution to baseflow in the K90A catchment to be 3.58 million m^3/a. Dennis and Pretorius (2006) excluded protected areas in the catchment from their study as they were completing a groundwater reserve study and assumed that no groundwater abstraction was allowed in a protected area. Thus, a smaller catchment area (178 km^2) was used in the model than the actual size of the catchment area, which is 214 km^2.

Xu et al. (2009) estimated baseflow using baseflow separation in the K90A catchment to be 7.5 million m^3/a (24.9% of the MAR). The GRA II[2] groundwater baseflow zones of South Africa illustrates that the study area is located within a high groundwater baseflow zone (Figure 14) (DWAF, 2006).

---

[2] Groundwater Resource Assessment Phase II project
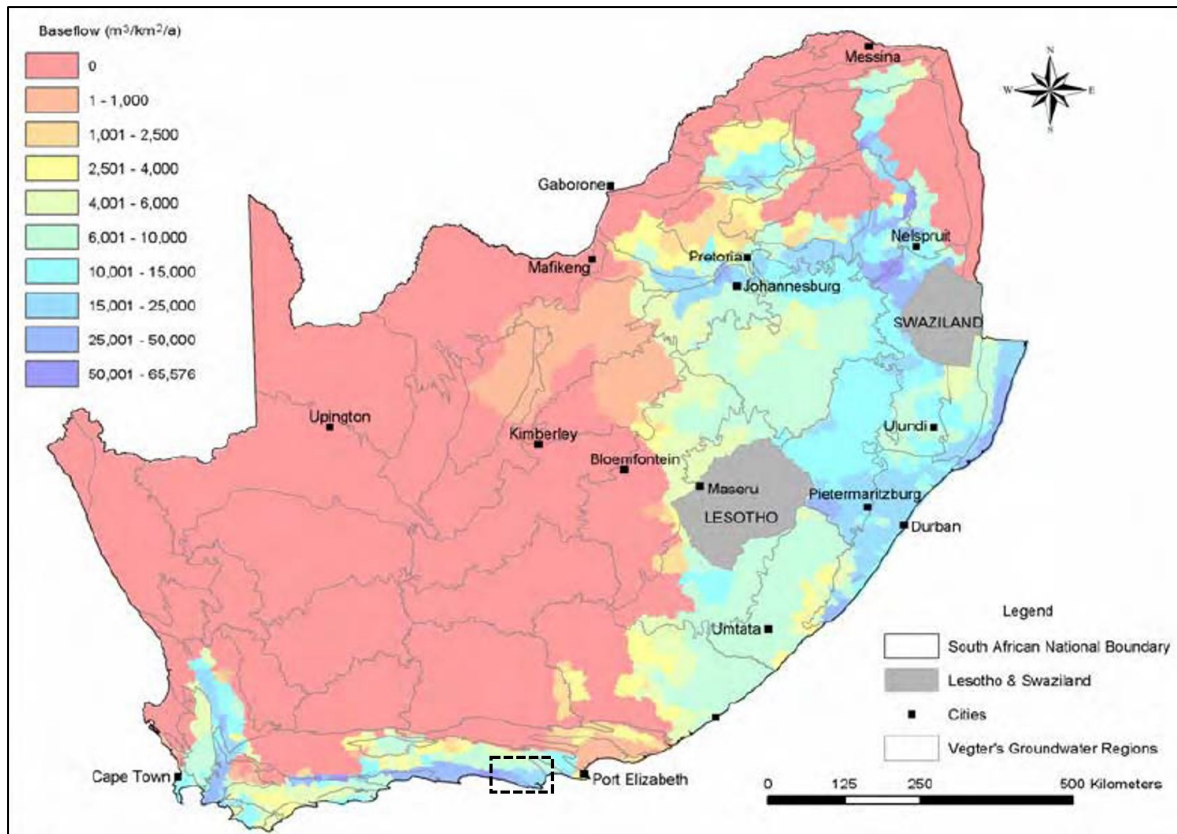
Figure 14: Mean annual groundwater contribution to baseflow map of South Africa in $m^3/km^2/a$ (DWAF, 2006). Study area is highlighted by a black stippled box

3.3   Data Collection

The investigation focused on the small-scale dynamics of the palmiet wetland system to increase the general understanding of the surface water and groundwater processes of these palmiet wetland systems. Most fieldwork was thus focused on the Kompanjiesdrif wetland system and the associated alluvial fans with some fieldwork being undertaken at the upstream Krugersland wetland. A severe drought was experienced in the study area over most of the study period and data collection was affected adversely.

3.3.1   Hydrocensus

The Department of Water and Sanitation (DWS) National Groundwater Archive, DWS Water Authorisation Management System database, and a local borehole expert were consulted to determine the location of boreholes in the study area. A borehole (BH1) is located upstream of the Krugersland wetland, but no boreholes were found in the vicinity of the Kompanjiesdrif wetland (Figure 15). Several other boreholes are located higher up in the catchment (but outside the study catchment).
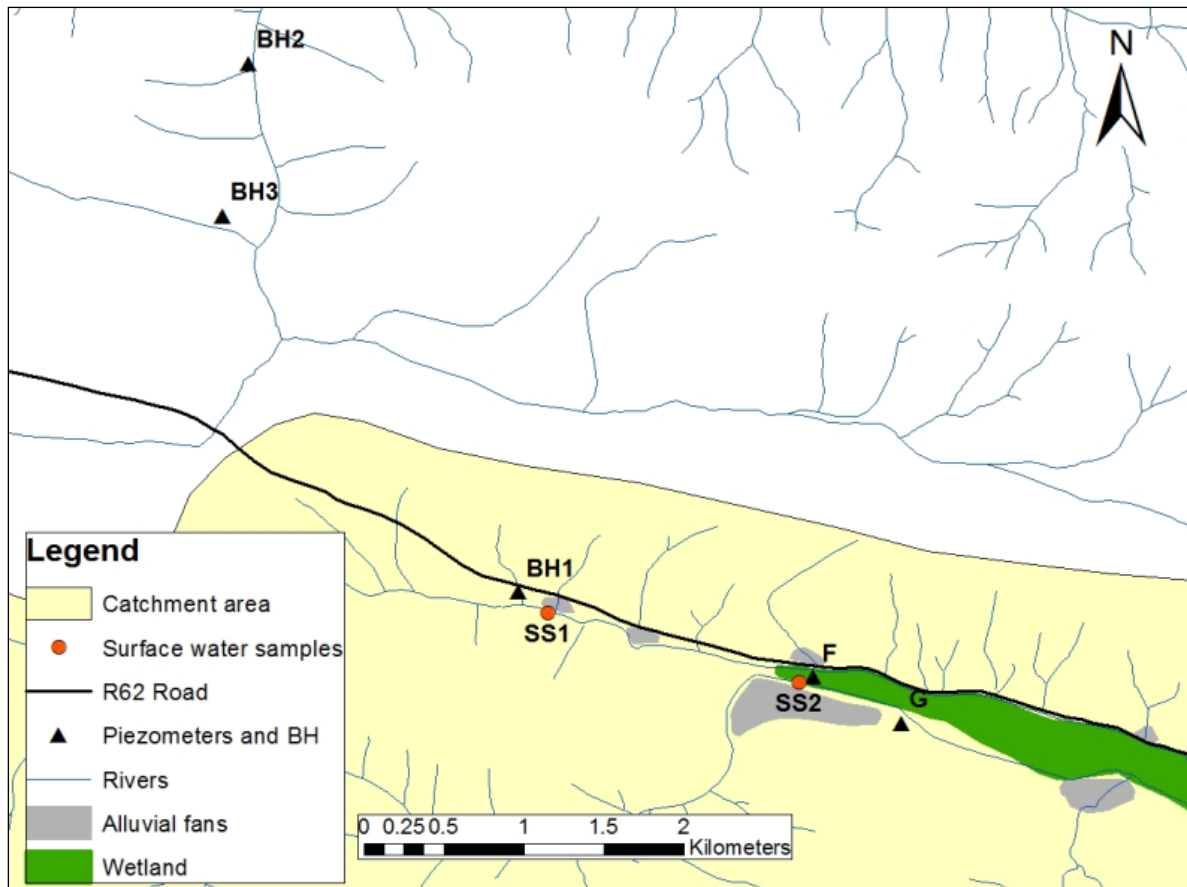
Figure 15: Location of piezometers and surface water sampling sites at the Krugersland wetland and the borehole upstream of the wetland. Two additional boreholes (BH2 and BH3) located outside the study catchment and their locations were also sampled

3.3.2 Installation of piezometers

Four alluvial fans encroach onto the northern bank of the Kompanjiesdrif wetland basin from tributaries of the Suuranys Mountain range. The intention was to install piezometers on the first alluvial fan (westernmost fan) to determine if there is preferential flow through the boulder material of this fan into the wetland. Holes were drilled using a handheld Dutch auger. Holes drilled towards the top of the fan were unsuccessful because hard boulders, which are typically found at the head of an alluvial fan, were intersected. These holes did not reach the water table despite deep pits being dug (maximum 2 m deep). Several auger holes, located on the outer edges of the alluvial fan were, however, successfully drilled through to the water table and in some cases to bedrock. Holes were also drilled in the wetlands and piezometers were installed (Figure 15, Figure 16, and Table 3).

Piezometer pipes were installed in the successful holes along with data loggers in selected piezometers for measuring variations in water height. Data loggers were installed in June 2016 in PZA, PZB, PZC, PZD, and in BH1. The data loggers monitored water levels for a period of eight months. These loggers were removed and reinstalled in different holes in February 2017, May 2017 and August 2018. This was both due to the drought (some piezometers dried up completely) and because we wanted to obtain information in different areas of the site. A Geomax Zenith 10/20 differential global positioning system (DGPS) was used to measure the location and elevation of the piezometers as well as cross-sectional transects through the river. During the drought experienced in 2017, some of the piezometers dried up, and the data loggers were therefore above the water level.
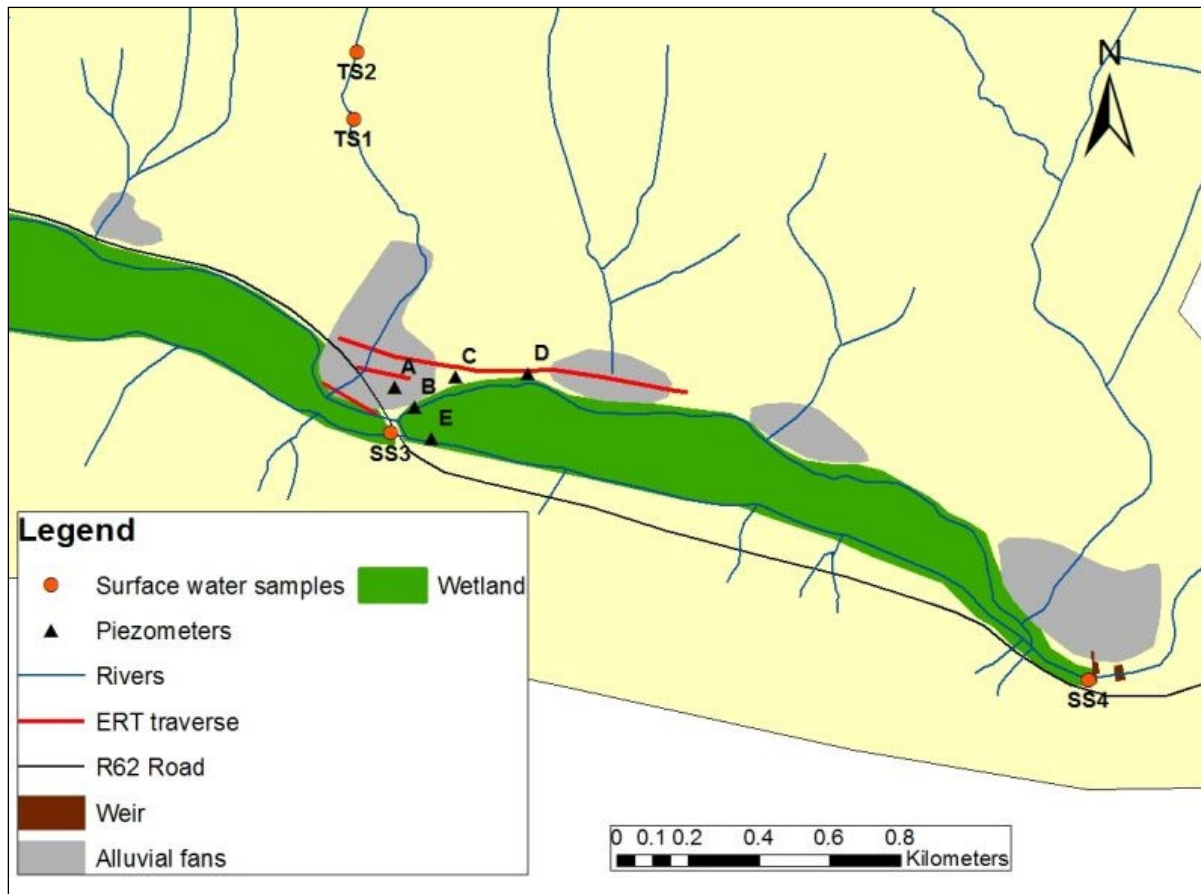
Figure 16: Location of piezometers, surface water sampling sites and electrical resistivity tomography (ERT) transects in the vicinity of the Kompanjiesdrif Wetland

Table 3: Details of piezometers and boreholes

Piezometer/ borehole	Location (decimal degrees)	Elevation (top of pipe/casing in masl)	Depth of hole (below top of pipe/casing in m)	Comments
PZA	−33.877281° 24.053235°	359.39	4.25	
PZB	−33.877793° 24.053720°	355.60	1.9	
PZC	−33.877018° 24.054751°	355.77	4.45	
PZD	−33.876941° 24.056576°	354.63	4.27	
PZE – in Kompanjiesdrif wetland	−33.878577° 24.054145°	356.22	4.5	

Piezometer/ borehole	Location (decimal degrees)	Elevation (top of pipe/casing in masl)	Depth of hole (below top of pipe/casing in m)	Comments
PZF – in Krugersland wetland	−33.867201° 24.017502°	391.70	2.98	
PZG	−33.869800° 24.022436°	380.885	3	
BH1	−33.862396° 24.000902°	422.691	55.55	Appears to be located at the contact between the Baviaanskloof Formation sandstone and Bokkeveld Group shale. Data logger was removed from the borehole by the landowner at the end of January 2017 so that the borehole could be pumped to provide water during the drought.
BH2	−33.832670° 23.985720°	498	−	Located outside the study catchment within the Peninsula Formation.
BH3	−33.841250° 23.984270°	518	−	Located outside study catchment within the Peninsula Formation (close or at the Peninsula Formation – Cederberg shale contact).

Table 4: Details of surface water sampling sites

Surface water samples	Location (decimal degrees)	Comments
River sample 1 (Krom) – upstream of wetlands (SS1)	−33.863561° 24.002574°	
River sample 2 (Krom) (SS2)	−33.867476° 24.016712°	
River sample 3 (Krom – under R62 bridge) (SS3)	−33.878393° 24.053147°	No samples were taken during 2017 during field visits due to the drought. Only one sample taken during May 2018.
River sample 4 (Krom – bottom of Kompanjiesdrif wetland) (SS4)	−33.884654° 24.070770°	

Surface water samples	Location (decimal degrees)	Comments
Tributary of Krom 1 (May 2017) (TS1)	−33.870520° 24.052180°	Both samples are from the same tributary but were collected on different dates. The second sample was also collected slightly higher up in the tributary than the first. Located within the Nardouw Subgroup, also receives water from the Peninsula Formation.
Tributary of Krom 2 (May 2018) (TS2)	−33.868820° 24.052270°	

3.3.3 Electrical resistivity tomography survey

An ERT survey was undertaken at the Kompanjiesdrif wetland in February 2017 to investigate the subsurface dynamics within the alluvial fans (Figure 16). An Abem SAS 1000 Terrameter and ES 10-64 switching unit were used in the field survey. Three ERT transects were undertaken using the Wenner measuring protocol at an electrode spacing of 4 m. The maximum investigation depth with this electrode spacing and measuring protocol is 24 m.

3.3.4 Water quality sample collection and analysis

Water samples were collected from all piezometers, the borehole (BH1), the Krom River, and a tributary of the Krom River (Figure 16 and Figure 15). In May and August 2017, no surface water sample could be collected from the river under the R62 bridge (top of Kompanjiesdrif wetland) and from certain piezometers due to the drought (Figure 22). No tributary sample was collected in August 2017 as the tributary could not be accessed. Electrical conductivity (EC) and pH were measured in the field using a Hanna HI98129 pH EC tester, YSI Pro Plus multiparameter water quality meter, Hanna HI9829 multiparameter water quality meter, and Hach SL1000 water quality meter. Chloride was measured in May 2018 using the Hach SL1000 chloride probe.

Two additional boreholes (BH2 and BH3) were also sampled in May 2018. These boreholes are located just outside of the study catchment within the Peninsula Formation quarzitic sandstones – with one being located at or close to the contact between the Peninsula Formation and the Cederberg Formation shale. These boreholes are situated in the same geology as the groundwater that would flow from tributaries into the wetlands in the study catchment. Therefore, they were considered representative of the groundwater in the catchment area. All water samples were analysed for $^2H/^1H$ and $^{18}O/^{16}O$ ratios in the laboratory of the Environmental Isotope Group of iThemba Laboratories, Johannesburg. The Mg, Ca, K, Al and Si content was tested at Rhodes University using a Palintest Photometer 7100.

3.3.5 Data loggers in the river

Data loggers were installed in three positions upstream and downstream of the wetlands in the Krom River channel to measure changes in water height and assist with developing the rating curve (Figure 17). The nature of the river channel, which was affected by artificial weir and culvert structures, made it difficult to find good locations to install data loggers. Unfortunately, the data loggers were also above water for large periods of time during the drought in 2017.

Figure 17: Location of the data loggers in the river

15 June 2016	2 February 2017
31 May 2017	11 August 2017
22 May 2018	
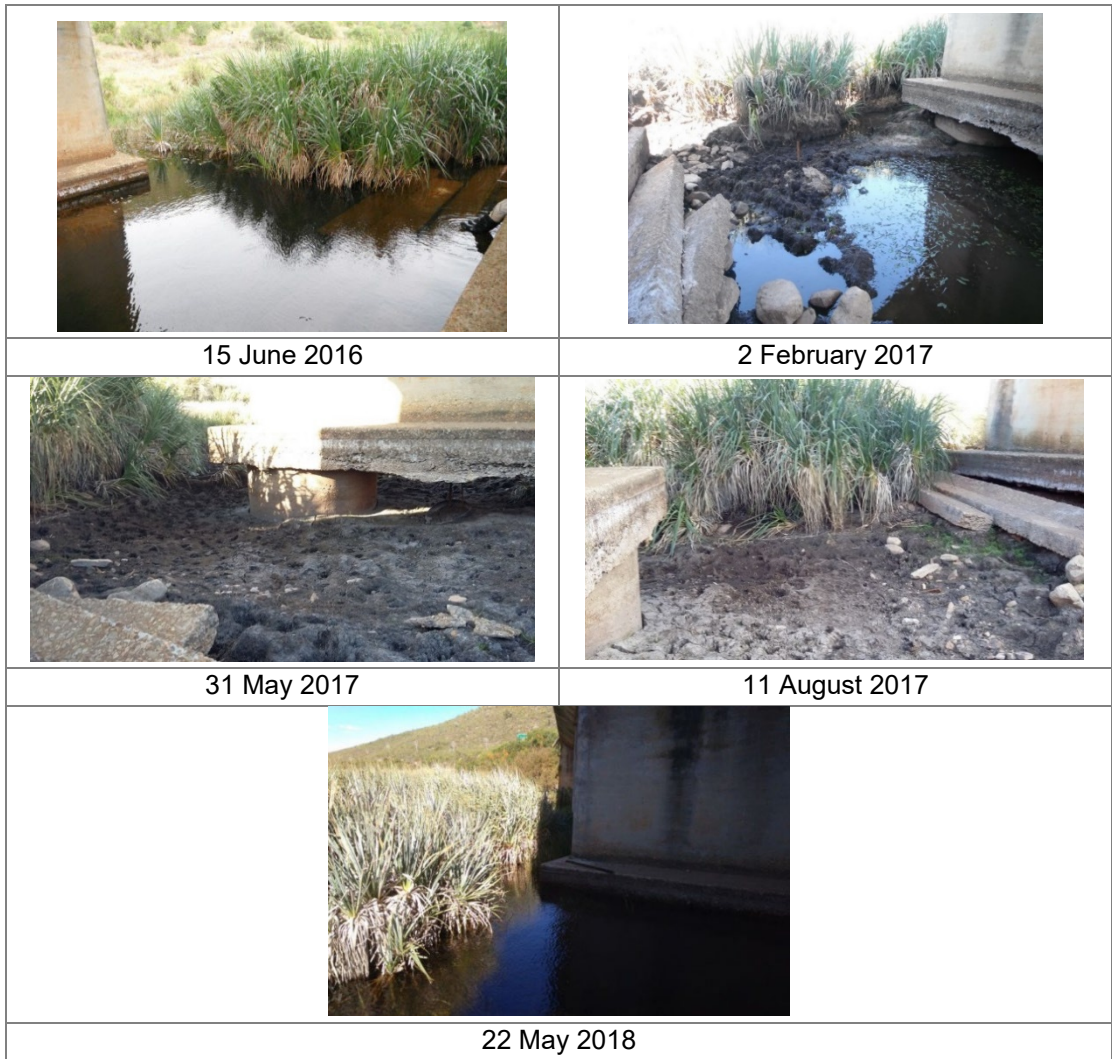
Figure 18: Variation in water levels at the top of Kompanjiesdrif wetland (underneath the R62 bridge: −33.878420°, 24.053210°). A particularly dry period was experienced between February and August 2017

4   AIM 1: DETERMINING THE SURFACE WATER AND GROUNDWATER DYNAMICS OF THE KROM RIVER WETLAND

4.1   Results of Data Collection

4.1.1   Subsurface water levels

The surface (where available and measured) and subsurface water levels for the period between June 2016 and May 2018 are illustrated in Figure 19, Figure 20 and Figure 21. There has been a decline in rainfall in the study area since August 2016 and the area experienced a severe drought in 2017. This is also reflected in the decline in elevation of the surface and subsurface water levels. Manual dip readings taken at Piezometers A–D[3], and the borehole (BH1) in June 2016 and at the end of January 2017 indicated an average drop in subsurface water level of between 0.5 m and 0.7 m.

Dip readings of all holes (PZA–PZG and borehole) in May 2017 indicated a further drop in water levels of between 0.4 m and 0.7 m since January 2017. Water levels had dropped even further (average of 0.3 m) in August 2017. This equated to an average drop in water level in the piezometers of about 1.4 m over the period between June 2016 and August 2017. PZB (edge of Kompanjiesdrif wetland) and PZF (in Krugersland wetland) were dry in May 2017 and August 2017. Manual dip readings taken in May 2018 indicated that subsurface water levels had increased by an average of about 0.8 m since August 2017. Most water levels measured in May 2018 were, however, still lower than initial readings taken when fieldwork began in June 2016.
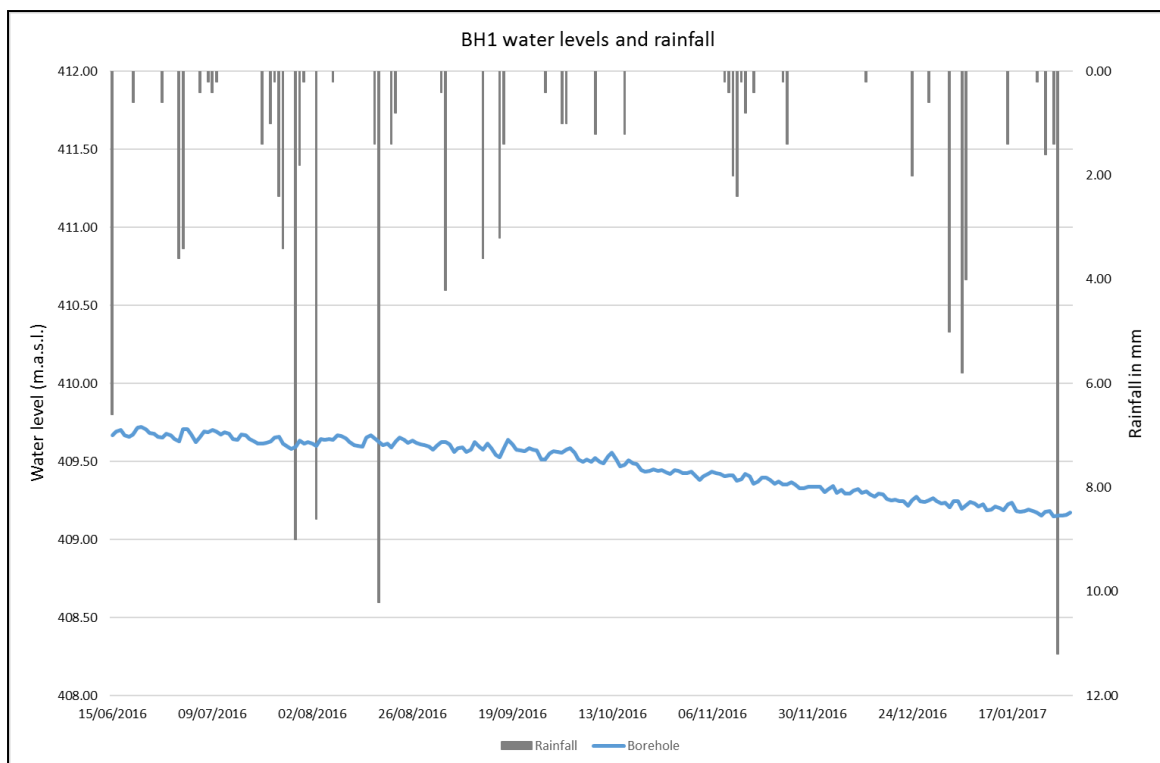
Figure 19: BH1 water levels between June 2016 and January 2017 (water levels ceased to be measured by a data logger in January 2017 as the farmer started pumping the borehole)

---

[3] The following notation will be used to indicate individual piezometers: Piezometer A (PZA); Piezometer B (PZB); and so forth.
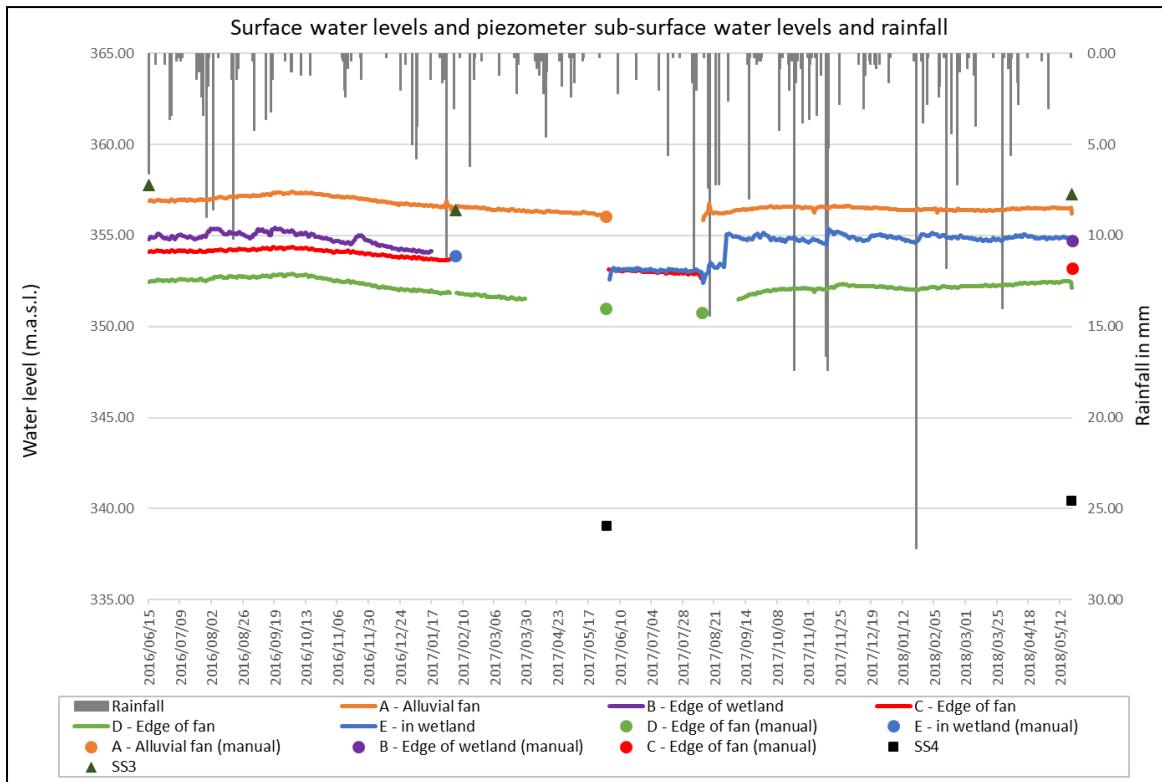
Figure 20: Surface and subsurface water levels at Kompanjiesdrif. Piezometer water level measurements were taken using a data logger. Manual piezometer readings taken with a dip metre are illustrated as dots
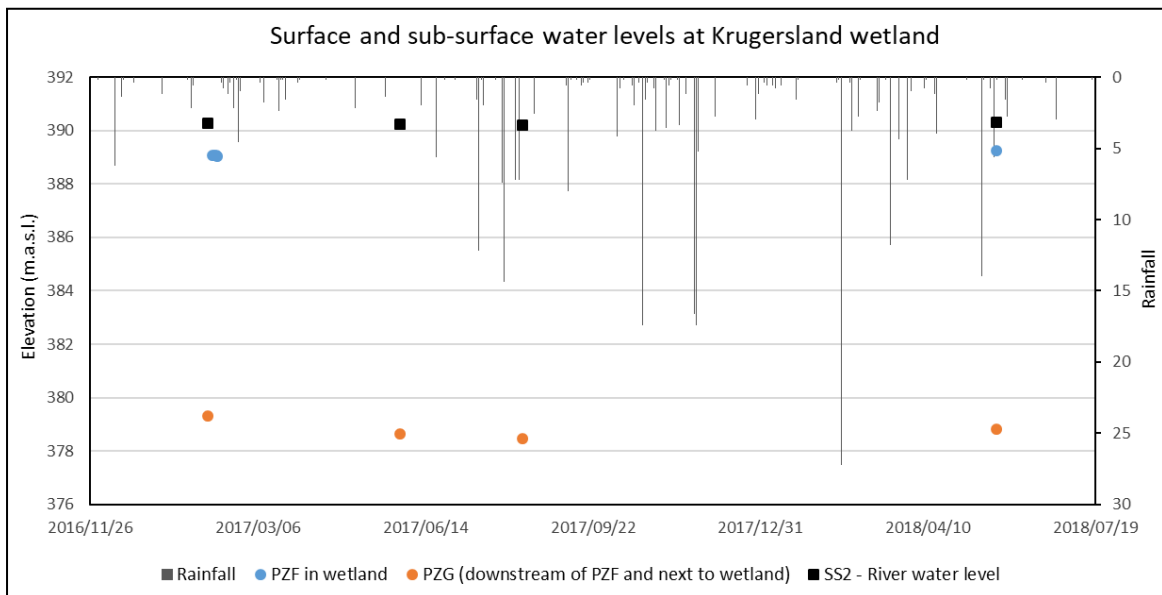
Figure 21: Surface and subsurface manual water level measurements at the Krugersland wetland. PZF was dry when it was measured in May and August 2017

The water level of the borehole (BH1) was at 407.19 masl in May 2018 (compared with 409.67 masl in June 2016 when the study began). The borehole had not been pumped for six months prior to this water level measurement. The farmer indicated that he had ceased pumping from this borehole due to the salty water affecting his equipment (indicating that the groundwater is moving through or in contact with shale-rich rock).

A floodplain cross section was surveyed using a DGPS running from BH1 (north) and across the river channel below it (south) in May 2017 (Figure 22 and Figure 23). The cross section illustrates the change in water level in the borehole over various months. The reading taken in May 2017 was affected by pumping of the borehole that took place during that month. It is evident that the borehole level is lower than the adjacent river channel in the months that it was monitored, which indicates that it is unlikely that the river at this point is receiving a significant amount of diffuse groundwater input from the aquifer. The borehole was monitored during a predominantly dry period though and its level in relation to the river channel could change during much wetter periods. Also illustrated in Figure 22 is the surveyed downstream water level in the river channel in May 2017.

Interestingly, the surface water elevation at SS3 (Figure 20) is higher than the water elevation of PZA (in June 2016 and May 2018) and the water elevation of PZE (in the wetland), which is located about 80 m downstream of SS3. The higher water level at SS3 compared with PZE and PZA is understandable considering the steep longitudinal slope of the Kompanjiesdrif wetland and the fact that SS3 is situated between two large bridge pylons in a pool-type environment (raising the water level) where the water flows slowly into the wetland. The surface water at SS2 remained quite shallow and the water level remained relatively constant throughout the study period (Figure 21).
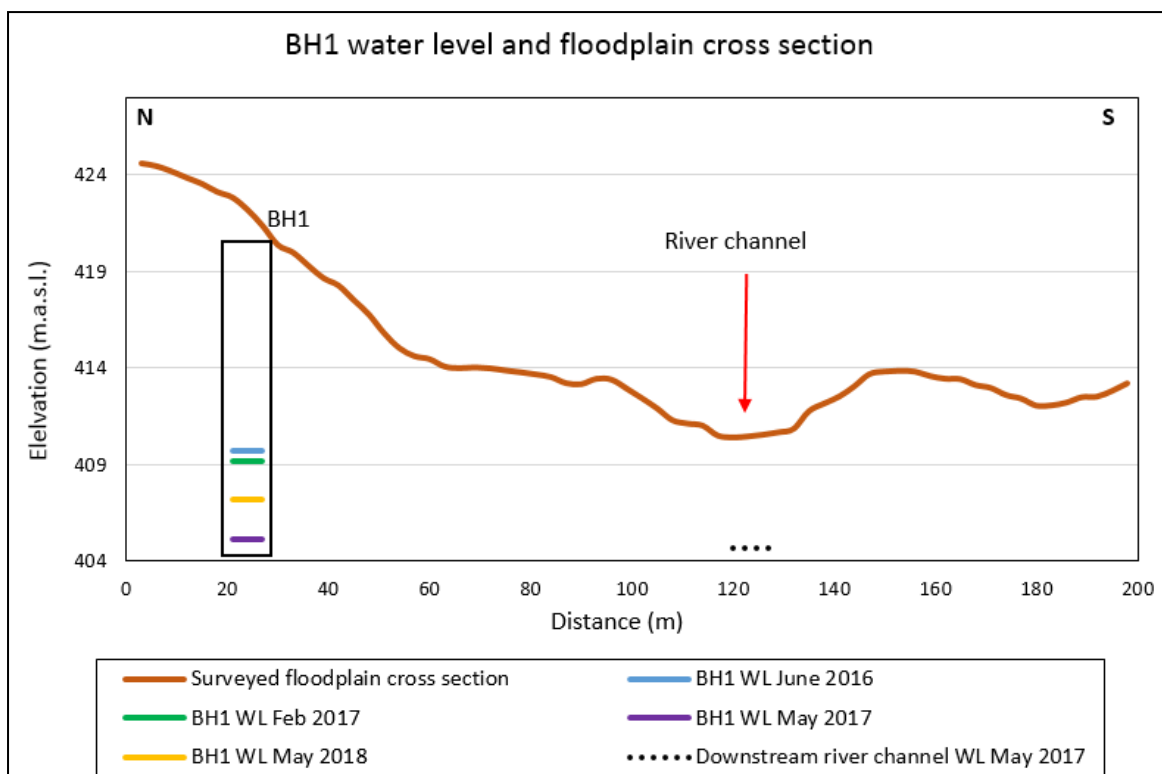
Figure 22: Surveyed floodplain cross section completed in May 2017 with the location of BH1 and the river channel from north to south illustrated. BH1 water levels are also illustrated over various months. The May 2017 borehole level is probably slightly lower than it would be naturally due to borehole pumping by the farmer that took place that month. Also illustrated is the water level of the river channel in May 2017 (the dotted line), which is located 200 m downstream of the borehole

Figure 23: Location of the surveyed cross section (illustrated by a white line) and downstream surveyed

4.1.2 Electrical resistivity tomography survey

The ERT survey conducted at the Kompanjiesdrif wetland indicated a distinct increase in resistivity along the alluvial fans (red, purple, orange areas) with lower resistivities between the fans (Figure 24 and Figure 25). This confirms the likelihood of the presence of distinct preferential subsurface flow paths through alluvial fan material to the wetland.
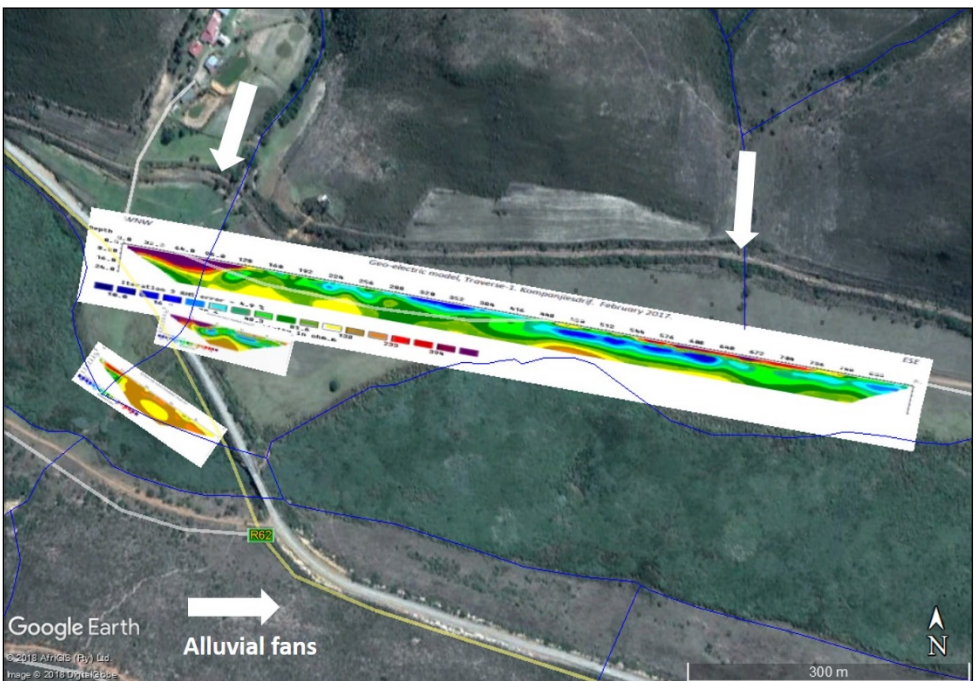
Figure 24: ERT survey results for transects at the Kompanjiesdrif wetland with alluvial fans entering the wetlands illustrated by white arrows
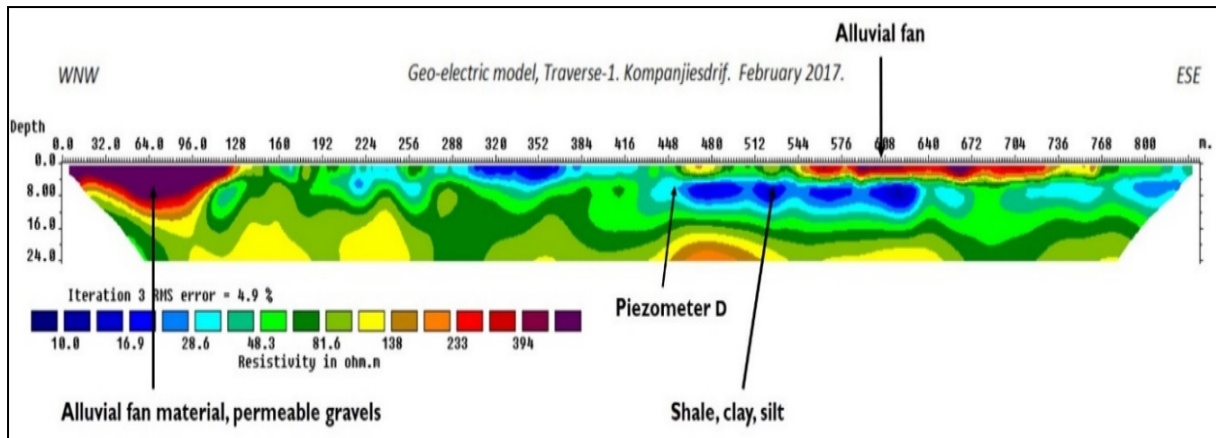
Figure 25: ERT survey results for the upper ERT transect at the Kompanjiesdrif wetland (across the alluvial fans and parallel to the wetland). The location of PZD, which fell on the ERT transect line, is also illustrated

The material between the fans, with a lower resistivity, appears to be a combination of shale, silt and clayey material. The resistivities shown are consistent with those described for these geological materials by Palacky (1988). The survey also indicates that PZD is located within the lower resistivity material (shale, clay and silt). Similar ERT profiles and resistivity values across alluvial fan environments are described by Giocoli et al. (2008) and Amaya et al. (2016) who highlighted the effectiveness of using ERT surveys for mapping aquifer systems in alluvial fans.

4.1.3 Water quality and stable isotope analysis

The nature of some of the surface water sampling points along the Krom River that are located in pool-type environments due to artificial weir structures needs to be considered when interpreting the water quality results. The SS1 and SS4 sampling sites would have experienced higher rates of evaporation and slower flow during the drought in 2017 due to the weir structures affecting flow at these locations.

The sampling event in May 2018 was during a wetter period than in 2017 when there was a higher water level in the main Krom River channel and water was flowing faster over the weir structures (instead of pooling behind the structures). The May 2018 surface water samples could thus be treated as being generally more representative of the typical surface water quality in the study catchment than the 2017 surface water samples.

Stable isotopes

The stable isotope plots for the various surface water, piezometer, and borehole samples are illustrated in Figure 26, Figure 27 and Figure 28. A single rainwater sample was collected in August 2017 and is presented in the August 2017 graph. No tributary sample was collected in August 2017. No SS3 and PZF sample was collected in May 2017 and August 2017 due to the drought. No PZD sample was collected in August 2017 due to the drought. The global meteoric water line (GMWL) developed by Craig (1961) is plotted on the graphs along with the local meteoric water line (LMWL). The LMWL was taken from Diamond (2014), which was determined using rainfall data collected at the Lentelus rainfall station in the Kouga Mountains (located approximately 50 km from the study catchment). Two additional borehole samples (located approximately 50 km north-west of the study catchment) were collected in May 2018 and the isotope results for these are shown in Figure 28.

The graphs illustrate an enrichment in lighter isotopes for the rainwater and borehole samples compared with the surface water and piezometer samples. SS1 (upstream) is more enriched in heavier isotopes than SS2 and is the most enriched sample in May 2018. This is possibly because the sample was taken from a weir structure (and downstream of the weir structure) where water was standing still and not flowing at times (subjected to high evaporation). The SS1 sample is thus not a good upstream representative sample. All samples plot relatively close to or on the LMWL. The August 2017 rainfall sample plots right next to the LMWL confirm that the LMWL gives a good indication of the isotopic signature of rainfall in the study area.

The fact that the tributary sample is more enriched in lighter isotopes than the other piezometer and surface water samples and plots relatively close to the borehole samples confirms the likelihood that this tributary receives considerable groundwater input (especially since there were no significant rainfall events during or immediately prior to sampling of the tributary).

As noted by Barrow, 2010, the interpretation of stable isotopic signatures of wetlands and river samples in the TMG can be complex because they are affected by evaporation and may receive various quantities and have various sources of groundwater and surface water. There is no immediately obvious link between the groundwater isotopic signatures and the wetland isotopic signatures (PZE, PZF, SS3, and SS4) in Figure 26 to Figure 28.
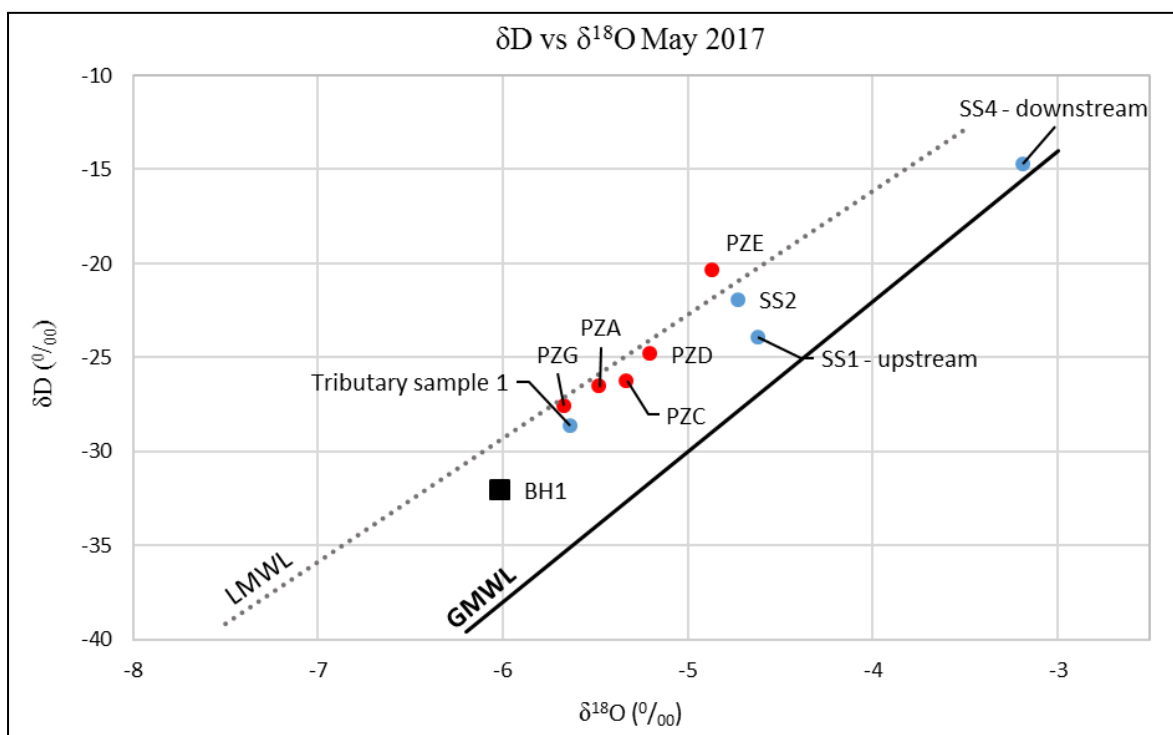
Figure 26: Plot of δD vs δ18O for May 2017. LMWL (Diamond, 2014); GMWL (Craig, 1961)
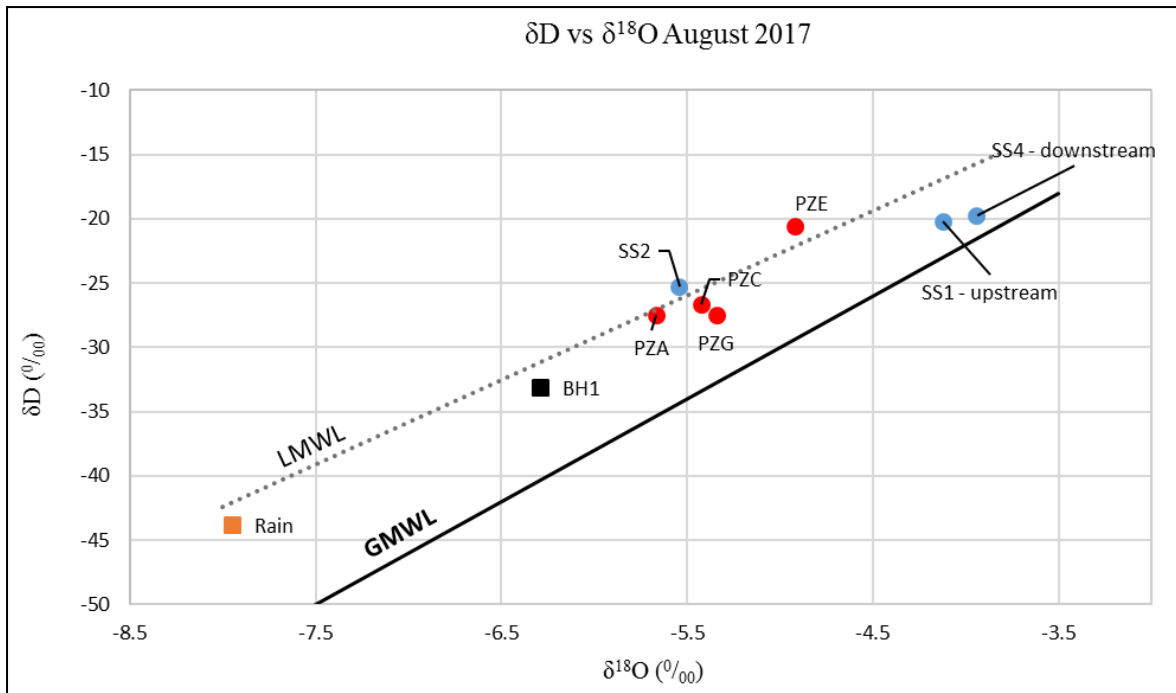
Figure 27: Plot of δD vs δ18O for August 2017. LMWL (Diamond, 2014); GMWL (Craig, 1961)
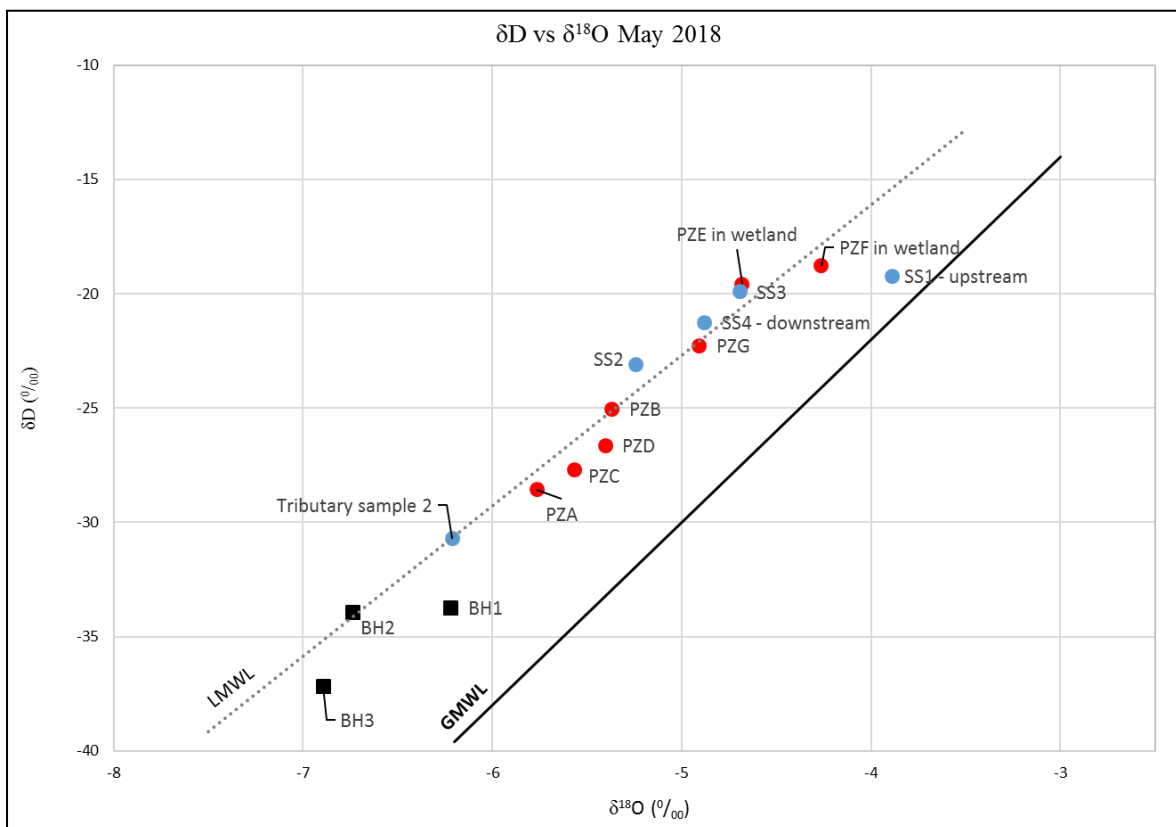
Figure 28: Plot of δD vs δ18O for May 2018. LMWL (Diamond, 2014); GMWL (Craig, 1961)

Change in water quality and isotope signature with distance along the Krom River channel

Figure 29, Figure 30 and Figure 31 illustrate the EC, chloride and $\delta^{18}O$ content of water at various sampling points moving from the top to the bottom of the catchment in May 2018. Sampling points located in the main Krom River channel are plotted on the red or purple lines. Wetland piezometer or surrounding sampling points are represented as dots. Large tributaries that enter the main river channel from the north and south are illustrated by dark blue arrows.

There was no significant rainfall in the months preceding the sampling event in May 2018. It is thus reasonable to assume that the tributaries flowing into the wetlands and main river channel consist pre-dominantly of groundwater.

The chloride and EC graphs show high concentrations at BH1. According to Smart and Tredoux (2002), TMG aquifers usually have an EC below 100 mS/m (1000 µS/cm) with an average range of 20–50 mS/m (200–500 µS/cm). Higher ECs are common in more shale-rich rocks. Smith, Clarke and Cavé (2002) analysed the water quality of boreholes in the Nardouw Subgroup and Peninsula Formation (within the Dysselsdorp and Calitzdorp area) and found that the Nardouw Subgroup had a mean EC value of 30 mS/m (maximum of 155 mS/m) and peninsula boreholes had a mean EC of 10.4 mS/m (maximum of 26.3 mS/m).

BH1's chloride content is higher than the mean value for the Nardouw aquifer reported by Smith et al. (2002) but is within the maximum range. Field observations and consultation of the 1:250 000 geological map of the area (Toerien, 1986) indicated that the borehole is located within the Gydo Formation (Bokkeveld Group) or at the contact of the Gydo Formation (shale-rich) and the Baviaanskloof Formation (sandstone and minor shale). The EC and chloride content of BH1 confirmed that the ground-water is coming into contact with the Bokkeveld shale.

The EC values of BH2 and BH3 were within the range reported for the Peninsula Formation by Smith et al. (2002), but the chloride content was slightly higher. BH3 also had a slightly higher chloride and EC value than BH2, which was expected based on its location at or close to the Cederberg shale – Peninsula Formation contact.

The high chloride and EC content of the SS1 sample are likely due to high evaporation at the sampling point. It is also unlikely that the higher EC and chloride content at SS1 is caused by groundwater input from the Bokkeveld shale at this point as Figure 29 illustrates that the water table at BH1 is lower than the elevation of the nearby stream channel. Also, the isotope signature is enriched with heavier isotopes at SS1, which can be explained by the high evaporation at this sampling point. There is a spike in the chloride and EC content at PZF and PZE. This is probably due to ET in the wetland (the wetland plants exclude certain salts such as chloride during transpiration) and the tributaries carrying in groundwater (which tends to have a slightly higher EC and chloride content than surface water) just before these points. The tributary sample had a slightly higher EC and chloride content than the river samples. The fact that the tributary has been subjected to evaporation and receives continuous groundwater input (with a slightly higher EC and chloride content than river samples – see BH2 and BH3) could explain this.

The gradual increase in EC and chloride in the surface water samples (SS2, SS3, and SS4) moving downstream can be attributed to evaporation and groundwater input from the tributaries. If the main river channel and wetlands were receiving large volumes of groundwater input from the Bokkeveld aquitard (via diffuse flow), then the EC and chloride content of SS2, SS3, SS4, PZF, and PZE would be expected to be much higher (based on the water quality of BH1).
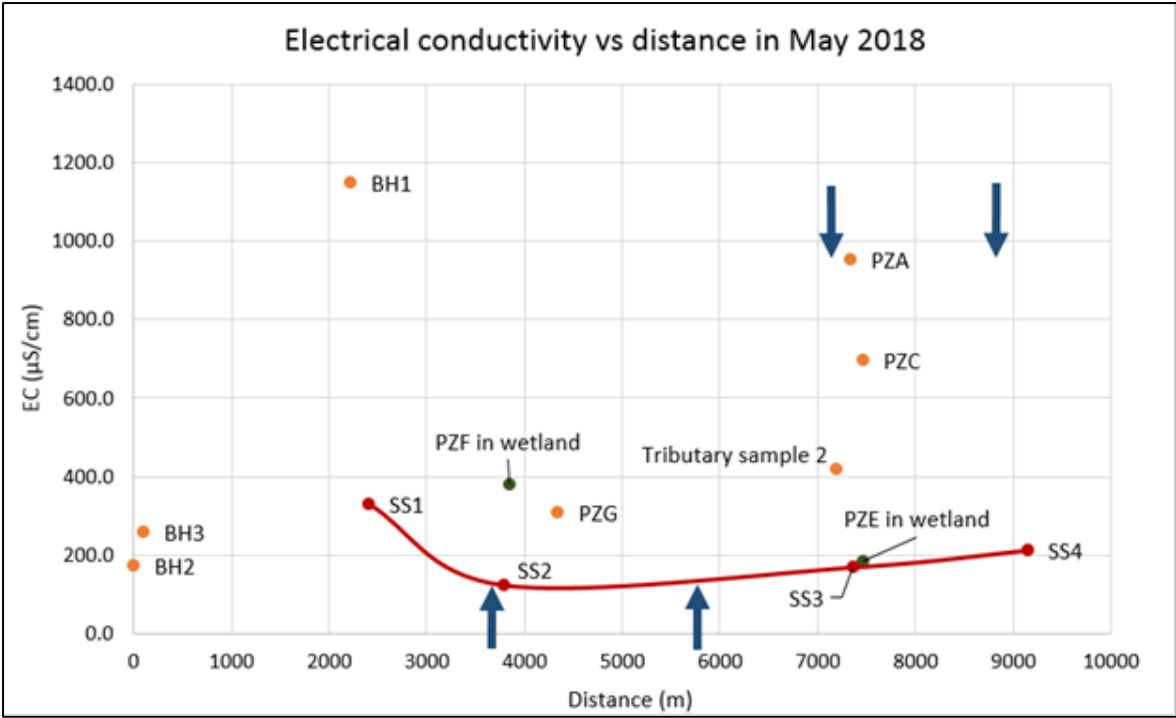
Figure 29: EC vs distance for May 2018 at various sampling points moving from top to bottom of the catchment. Dark blue arrows indicate the approximate location of large tributaries entering the main Krom River channel. Sampling points located in the main Krom River channel are plotted on the red line and wetland piezometer or surrounding sampling points are represented as dots. PZD has a very high EC, which skews the graph and it was thus left out
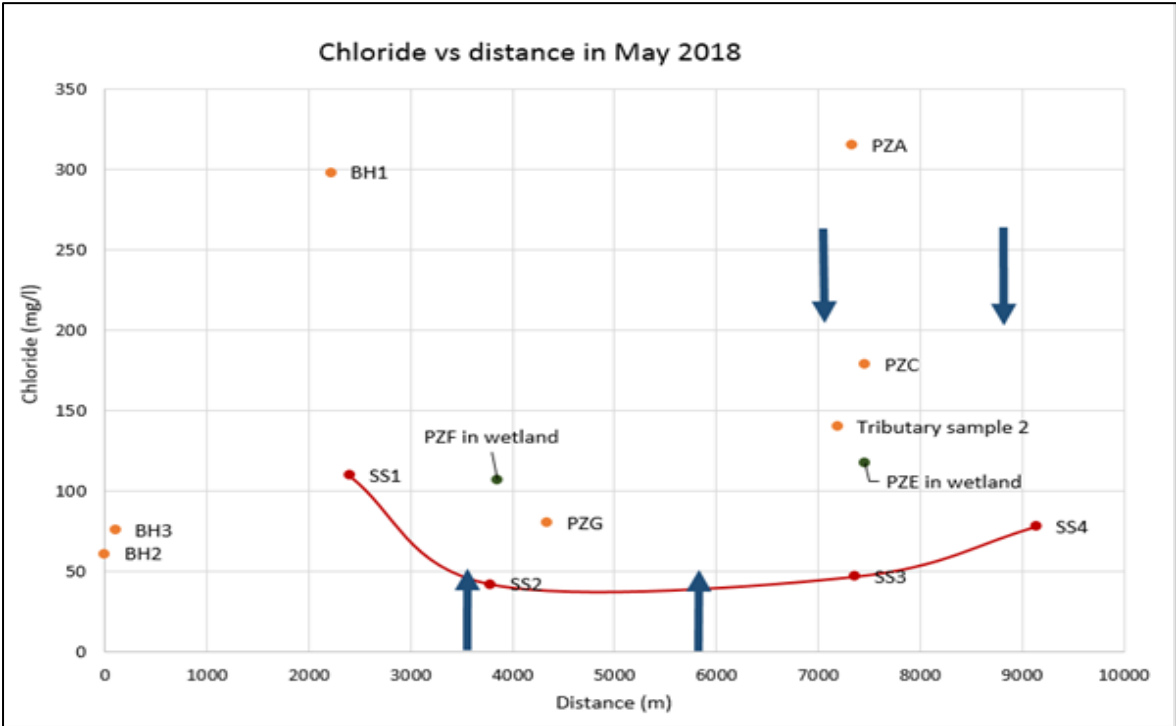
Figure 30: Chloride (red line) vs distance for May 2018 at various sampling points moving from top to bottom of the catchment. Dark blue arrows indicate the approximate location of large tributaries entering the main channel. Sampling points located in the main Krom River channel are plotted on the red line and wetland piezometer or surrounding sampling points are represented as dots. PZD has a very high value, which skews the graph and it was thus left out

The δ¹⁸O graph (Figure 31) illustrates that the river samples become lighter downstream (from SS2 onwards) even though it would be expected that the samples become more enriched in heavier isotopes due to evaporation (in particular the SS4 sample). This indicates that the tributaries are probably carrying in fresh groundwater (lighter δ¹⁸O concentration) before these sampling points. The spike at SS2 can be attributed to the large tributary flowing into the main channel (carrying in lighter groundwater) before that sampling point.

SS4 is more enriched in heavier isotopes than the other surface water samples in 2017 (Figure 26 and Figure 27), which is likely due to the drought, lower inflow from the tributaries and higher evaporation over that period.
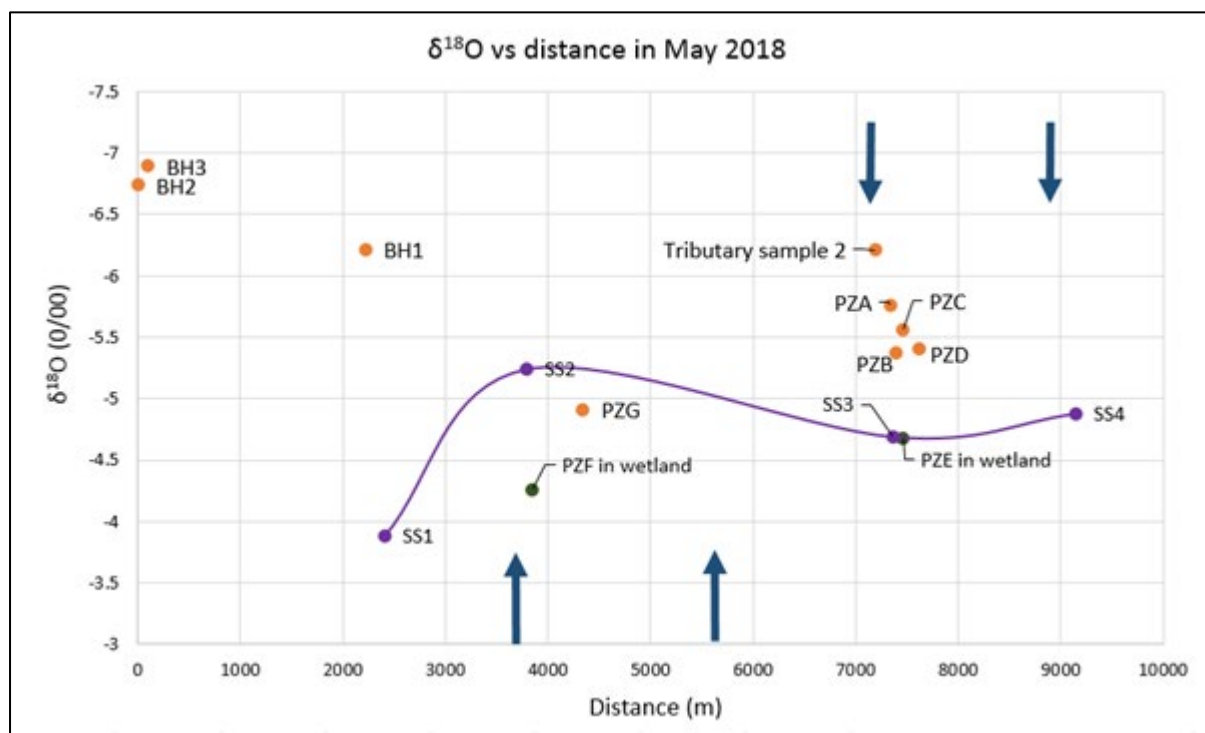
Figure 31: δ18O (purple line) vs distance for May 2018 at various sampling points moving from top to bottom of the catchment. Dark blue arrows indicate the approximate location of large tributaries entering the main channel. Sampling points located in the main Krom River channel are plotted on the purple line and wetland piezometer or surrounding sampling points are represented as dots

Physico-chemical water quality results

Table 5 to

Table 7 provide the results of all physico-chemical parameters analysed for water samples.

Table 5: Water quality results for May 2017 (units in µS/cm, pH units and mg/ℓ)

Sample	EC	pH	Cl	Ca	Si	Mg	Al	K
SS1	519	7.38	–	2.8	5.60	5	0	2.1
SS2	200	7.40	–	0	3.30	5	0	1.4
SS3	no sample							
SS4	380	7.00	–	1.6	4.60	6	0	1.2
TS1	575	6.70	–	5.6	7.00	10	0	0.9

Sample	EC	pH	Cl	Ca	Si	Mg	Al	K
PZA	1248	5.84	–	37.6	3.60	30	0.08	4.0
PZC	848	6.23	–	8.4	9.15	16	0	3.7
PZD	6750	5.52	–	0	10.55	220	0.28	11.5
PZE	308	–	–	0	5.86	7	0.03	3.9
PZF	no sample							
PZG	425	5.96	–	3.6	6.80	9	0.06	5.6
BH1	1438	6.32	–	4.8	15.50	23	0.04	4.0

Table 6: Water quality results for August 2017 (units in µS/cm, pH units and mg/ℓ)

Sample	EC	pH	Cl	Ca	Si	Mg	Al	K
SS1	463	5.86	–	1.6	4.30	9	0.06	0.5
SS2	156	5.31	–	3.0	2.70	6	0	1.0
SS3	no sample							
SS4	320	7.05	–	2.0	4.30	7	0	0.6
PZA	1014	6.22	–	24.0	13.10	28	0.19	22.0
PZC	874	6.24	–	6.4	7.97	18	0.17	2.3
PZD	7277	5.32	–	not enough sample				
PZE	243	6.53	–	1.6	5.63	7	0	5.6
PZF	no sample							
PZG	353	6.90	–	not enough sample				
BH1	1051	5.97	–	17.2	13.40	22	0	3.3

Table 7: Water quality results for May 2018 (units in µS/cm, pH units and mg/ℓ)

Sample	EC	pH	Cl	Ca	Si	Mg	Al	K
SS1	332.0	6.94	110.0	1.6	5.20	1	0	0.9
SS2	124.0	6.34	42.3	0	2.60	3	0	0.6
SS3	169.4	6.46	47.1	0.8	5.60	5	0.03	0.4
SS4	212.3	7.38	78.4	0.8	5.60	7	0.02	1.0
TS2	419.0	6.37	140.0	6.0	4.03	10	0.38	1.8
PZA	955.0	6.05	315.0	23.6	15.90	47	1.10	6.9
PZC	699.0	6.04	179.0	8.4	10.08	15	0.06	2.7
PZD	6547.0	5.03	2540.0	0	15.01	310	1.20	3.4
PZE	183.9	5.81	118.0	0	5.16	11	0.18	4.0
PZF	381.0	5.76	107.0	0	5.86	13	0.01	2.4
PZG	308.0	5.84	80.6	0	7.50	13	0	6.5
BH1	1149.0	6.21	298.0	13.6	12.70	27	0.05	3.3
BH2	174.0	5.46	61.2	0	3.94	5	0	0
BH3	258.0	5.92	76.2	1.2	9.38	9	0	2.8

4.2   Building the Conceptual Model

The conceptual models evaluated during the field investigation and modelling exercise included:

- Groundwater/interflow is not a significant contributor to the system: the system is sustained purely by surface water (surface run-off and direct precipitation). In this model, surface water is stored within the alluvium and wetland leading to the evident baseflow seen in the river.

- Subsurface water (groundwater, interflow or both) contributes to the system via preferential flow paths in the alluvium, which are fed by the surrounding quartzite TMG geology.

- Subsurface water (groundwater, interflow or both) contributes to the system via diffuse flow through the surrounding Bokkeveld shales and sandstones, which are recharged by the surrounding quartzite TMG geology.

During the first site visit in June 2016, the river was flowing and instrumentation of the catchment began. During subsequent site visits in February and May 2017, however, a severe drought resulted in many parts of the river drying out completely. It was evident, nevertheless, that water was still continuously flowing in certain tributaries of the Krom River despite the severe drought. This was particularly evident at the main Kompanjiesdrif tributary where water emerged at the top of a steeply dipping sandstone outcrop of the Nardouw Subgroup. Water flowed through the tributary towards the valley, disappeared into the subsurface (alluvial material) and then, presumably, emerged again within the wetland. A local farmer below the tributary used some of this water for household use and farming. The farmer indicated that his family has lived on the land for several years and that the tributary has never run dry. The larger tributaries in the entire wetland catchment all behaved similarly and did not stop flowing throughout the study period. This is evidence of significant storage within the Peninsula and Nardouw aquifers.

Based on the results of the data collection (water quality, stable isotopes and ERT survey), we propose that the palmiet wetlands are sustained by subsurface water (both groundwater and interflow) moving through preferential flow paths in the alluvial fans, which are sustained by groundwater discharge from the surrounding sandstone and quartzites of the Nardouw Subgroup and Peninsula Formation. The conceptual model (Figure 32) shows the various flow paths proposed here and the probable Bokkeveld and Cederberg Formation aquitards (as described by Rosewarne, 2002) separating individual aquifers.

A similar situation exists in the Hex River Valley, which has also formed along a syncline. There are strong linkages between the alluvial fans within the valley and the TMG/Bokkeveld groundwater (Rosewarne, 2002). The TMG alluvium is a prominent groundwater storage reservoir: an estimated 5 million m^3/a seeps into the TMG/Bokkeveld aquifer beneath it (Rosewarne, 1981; 2002). According to Colvin, LeMaitre and Hughes (2003:26) who described typical TMG groundwater discharge settings, "*the colluvial and alluvial deposits formed from the quartzites result in many streams which appear and disappear as surface flows, particularly on the alluvial fans that are a prominent feature in many valleys*".

Brown et al. (2003) described similar scenarios for the interaction between the TMG aquifer and alluvium or rivers. They indicated that the Skurweberg aquifer (Nardouw) generally provides water directly to river baseflow in the main river channel, while water from the Peninsula Aquifer mainly flows into tributary rivers contributing to the main river channel. Springs associated with the Nardouw aquifer are usually low volume and intermittent while Peninsula Formation springs are generally perennial.

The folded and fractured nature of the TMG and Bokkeveld rocks mean that despite the proposed aquitards and boundaries between the individual aquifers (Figure 32), there is probably still some groundwater flow between the aquifers via fractures. Water level data (Section 4.1.1) and water quality data (Section 5.1.3) illustrate that it is unlikely that there is a significant groundwater discharge from the surrounding Bokkeveld shale into the palmiet wetlands.
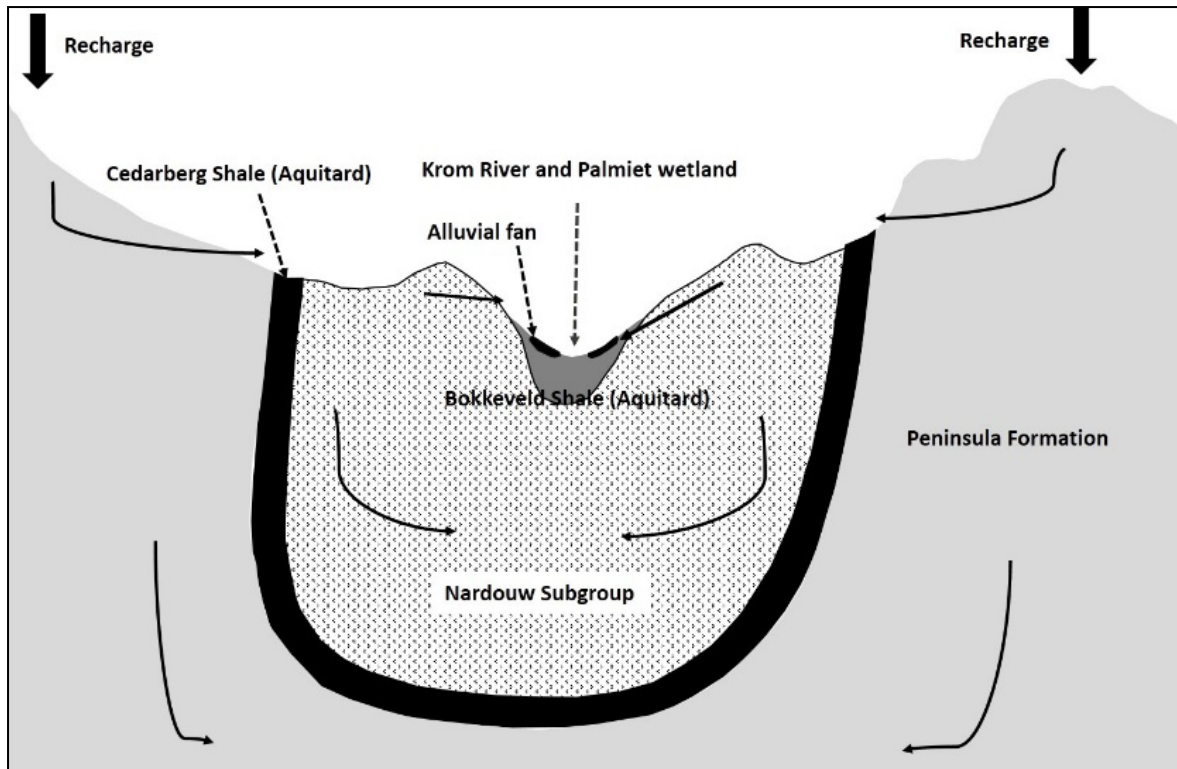
Figure 32: Conceptual model illustrating the flow of groundwater to the wetlands via alluvial fans and tributaries, which in turn derive this water from the Nardouw and Peninsula aquifers

4.2.1 Small-scale alluvial fan dynamics

Recovery of piezometer water levels at the Kompanjiesdrif wetland

A simple recovery test was undertaken for PZA, PZB, PZC and PZD (Figure 33) in February 2017 by emptying the piezometers and taking regular manual dip readings of the water level (every half hour). PZB and PZC took just over a day to recover fully, whereas PZA and PZD recovered relatively quickly (within 7.5 hours and 5 hours respectively). This provides an indication of the transmissivity of the alluvial fan material and surrounding alluvium. PZA is located near to the expected main trunk section of the alluvial fan and a higher transmissivity was expected, while PZD was located off of the alluvial fan.

These tests were repeated during each study visit and gave variable results. It is assumed that the variability in piezometer recovery times is linked to the extreme drying out of the catchment prior to wetting up in 2018. The outcomes of the recovery tests are summarised below.

- In May 2017, PZA, PZC, PZD, and PZE (in the wetland) were emptied again and dip readings were taken the next day. PZB was already dry and was thus not measured. PZA and PZC recovered within a day, but PZD took just over a day to recover. The slower recovery of PZD could be as a result of the lower water table due to the drought and a resulting change in the preferential flow paths at this site.

- In August 2017 after emptying all piezometers again, PZA, PZD and PZE did not recover fully within 24 hours, but PZC did.

- In May 2018 (subsurface water levels had improved in the catchment), PZA, PZC, PZD, and PZE all recovered within 24 hours of being emptied. PZE was filling up rapidly while being emptied. PZB did not recover fully.

Generally, the piezometers within the alluvial fan and in the surrounding alluvium appear to have an overall low hydraulic conductivity.

Figure 33: Location of piezometers where recovery tests were undertaken

Subsurface dynamics of piezometers at the Kompanjiesdrif wetland

The elevation of the water table at PZD (Figure 20) is consistently lower than the elevation of the water table in the wetland. Lagesse (2017) surveyed the water level of the Kompanjiesdrif wetland along a number of transects using a DGPS in May 2015 (Figure 33). At the time of the survey, the water level was sufficiently elevated throughout the wetland that it could be measured without using an auger or by installing piezometers. The direction of the slope of the water table changes along certain transects of the wetland (Figure 32).

In Transects 1 and 5, the water table slopes towards the northern edge of the wetland. In Transects 2, 4 and 6, the water table slopes primarily towards the southern edge of the wetland. This is linked to the presence of alluvial fans that constrict the wetland and steepen the land surface on the northern side at Transects 2, 4 and 6. At Transects 1 and 5 there are no alluvial fans present and the land surface on the northern side of the wetland has a gentler slope than the southern side (land surface is higher on this side). The water table at Transect 3, however, does not follow the trend and appears to slope gently towards the southern side even though there are no alluvial fans present on the northern edge of the wetland at this transect.
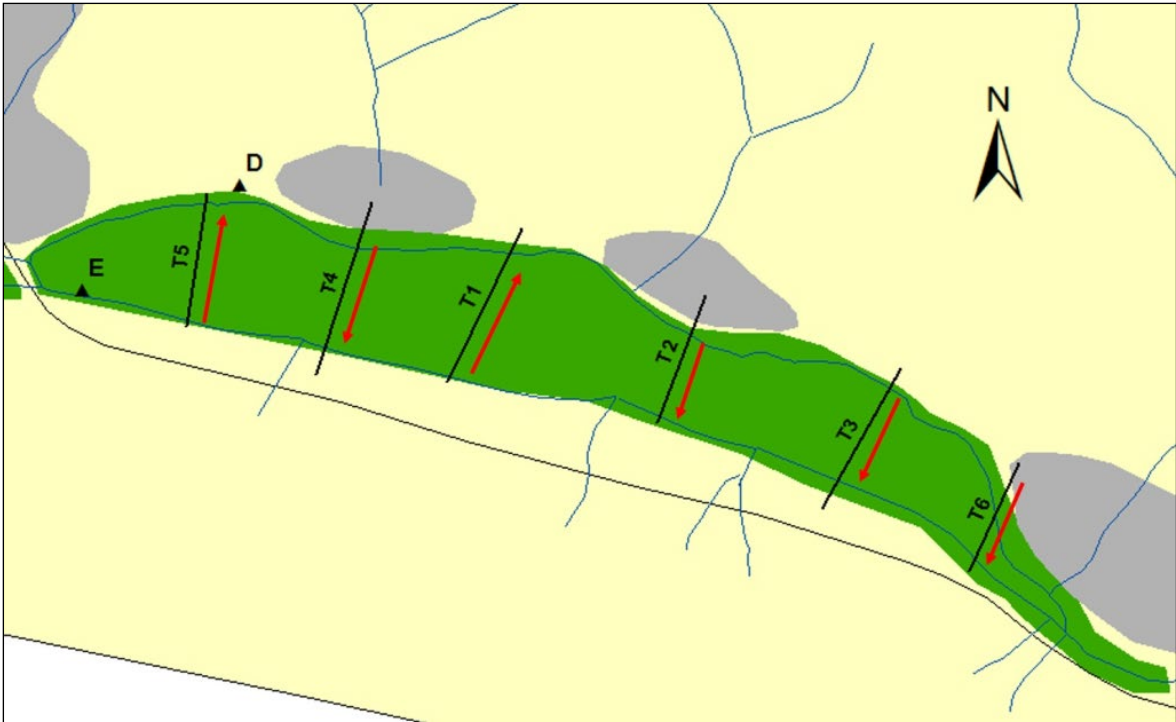
Figure 34: Direction of the slope of the water table along various transects in the Kompanjiesdrif wetland according to Lagesse (2017). The location of PZE and PZD and the alluvial fans (in grey) in relation to the wetland transects are also indicated. The direction of slope of the water table is indicated by red arrows

Figure 35: Proposed subsurface flow directions at the Kompanjiesdrif wetland with water levels measured in May 2018

Figure 35 illustrates the subsurface water levels measured in May 2018 for the piezometers at the Kompanjiesdrif wetland (illustrating that PZD has a lower water level than the wetland). The probable subsurface flow directions (based on field observations and water level data) are also illustrated. The observed water level data and the directions of slope of the water table described by Lagesse (2017) indicate that as subsurface water enters the Kompanjiesdrif wetland, it appears to flow towards (and recharge) PZD (representing the valley-bottom areas between the alluvial fans) and then flow down-stream. According to these water levels, it appears as though the alluvial fans recharge the wetland and the wetland recharges the valley-bottom alluvium between the fans.

Water quality of piezometers at the Kompanjiesdrif wetland

The EC and chloride content of PZA, PZC and PZD are higher than those of the tributary, river samples and PZE in the wetland at Kompanjiesdrif. PZD has a significantly higher EC and chloride content than the other piezometers and surface water samples (Figure 36).

The very high EC value reported for PZD correlates with the ERT results described in Section 4.1.2 (located off the alluvial fan in shale/clayey material with a low resistivity and high conductivity). The very high EC and chloride content of PZD in comparison to the others can only be explained by its location in shale/clay-rich material (with a high salt content), the fact that it is located off the alluvial fans in material with a lower transmissivity (recharged slower), and is subjected to higher evaporation.
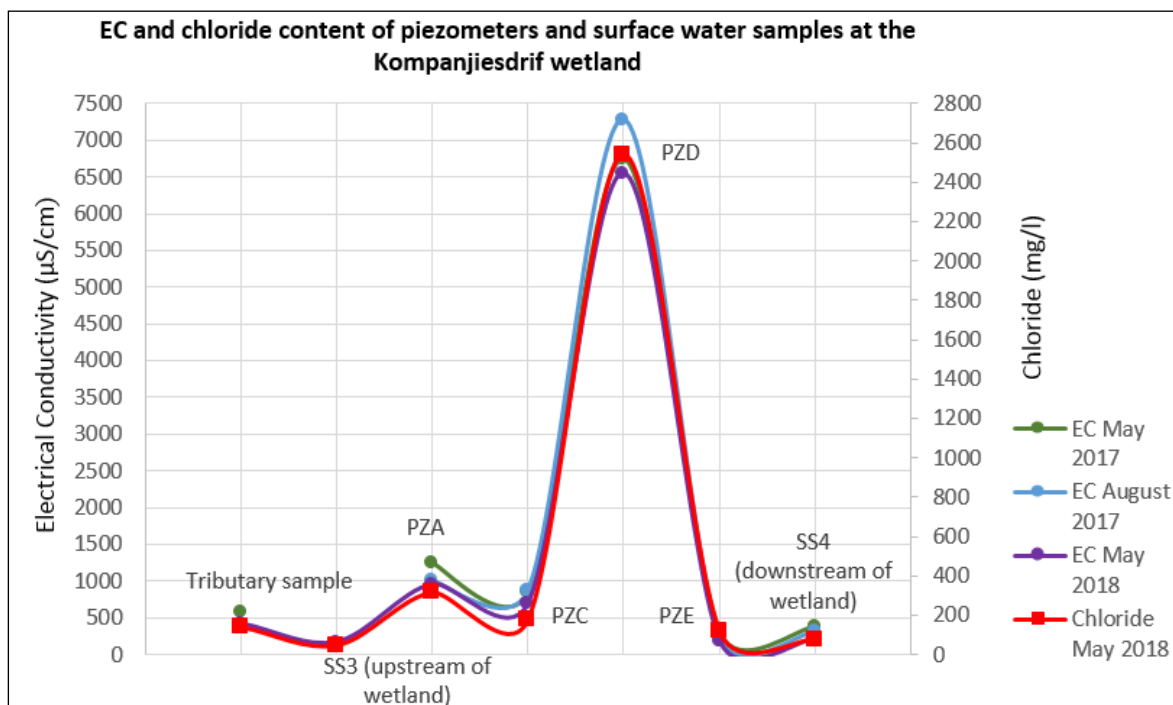
Figure 36: EC and chloride content of piezometer and surface water samples at the Kompanjiesdrif wetland

5 AIM 2: IDENTIFY THE RELATIONSHIP BETWEEN WETLANDS AND THE HYDRO-LOGICAL FUNCTIONING OF THE CATCHMENT

Two models were set up to test hypotheses of hydrological functioning in the upper Krom catchment palmiet wetlands. The modified Pitman model (Hughes, 2013) was set up together with a wetland sub-model (Hughes et al., 2014) and an MCM (Adar, 1996). Although we originally envisaged using the modified Pitman model together with the MIKE-SHE model, the lack of flow data in the catchment due to the severe drought meant there was too little calibration information with which to interrogate wetland functioning. As a result, it was decided to apply an MCM that used the water quality and isotope information and could identify the source contributions to the wetlands.

5.1 Hydrological Modelling of the Krom River Valley and Palmiet Wetlands

The Pitman model was set up using local climate data from a weather station run by DuToit fruit farmers, located 13 km away from the study site. The weather station measured hourly rainfall, temperature, relative humidity, solar radiation and wind speed. The Penman-Monteith equation was used to produce a time series of potential evapotranspiration (PET). The weather station has been recording climate information since 25 May 2011 and compared well with daily rainfall measurements obtained from farmers within the study site. A comparison of the DuToit PET and the PET from the WR2012 database (for the whole K90A catchment) is shown in Figure 37.
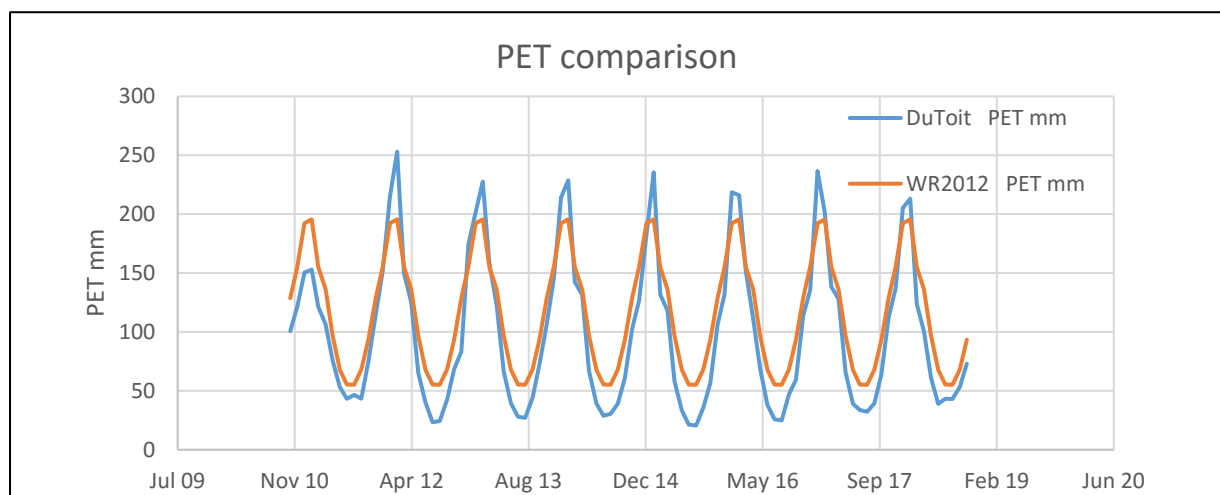
Figure 37: Comparison of PET between the WR2012 database and a local weather station

The Pitman model was set up in a semi-distributed manner according to the subcatchments shown in Figure 38. The subcatchments surrounding the wetlands were set up to represent a fast-responding steep rocky catchment typical of the Cape Fold Belt geology, with a significant portion of both interflow and groundwater contribution to baseflow (witnessed during the drought period) within the tributaries.

Similarly, the wetland submodel was set up to represent the wetlands as sensibly as possible; however, without adequate catchment outflow data, it was not possible to identify key hydrological information regarding wetland hydrological behaviour. It was not straightforward to determine the spill relationship (the release of water from the wetland) without observed data. Therefore, the model was set up to represent spill as we envisaged from our time working in the catchment. The wetland submodel was calibrated against wetland size and amount of evaporation expected from the wetland. This was based on ET from other palmiet wetlands as determined by Fruitlook data (www.fruitlook.co.za) and MODIS (Mu, Zhao & Running, 2011) (Section 2.4).

Figure 38: Subcatchments represented by the modified Pitman model

The parameters used to set up the model are given in Appendix A. The wetland parameters are provided in Table 8, with an explanation of their meaning, which is also provided in Appendix A.

Table 8: Wetland parameters

Parameters	Upper wetland	Lower wetland
Local catchment area (km^2)	1.7	0.8
Residual wetland storage (MCM)	0.6	0.25
Initial storage (MCM)	2.1	1
A in Area (m^2) = A × Volume (m^3)^B	5000	1500
B in Area (m^2) = A × Volume (m^3)^B	0.35	0.4
Channel capacity for spillage (MCM)	0	0
Channel spill factor (fraction)	1	1
AA in (Ret.Flow = AA × (Vol/RWS)^{BB})	0.2	0.2
BB in (Ret.Flow = AA × (Vol/RWS)^{BB})	0.9	0.8
Annual evaporation (mm)	1200	1200
Annual abstraction (MCM)	0	0
AA scaling factor	0	0
Max. return flow fraction (or −1)	10.95	10.95

The resulting area-volume relationship and associated wetland spill are given in Table 9. The spill from the wetland was set up to proportionally increase with flood size until the upstream inflow was moving directly over the wetland at the largest floods (100% spill).

Table 9: Wetland area-volume relationship and wetland spill as simulated in the model

Upper wetland			Lower wetland		
Volume	Area	Spill	Volume	Area	Spill
mcm	km²	mcm	mcm	km²	mcm
2.04	0.81	0.87	0.30	0.30	0.01
2.80	0.90	1.76	0.40	0.40	0.04
3.60	0.99	3.01	1.00	0.50	0.45
5.50	1.14	5.50	2.00	0.60	2.00
7.80	1.29	7.80	3.50	0.70	3.50
11.90	1.50	11.90	3.65	0.80	3.65

The downstream outflow from the Kompanjiesdrif (lower) wetland is shown in Figure 39.
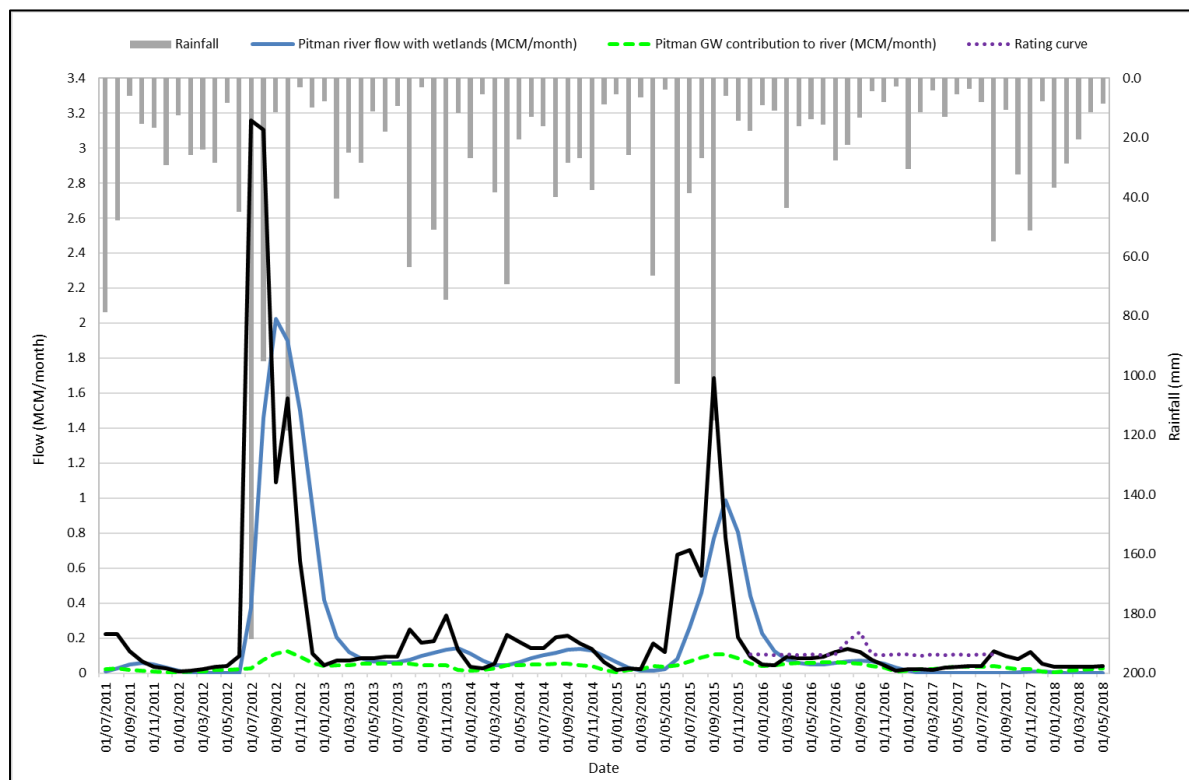
Figure 39: Pitman outflow (black without wetland and blue with wetland), groundwater contribution to the river (green) and rainfall (grey) between 2011 and 2018. Included is the limited observed flow data obtained via a pressure transducer installed in the river below the wetland, and the resulting rating curve obtained through flow measurements and the surveyed cross section

As shown in Figure 39, the model is simulating fairly significant attenuation of flows with the wetland submodel when compared with the flashy high flows, which are typical of TMG environments, shown without the wetland submodel included. The average water balance components are shown in Table 10 and Table 11.

Without further flow data, it is not possible to identify whether this is a realistic representation of wetland dynamics.

Table 10: Simulated modelled average water balance components of the wetland over the simulation period given in m^3 × 106

Variable	Upper wetland (Krugersland)	Lower wetland (Kompanjiesdrif)
Wetland inflow	0.19	0.19
Wetland outflow (spill)	0.15	0.18
Wetland evaporation	0.06	0.03
Storage volume	0.90	0.57

Table 11: Simulated modelled average contribution of groundwater and interflow to low flows in the tributaries and rivers supporting the wetland given in m^3 × 106

Variable	Upper wetland (Krugersland)	Lower wetland (Kompanjiesdrif)
Groundwater contribution to baseflow	0.03	0.009
Interflow contribution to baseflow	3.85	3.57
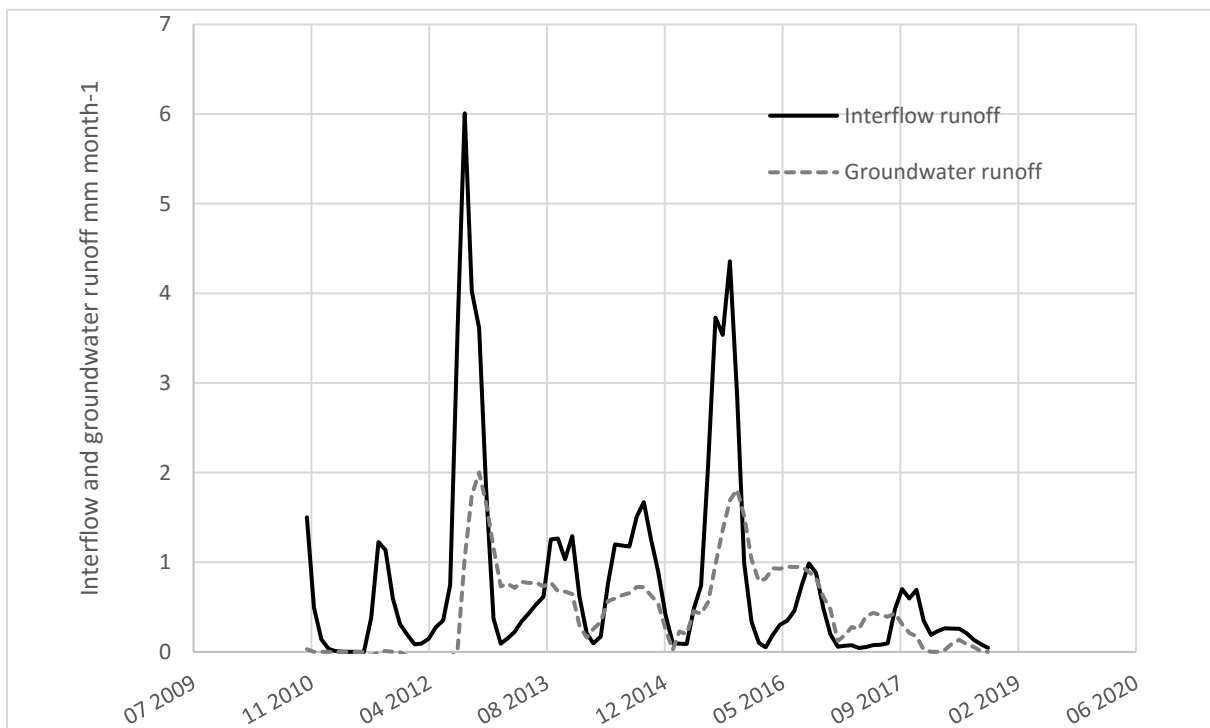
Figure 40: Interflow and groundwater contribution to baseflow in upstream tributary

The monthly average total groundwater contribution to baseflow in the catchment is 0.04 mcm·month^{-1} while the monthly average total interflow contribution to baseflow in the catchment is 7.43 mcm·month^{-1}. As expected, the simulated interflow component is higher but also more variable than the groundwater component. The interflow and groundwater component for Subcatchment 1 (the most upstream tributary) is shown in Figure 40.

Figure 41 compares the ET of the wetland with the ET of other palmiet wetlands. Comparison of ETa estimates from MOD16, Pitman model and Fruitlook for the Krom wetlands showed that the Pitman model produced the highest ETa estimates. MOD16 and Fruitlook estimates were comparable with MOD16, slightly higher than Fruitlook. The Pitman annual estimate 1205 mm/year is comparable to the ETa of 1332 mm/year, which was adopted for the Jonkershoek wetland based on comparisons of stomatal conductance of palmiet plants with other riparian plants (Rebelo, 2012). The lower MODIS values are probably due to the MODIS pixel size and the comparatively small size of the palmiet wetlands. MODIS is therefore probably not picking up the full wetland ET signal.
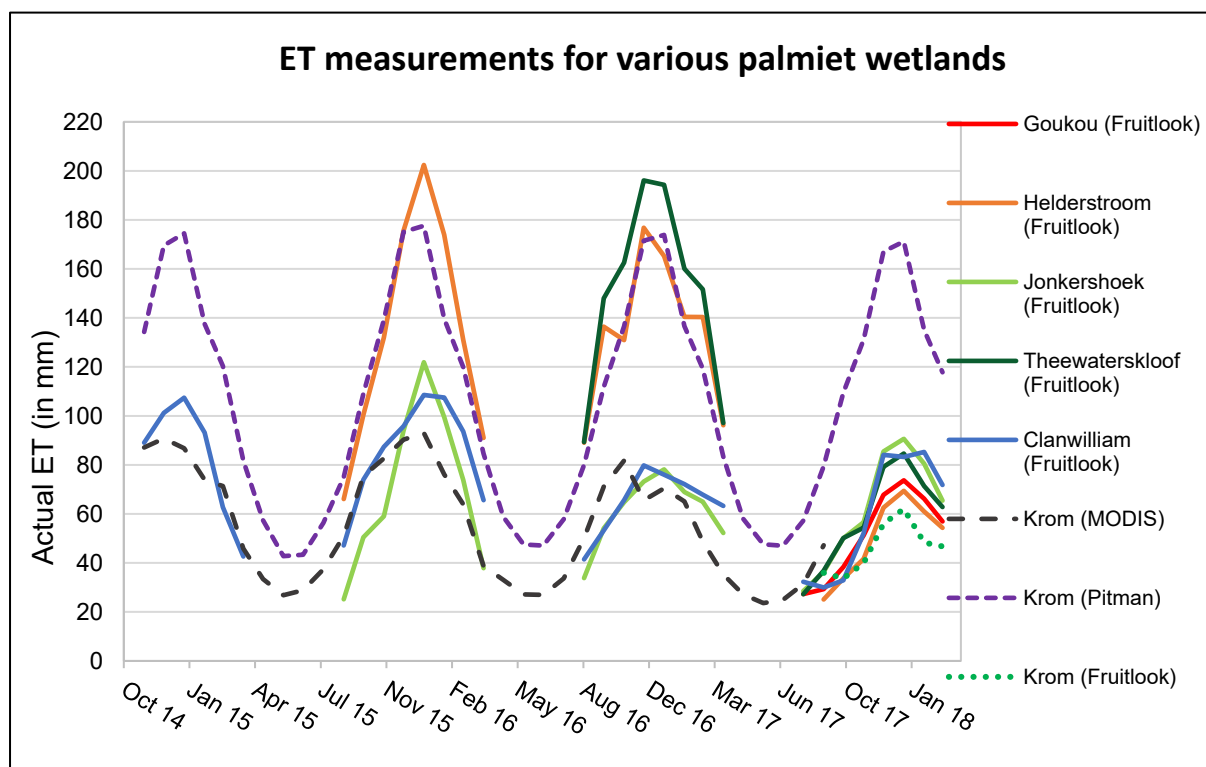
Figure 41: ETa simulated by the modified Pitman Model compared to other palmiet wetlands in the Western Cape

5.2   Simulating Source Contributions to the Wetlands Using a Mixing Cell Model

Mixing models have been used by various authors to model hydrological systems successfully (Robson & Neal, 1990; Harrington et al., 1999; Liu, Williams & Caine, 2004; Partington et al., 2011; Wilson, 2015). These models can be used to estimate the groundwater component of baseflow in a river. This has been demonstrated by Matthews (2013) who used an MCM developed by Adar (1984) to quantify the groundwater component of baseflow at a test site along the Modder River in Bloemfontein, quaternary catchments A42A, A42B and A42C in Limpopo, and quaternary catchment D73F in the Northern Cape, South Africa. Matthews (2013) validated the model by comparing results with another tracer model and baseflow separation model results.

In an MCM, the flow of mass in a system is modelled by separating the system into a number of mixing cells and then formulating a mathematical algorithm to describe flow into, out of, and within the cells (Campana, 1975). The basic principle of the MCM is that the volume of inflow into a system equals the volume of outflow for the relevant time step (Figure 42). A water balance equation is applied to each cell. A tracer concentration (for example, dissolved chemicals, stable isotope ratios, and EC) is required for each inflow included in the water balance (as well as for the cell itself). Chemical mass balance equations are developed for each cell using the available tracer data. These mass balance equations aid in restricting the water balance equation to yield more accurate estimates of the unknown inflows into the system in contrast with estimates developed using a water balance equation only (Matthews, 2013).

The MCM developed by Adar (1984) and used by Matthews (2013) was applied to this study area to quantify the amount of groundwater (and other inflows) entering and sustaining the palmiet wetlands.
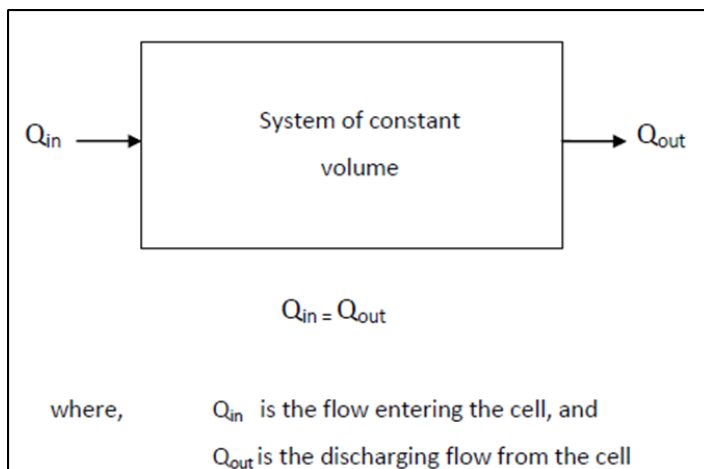
Figure 42: Illustration of the MCM concept (Matthews, 2013)

5.2.1 Setup of model

The MCM created by Adar (1984) has originally been designed to determine multiple inflow sources into aquifer(s) by dividing these aquifers into separate MCM cells. The MCM was adapted here to determine the number of groundwater inflows into the palmiet wetlands. The two palmiet wetlands were thus defined as wetland cells with various unknown inflows (groundwater and surface water) contributing to them. The MCM could not be set up for 2017 as water quality data was unavailable for certain key sampling points due to the drought. A single-cell MCM and a two-cell MCM were set up for May 2018 (using tracer data collected on 22 May 2018). Although the catchment was generally wetter, no significant rainfall was experienced in the catchment immediately prior to and over the sampling period (Figure 43).

There was no flow gauge at the outflow point of the study catchment, but a data logger (measuring changes in water height) was installed in the river at the outflow of the catchment for a limited period. The Pitman hydrological model (with wetland submodel) underestimated the river flow (or spill) at the outflow point of the wetlands during May 2018. The outflow volume was thus estimated for May 2018 using the rating curve (created using limited data from the data logger) over 2016 and 2017.
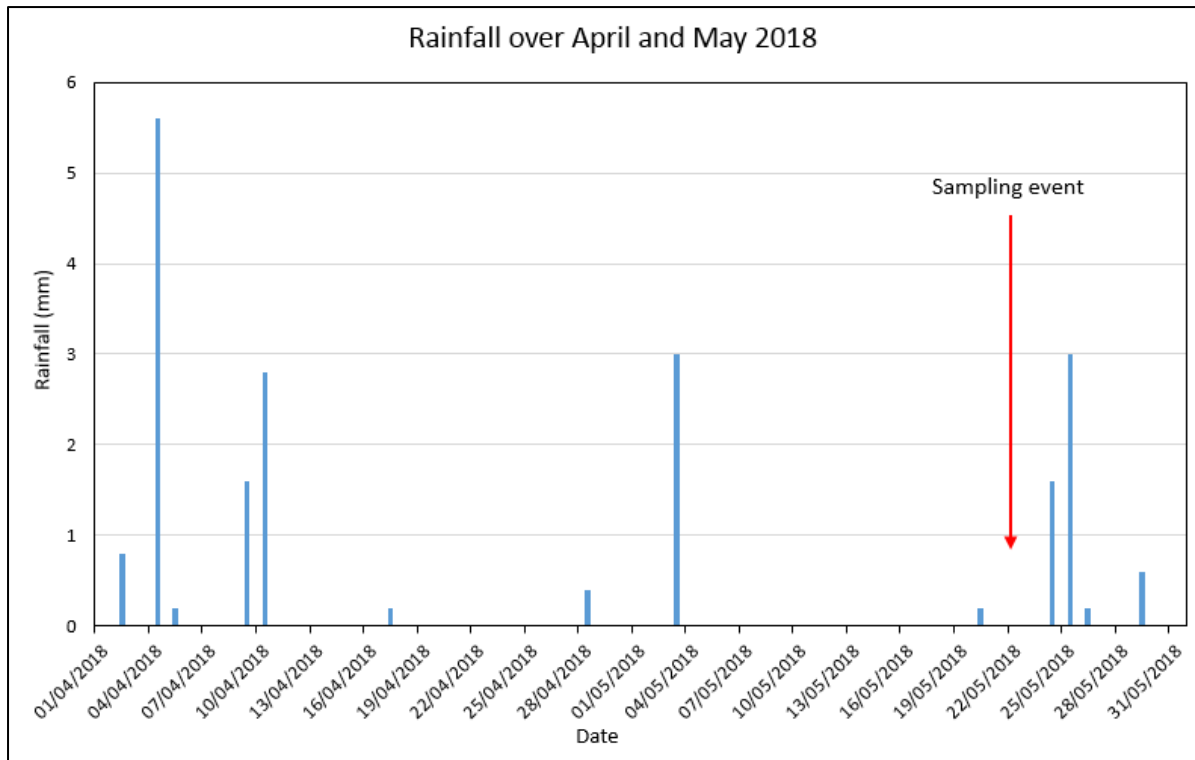
Figure 43: Rainfall for April and May 2018 for Krom River valley (from a weather station 13 km from study site)

Single-cell model

The downstream Kompanjiesdrif wetland was defined as the wetland cell in the single-cell model setup (Figure 44). The MCM software requires at least two mixing cells. Therefore, a fictitious wetland cell with exactly the same water quality data as the first cell was created. The chemistry of the wetland cell was defined using tracer concentrations obtained from the outflow point of the wetland. Inflow into the wetland was defined by tracer concentrations of the outflow point of the upstream wetland (Krugersland wetland). Tributary inflow into the wetland was defined by the tracer concentration of the main nearby large tributary that flows into the Kompanjiesdrif wetland.

Groundwater inflow into the wetland was defined by the tracer concentrations of BH1, BH2, and BH3, which were all entered separately into the model. BH1 is influenced by the Bokkeveld shale (confirmed by high EC measurements) representing diffuse groundwater flow into the wetland. Although BH2 and BH3 are located outside the study catchment, they were considered representative of the groundwater chemistry in the study area due to their location in the same geological formations (Peninsula Formation/Cederberg–Peninsula Formation contact). Shallow subsurface inflow into the wetland was defined by the tracer concentration of PZA. An ET loss volume (modelled in Pitman) for the wetland was included as an outflow volume. All tracers were given an equal weight for the model run.

44
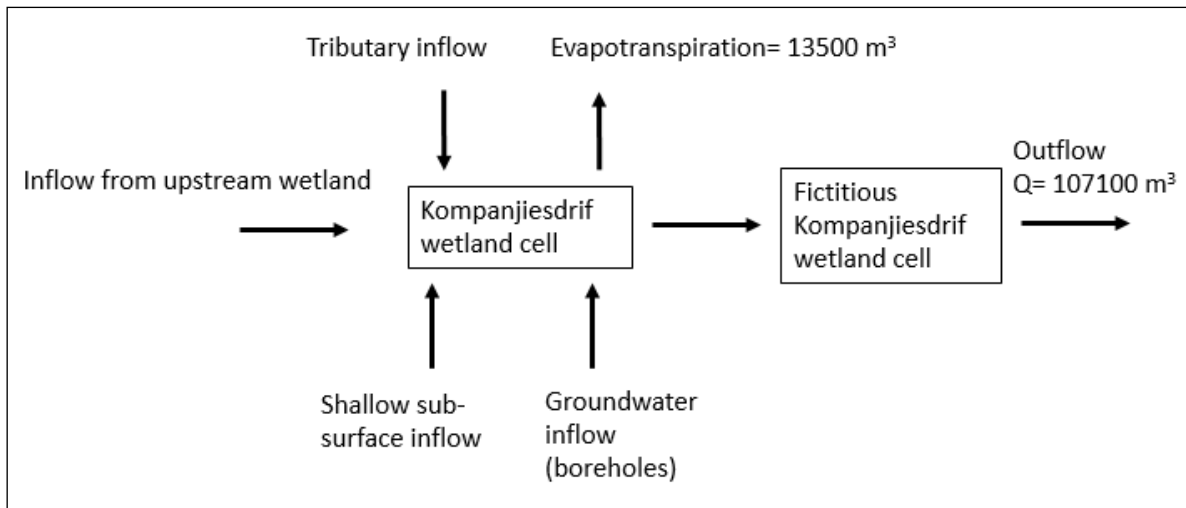
Figure 44: Single-cell model setup for the Kompanjiesdrif wetland in May 2018. Groundwater inflow (boreholes) represents three different groundwater inflows that were input separately. This includes water quality from BH1 (representing the valley-bottom Bokkeveld shale), BH2 (representing contributions from the Peninsula Formation) and BH3 (representing contributions from the Peninsula–Cederberg shale formation contact)

Two-cell model

In the two-cell model setup, the Krugersland wetland was defined as the first wetland cell (upstream). The Kompanjiesdrif wetland was defined as the second wetland cell (downstream wetland) (Figure 45). The chemistry of each wetland cell was defined using the tracer concentrations of their outflow points. Tributary inflow into the wetlands was defined using the tracer concentration of one of the main tributaries that enter the Kompanjiesdrif wetland (this tributary was also used as an inflow for the Krugersland wetland as it is considered to be generally representative of the chemistry of the tributaries in the catchment). Groundwater inflow into the wetland is defined by the tracer concentrations of BH1, BH2, and BH3. There was no shallow subsurface inflow (water quality from piezometers) volume identified when the two-cell model was first run and it was thus left off. All tracers were given an equal weighting for the model run.
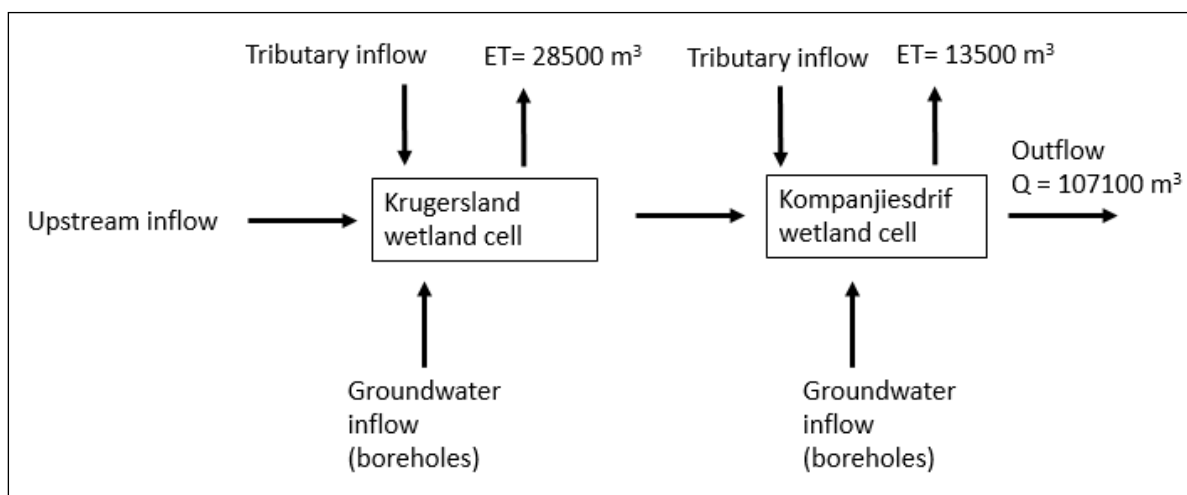
Figure 45: Two-cell model setup for the Krugersland and Kompanjiesdrif wetlands in May 2018. Groundwater inflow (boreholes) represents three different groundwater inflows that were input separately. This includes water quality from BH1 (representing the valley-bottom Bokkeveld shale), BH2 (representing contributions from the Peninsula Formation) and BH3 (representing contributions from the Peninsula-Cederberg shale formation contact)

45

Abstraction/loss volumes other than ET were excluded from the setup of the MCM. Tracers used in the model are illustrated in Table 12.

Table 12: Tracers used in the MCM

Unknown inflow or cell	pH	EC	Mg	Ca	K	Cl	Si	Al	D	O⁻¹⁸
Inflow into the Krugersland wetland	6.34	124.00	3.00	0.00	0.60	42.30	2.63	0.00	−23.09	−5.24
BH1 (groundwater)	6.21	1149.00	27.00	13.60	3.30	298.00	12.66	0.05	−33.74	−6.21
Tributary	6.37	419.00	10.00	6.00	1.80	140.00	4.03	0.38	−30.72	−6.21
Wetland 1 cell (Krugersland)	6.46	169.40	5.00	0.80	0.40	47.10	5.63	0.03	−19.90	−4.69
Wetland 2 cell (Kompanjiesdrif)	7.38	212.30	7.00	0.80	1.00	78.40	5.63	0.02	−21.25	−4.88
Wetland 2 cell (Fictitious cell)	7.38	212.30	7.00	0.80	1.00	78.40	5.63	0.02	−21.25	−4.88
PZA	6.05	955.00	47.00	23.60	6.90	315.00	15.95	1.10	−28.57	−5.76
BH2 (groundwater)	5.46	174.00	5.00	0.00	0.00	61.20	3.94	0.00	−33.95	−6.74
BH3 (groundwater)	5.92	258.00	9.00	1.20	2.80	76.20	9.38	0.00	−37.19	−6.89

We decided to first set up a single-cell model for the Kompanjiesdrif wetland as the MCM manual recommended that a single-cell model be used as a preliminary assessment before a more complex multi-cell model is set up (Adar & Kuells, n.d.).

5.2.2 Results

Single-cell model

The MCM flow results (unknown inflow volumes and percentages) for the single-cell model setup for the lower wetland (Kompanjiesdrif) are illustrated in Table 13 and Figure 46. The water balance error is 2.61% and average chemical mass balance error is −3.8%. These errors are within the acceptable range as described in the MCM manual (< 15 –20%). The 2.61% water balance error indicates that there is more water flowing out of the system than flowing in from known sources, which indicates that there are additional unidentified water sources not accounted for.

According to the single-cell run of the MCM, inflow from the upstream wetland contributes 67% of the total inflow into the Kompanjiesdrif wetland and groundwater contributes 33% of the total inflow (defined by BH1, BH2, and BH3). The upstream inflow is expected to consist of a mixture of surface water and groundwater. Shallow subsurface inflow (defined by the tracer concentrations of PZA) is 0%. This is interesting as it is evident that there is subsurface flow moving through preferential flow paths in the alluvial fan material to the wetland. The fact that PZA is not situated on the main trunk stream entering the wetland through the alluvial fan, and therefore within alluvium with low transmissivity, could be an explanation.

Also surprisingly, the tributary inflow (considered to be mostly groundwater during May 2018), based on isotope data and the lack of rainfall in the catchment) is 0%. The contribution from this tributary is

expected to be high as it flowed continuously during the drought and is one of the larger tributaries entering the wetland. The water quality of this tributary is thought to be a good representative sample for the general water quality of all tributaries entering the wetland (as it is situated in the same geology as the other main tributaries). However, the MCM indicates that it is not necessarily a good representative sample and only additional sampling of the other tributaries in the catchment would confirm this. Also, the tributary has been subjected to evaporation, which would alter its chemistry. Ideally, the sampling point should be at the source of the tributary where it first emerges from the aquifer. In this case, it was not possible to access the headwaters of the tributary to access more suitable seepage points.

The groundwater flow into the system is unusual since it becomes surface flow prior to reaching the wetlands. And it could be that the unusual way the groundwater system works is not able to be captured by the model, which instead recognises a groundwater contribution through BH2 and BH3 (which according to the water chemistry is quite similar to the tributary). The 0.4% inflow indicated for BH1 (located within Bokkeveld shale/Nardouw-Bokkeveld shale contact) is probably contributed via diffuse groundwater discharge into the wetland through the Bokkeveld aquitard. We hypothesise that the large groundwater contribution (32.6%) from BH2 and BH3 would enter the wetland via tributaries from springs higher up in the Peninsula Formation/Cederberg-Peninsula Formation contacts of the catchment.

The modified Pitman model estimates a groundwater contribution to the river (or wetland) for May 2018 of 5200 m^3, which is approximately seven times smaller than the groundwater contribution estimated by MCM as 38 797 m^3. The groundwater quantity estimated here by the MCM includes all groundwater contributions into the wetland from upstream sources and tributaries.

Table 13: May 2018 single-cell MCM results for unknown inflows

Name of inflow	Inflow volume (m^3/month)
Upstream inflow	78 659
Tributary inflow	0
Shallow subsurface inflow	0
BH1 (shale influenced groundwater)	496
BH2 and BH3 (sandstone influenced groundwater)	38 301
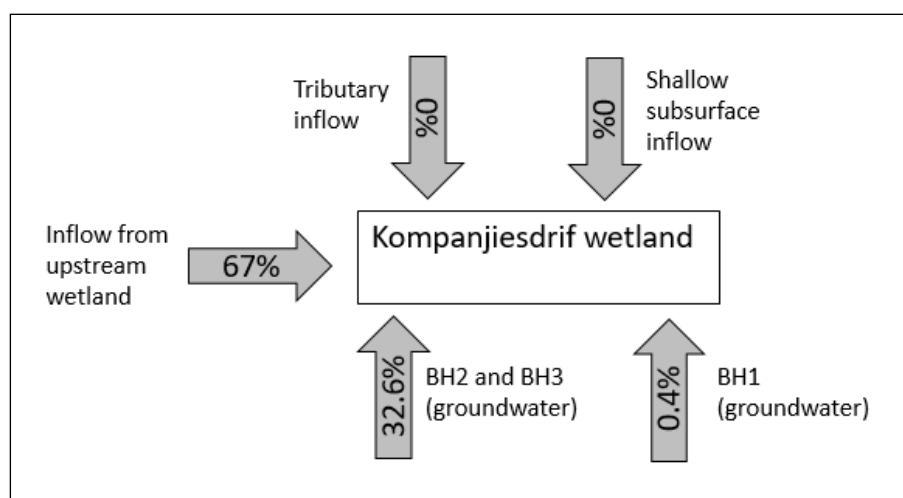
Figure 46: Inflow percentages determined by the MCM for the single-cell model

Two-cell model

The MCM flow results (unknown inflow volumes and percentages) for the two-cell model are illustrated in We tried different model runs by excluding and including certain inflows and ultimately the model always picked up a large contribution from BH2 and BH3 and no or little contribution from the tributary.

The MCM groundwater contribution results are generally significantly higher than the Pitman ground-water contribution volumes. The MCM cannot, however, be compared accurately with Pitman as Pitman simulates the groundwater contribution differently, i.e. the groundwater transitions into surface water prior to reaching the wetlands. The MCM can be seen as giving a more accurate estimate of ground-water contribution than Pitman. It is surprising that the two-cell model estimates a larger groundwater contribution to the Kompanjiesdrif wetland than the single-cell model. This highlights the uncertainty of the MCM. The two-cell model is a more realistic representation of the system, and gives the model a larger volume of water to work with, which could explain the different volumes. The single-cell model does, however, have a lower water balance error and thus theoretically could be considered to be slightly more accurate. Despite these uncertainties, the results from the MCM show that the ground-water contribution to the palmiet wetlands is significant and forms a large component of the wetland water balance.

Table 14 and Figure 47. The water balance error for the two-cell model is higher than the single-cell model at 13.89% and the average chemical mass balance error is −2.24%. These errors are still within the acceptable range as described in the MCM manual (< 15–20%). The 13.89% water balance error once again indicates that there are potentially additional unknown inflow sources into the wetlands that are not accounted for.

Upstream inflow into the Krugersland wetland accounts for 19.1% of the total inflow. The two-cell model does yield a contribution from the tributary (of 3.6 and 2.8% respectively), although this contribution is smaller than expected, but the fact that the model picks up a contribution indicates that the tributary is a source. As discussed above, there could be various reasons for the contribution being smaller than expected.

Groundwater inflow into the Krugersland wetland accounts for 18.1% of the total inflow and groundwater inflow into the Kompanjiesdrif wetland accounts for 56.4% of the total inflow. Inflow from BH1 would enter the wetlands as diffuse groundwater discharge, whereas the other groundwater inflow (BH2 and BH3) would likely enter the wetlands via tributaries.

The flow between the wetland cells (from Krugersland to Kompanjiesdrif) is calculated to be 32 224 m^3. The groundwater contribution to the Kompanjiesdrif wetland is 72 394 m^3 (higher than what was estimated in the single-cell model) and to the Krugersland wetland is 23 317 m^3. The groundwater contribution to the Krugersland wetland is similar to that estimated in Pitman of 20 600 m^3. The smaller tributary inflows (4562 m^3 and 3582 m^3 respectively) would likely mostly comprise groundwater and interflow. We tried different model runs by excluding and including certain inflows and ultimately the model always picked up a large contribution from BH2 and BH3 and no or little contribution from the tributary.

The MCM groundwater contribution results are generally significantly higher than the Pitman ground-water contribution volumes. The MCM cannot, however, be compared accurately with Pitman as Pitman simulates the groundwater contribution differently, i.e. the groundwater transitions into surface water prior to reaching the wetlands. The MCM can be seen as giving a more accurate estimate of ground-water contribution than Pitman. It is surprising that the two-cell model estimates a larger groundwater contribution to the Kompanjiesdrif wetland than the single-cell model. This highlights the uncertainty of

the MCM. The two-cell model is a more realistic representation of the system, and gives the model a larger volume of water to work with, which could explain the different volumes. The single-cell model does, however, have a lower water balance error and thus theoretically could be considered to be slightly more accurate. Despite these uncertainties, the results from the MCM show that the ground-water contribution to the palmiet wetlands is significant and forms a large component of the wetland water balance.

Table 14: May 2018 two-cell MCM results for unknown inflows

Cell	Name of inflow	Inflow volume (m³/month)
Cell 1 – Krugersland wetland	Upstream inflow	24 531
	Tributary inflow	4 562
	BH1 (groundwater)	1 399
	BH2 and BH3 (groundwater)	21 918
Cell 2 – Kompanjiesdrif wetland	Tributary inflow	3 583
	BH1 (groundwater)	1 239
	BH2 and BH3 (groundwater)	71 155
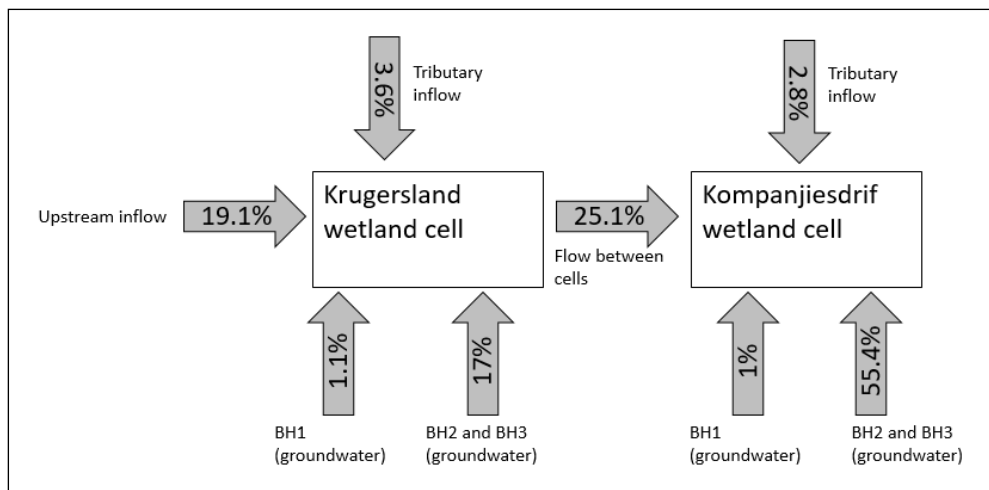
Figure 47: Inflow percentages determined by the MCM for the two-cell model

6 AIM 3: DETERMINE WHETHER WETLAND DEGRADATION IS AFFECTING THE HYDROLOGICAL INTEGRITY OF THE RIVER

6.1 Hydrodynamic Characteristics of the Krom Valley

Based on the observations of Pulley et al. (2018) who identified that most wetland gullies are linked with tributary alluvial fan deposit effects, Schlegel (2017) examined variations in hydrodynamic characteristics for a range of discharges. The investigation focused on the Kompanjiesdrif basin (around 250 m wide), which is confined in a downstream direction to a width of less than 50 m by a combination of a large impinging left bank alluvial fan that coincides with a resistant sandstone bedrock lithology. Schlegel (2017) used a two-dimensional raster-based flood inundation model, namely, Caesar-Lisflood, and a one-dimensional hydraulic analysis model, namely, Hydrological Engineering Center River Analysis System (HEC-RAS), to simulate different parameters associated with variations in discharge, including flow velocity, water depth, and stream power (using field measurements of surveyed data, river flow rates, measured wetland extent and vegetation measurements). Schlegel (2017) aimed to improve understanding of the hydraulic characteristics that promote the formation of gullies in the wetland.

This study demonstrated that variations in key hydraulic features (i.e. discharge, velocity, water depth, and stream power) are crucial in the spatial variations of gully initiation. In addition, alluvial fan deposits strongly influence the patterns of variation in hydraulic features by reducing the width of the wetland and increasing the slope downstream of the node of tributary fan deposition (Figure 48).
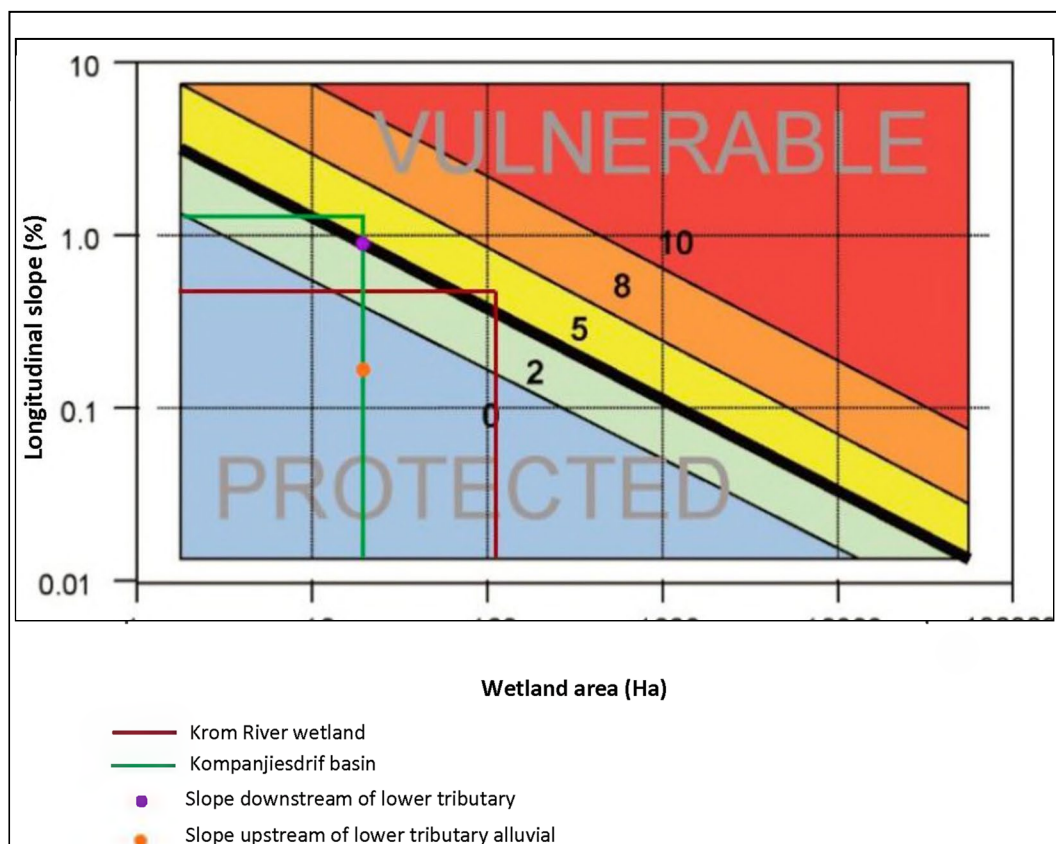
Figure 48: Wetland vulnerability to erosion graph depicting the Krom River wetland complex, Kompanjiesdrif basin, the slope downstream and upstream of the lower tributary alluvial fan (Ellery et al., 2009; Schlegel, 2017)

Stream flow characteristics, channel geometry, and basin features are inherently linked. The structural control that alluvial fans have on the Kompanjiesdrif basin wetland plays an important role in the distribution of velocity and water depth within the wetland, which results in the processes of erosion. Schlegel (2017) used Hjulstrom's diagram (Figure 49) together with the modelling results to show that the most common particle size (fine to medium sand) found in the basin can be lifted, transported and, therefore, eroded by velocities greater than 0.03 m·s⁻¹. Figure 50 shows the zones of potential erosion according to Hjulstrom's critical erosion velocity curve in the Kompanjiesdrif wetland. According to the modelled results, the most crucial of these zones occur where the valley is pinched by an alluvial fan, which has significantly reduced the width of the valley and increased the slope in the downstream direction.
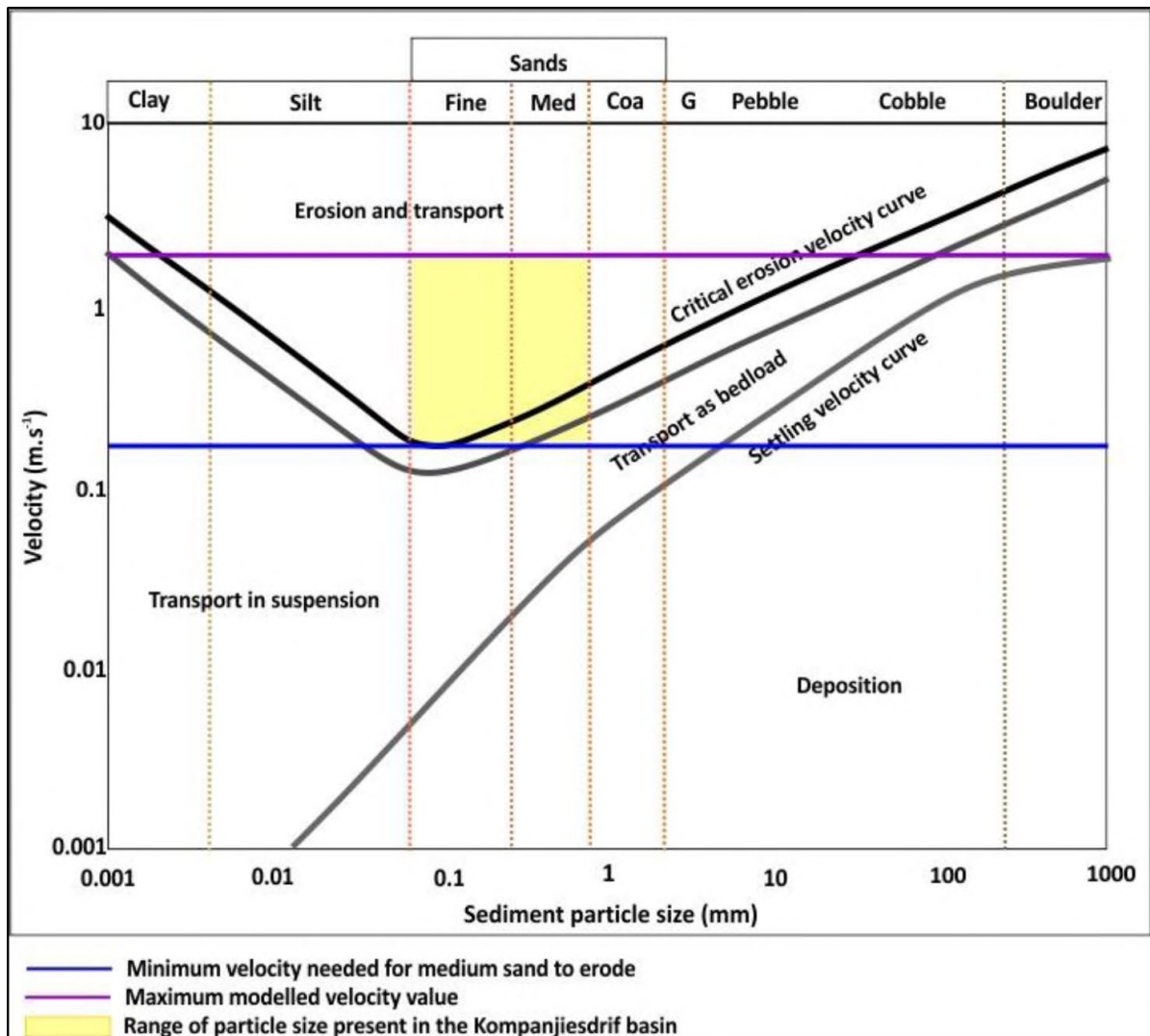
Figure 49: Hjulstrom's diagram illustrating the minimum velocity (blue line) required for medium sand to be eroded and the maximum modelled velocity (purple line) (Schlegel, 2017)
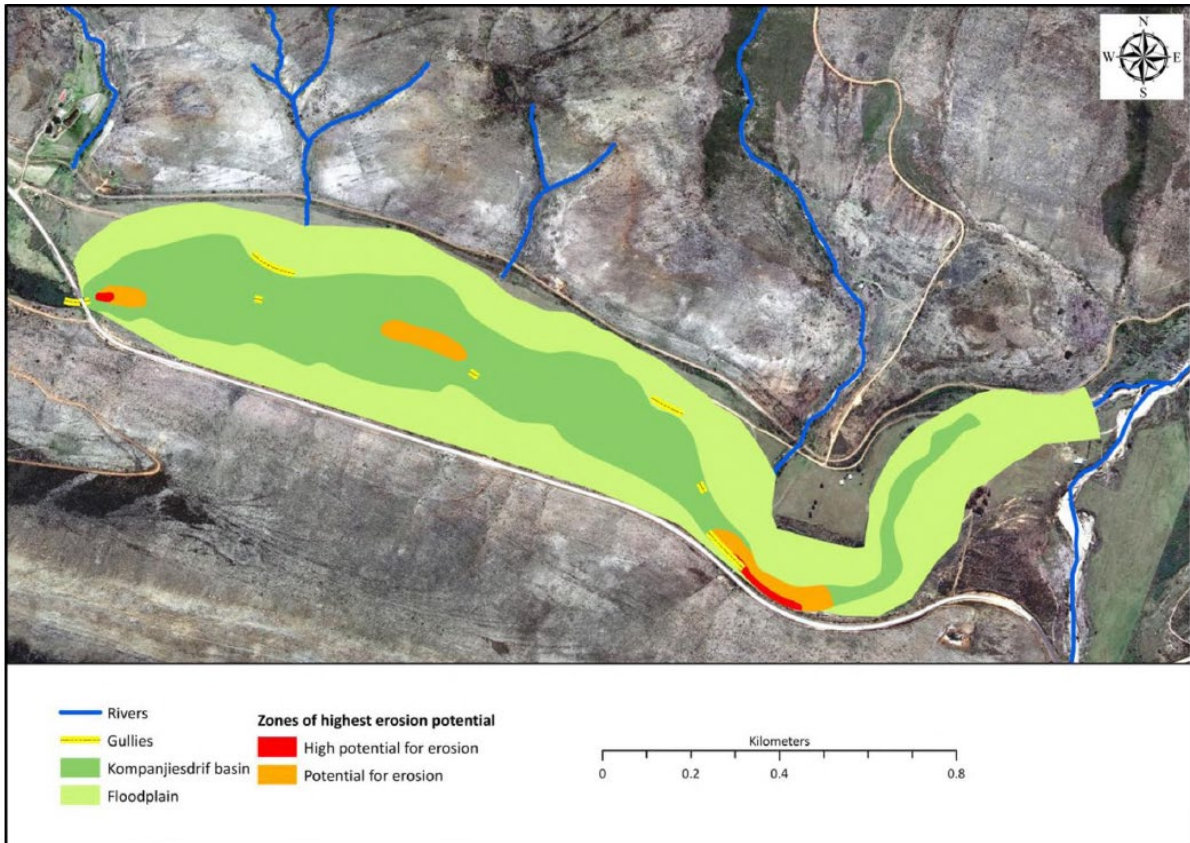
Figure 50: Zones of potential erosion in the Kompanjiesdrif basin in relation to the location of current gullies (Schlegel, 2017)

Schlegel (2017) presented a conceptual model (Figure 51) that relates to the presence of a broad near-flat valley with a gentle longitudinal slope. The first process in gully initiation is the delivery of sediment at the toe of the wetland basin to the valley floor by a large tributary alluvial fan (Figure 51B). This sediment deposit from a large, steep tributary stream pinches the valley floor and significantly decreases the width of the wetland (from approximately 350 m to 50 m). Schlegel (2017) identified that a reduction in cross-sectional width results in increased water depth, leading to increased velocity for a given discharge in the confined section. Eventually, the retarding effects of vegetation are overwhelmed as the floodwaters flatten the vegetation, initiating erosion (Figure 51C).

In summary, we concluded that the effect of impinging alluvial fans on hydraulic characteristics, such as flow velocity, water depth, and stream power, may lead to the initiation of gullies within the Krom River wetland.
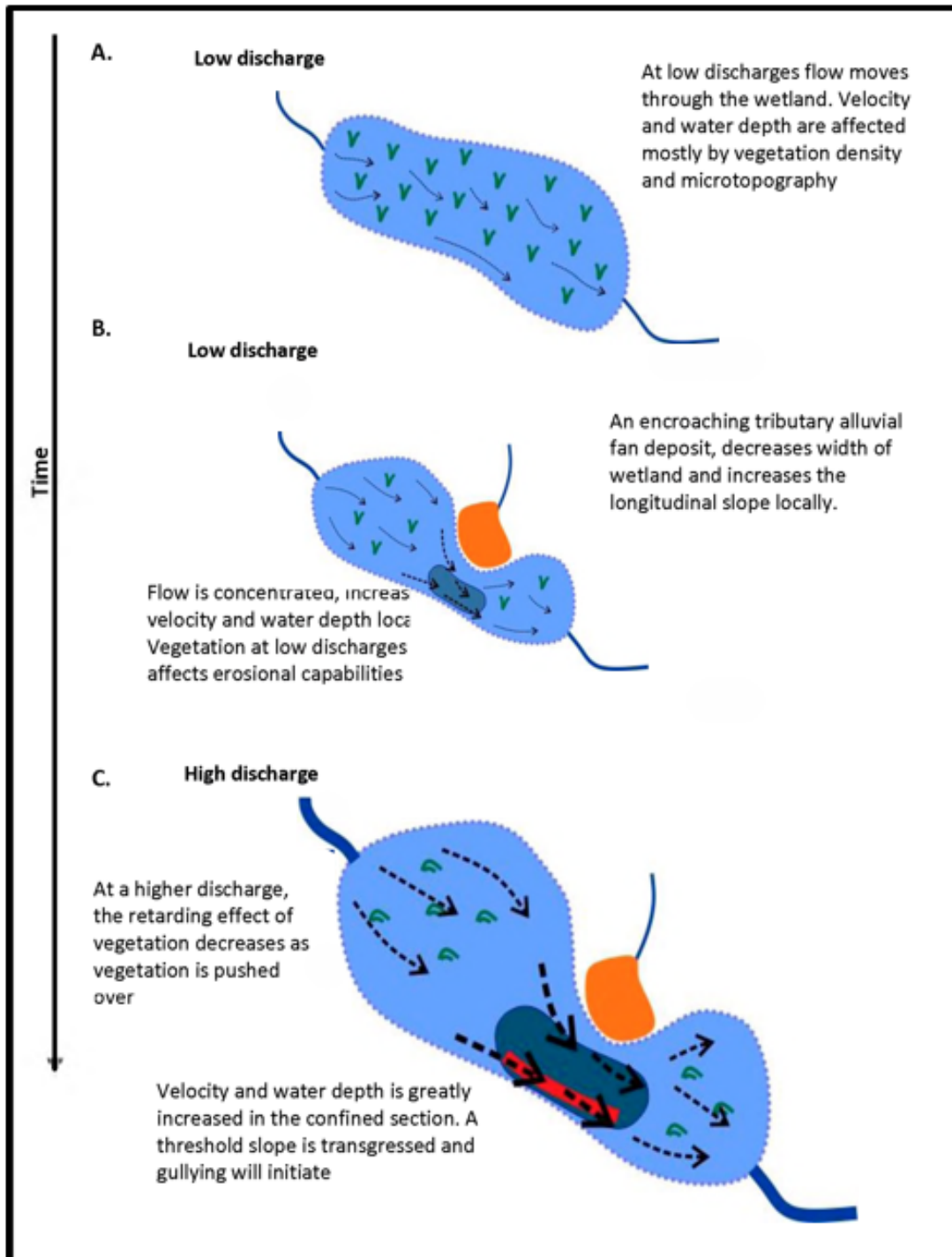
Figure 51: Conceptual model of how gully erosion may be initiated due to width reduction and localised slope steepening (Schlegel, 2017)

6.2 Gully Erosion As a Mechanism for Wetland Formation

Although this project focused on the hydrological functioning of palmiet wetlands, it is apparent that the hydrological functioning of palmiet wetlands is closely linked to geomorphological characteristics of the wetlands within the TMG.

Intensive gully erosion is common in palmiet peatlands (Job, 2014). While various authors attribute gully erosion in palmiet wetlands to human impacts, recent studies of the Krom River palmiet wetlands in the Eastern Cape by Lagesse (2017), Schlegel (2017) and Pulley et al. (2018) indicated that gully erosion may be a natural part of palmiet wetland functioning, and that human impacts only speed up this natural process. According to Pulley et al. (2018), gullying forms an essential function in terms of removing excess sediment that builds up within the wetlands, particularly due to commonly found alluvial fans constricting wetland extent in the Cape Fold Belt region. This erosion is deposited downstream, laterally flattening the valley bottom and decreasing the longitudinal slope, forming an environment fit for wetland formation downstream of the erosion point.

Gully erosion is commonly attributed to poor land management in South Africa. However, a number of studies have identified gullies which pre-date the introduction of European farming methods (Keen-Zebert et al., 2013; Lyons, Tooth & Duller, 2013; Pulley et al., 2018). Pulley et al. (2018) discuss how gully erosion forms part of the natural cut-and-fill cycles which are controlled by a number of different intrinsic and extrinsic factors.

According to Ellery et al. (2009), valley-bottom wetlands (such as those in the Krom River) are especially vulnerable to gully erosion. This is due to continuous accumulation of sediment in the wetlands, which produces a steep longitudinal slope. Erosion may be caused by human activity (for example, by confining flow when pipe culverts are placed beneath a road), but it may also take place naturally when "*the surface of a wetland is steepened longitudinally by prolonged sedimentation and ultimately exceeds a critical threshold of slope stability*" (Ellery et al., 2009:52). In the Kompanjiesdrif wetland, four gullies are located in the centre of the wetland opposite alluvial fans and are between 5.0 m and 8.2 m deep (Figure 52). Two gullies filled with sediment are also located on the alluvial fans. The age of the gullies is between 470 to 7060 YBP (pre-dating late eighteenth century European farming).
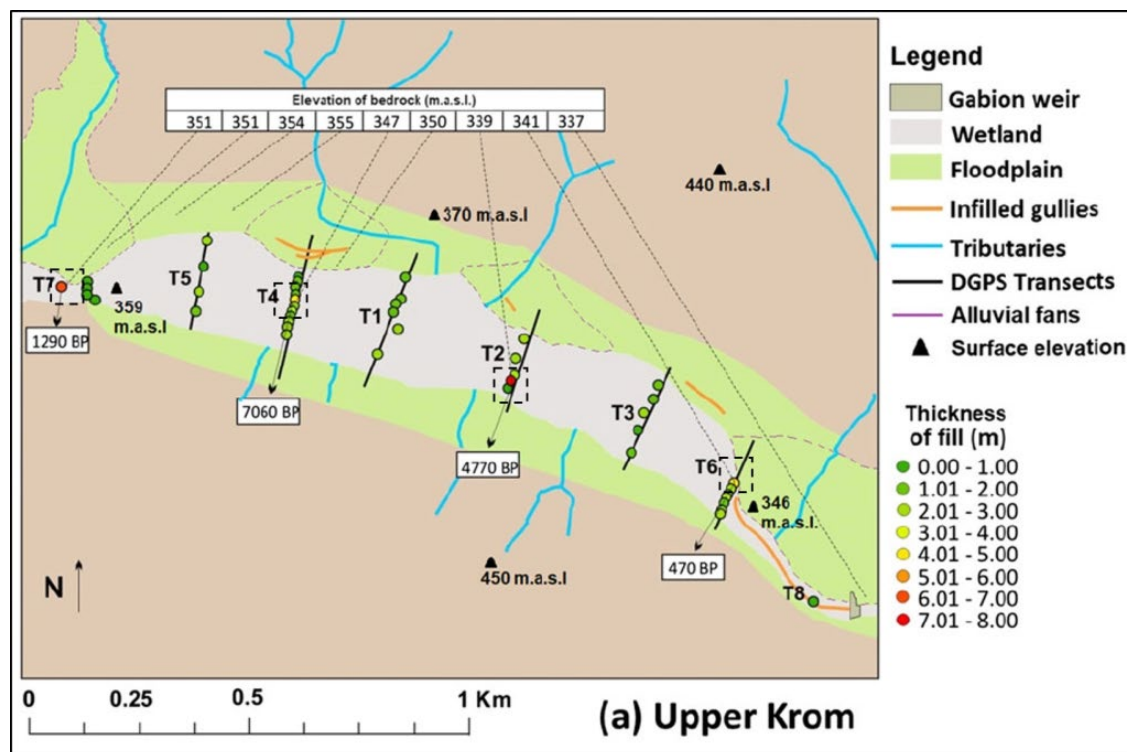
Figure 52: Age and thickness of infilled gullies in the Kompanjiesdrif wetland. Gullies in the wetland are smaller than the ones outside the wetland and are indicated by black stippled boxes. They are located in the deeper holes (Pulley et al., 2018)

According to Pulley et al. (2018:1762), when localised clastic sediment is deposited into the wetland, it results in a steeper longitudinal slope. This factor combined with the fact that alluvial fans also narrow the valley, focusing flows, enhances the probability that the "*threshold of land surface stability will be exceeded*" and gully erosion could begin (Figure 53). The bed of the gullies usually have a smaller slope than the wetland surface. Sediment deposited as a result of this erosion shapes the land surface to a slope closer to the river's regional slope. This gentler slope provides ideal conditions for wetland formation. Human factors such as poor land management or the presence of alien invasive vegetation can increase natural gully formation along the Krom River, but Pulley et al. (2018) showed that this gully erosion could also be caused by intrinsic factors.
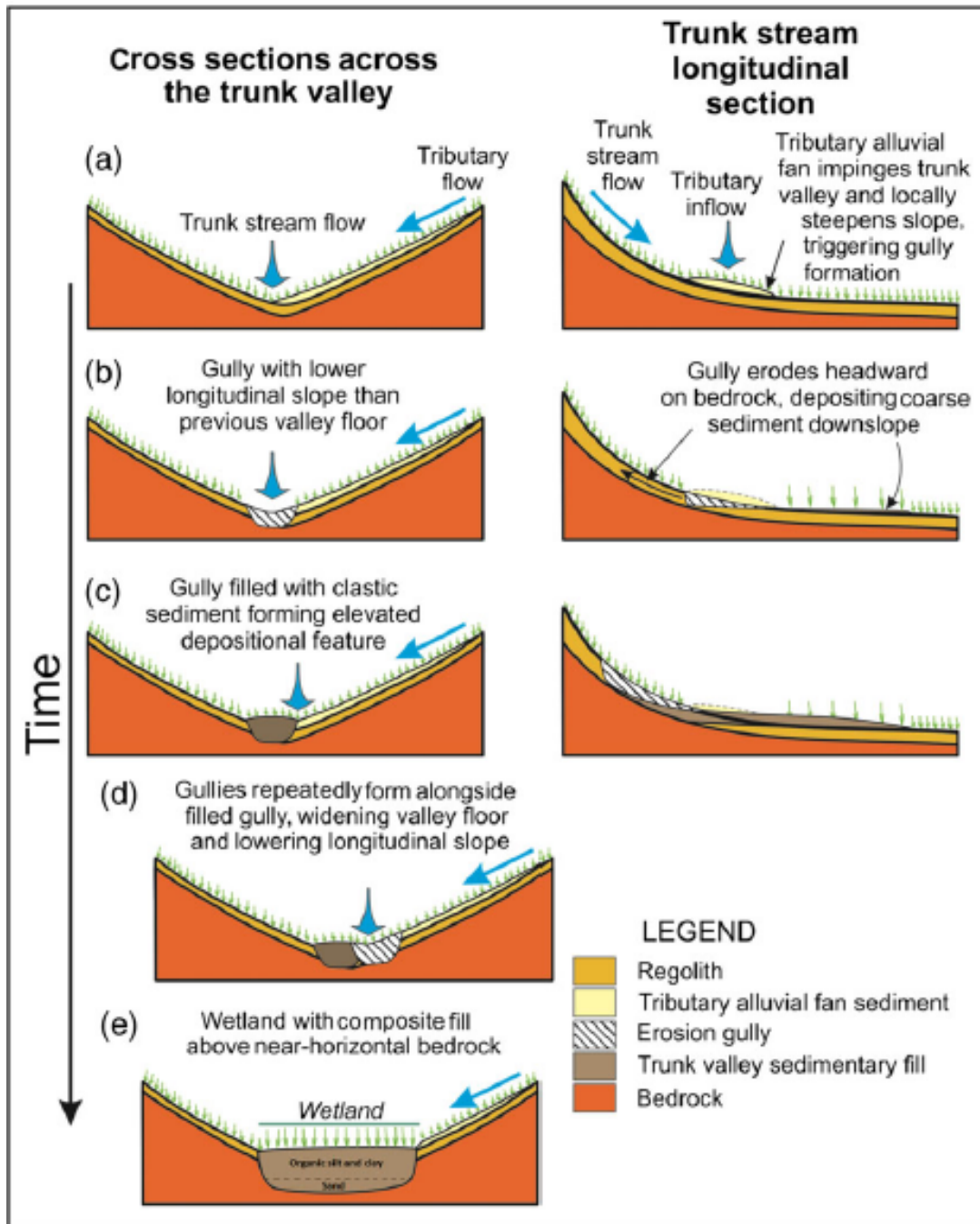
Figure 53: Diagram illustrating wetland formation by gully erosion (Pulley et al., 2018)

The regional slope along the Krom River is 0.35%; however, the longitudinal slope of the Kompanjiesdrif wetland is 1.02% (Figure 54a), illustrating the steepness of this erosional reach compared with the regional slope. The bedrock underneath the wetland has a slope of 0.85%. Gully incision causes the slope of the bedrock to decrease in comparison to the surface of the wetland (base of the gully has a slope of 0.18%) (Figure 54b). The gradient of the depositional reach downstream is higher than the gradient of the gully bed located immediately upstream and is closer to the regional slope (Figure 54c).
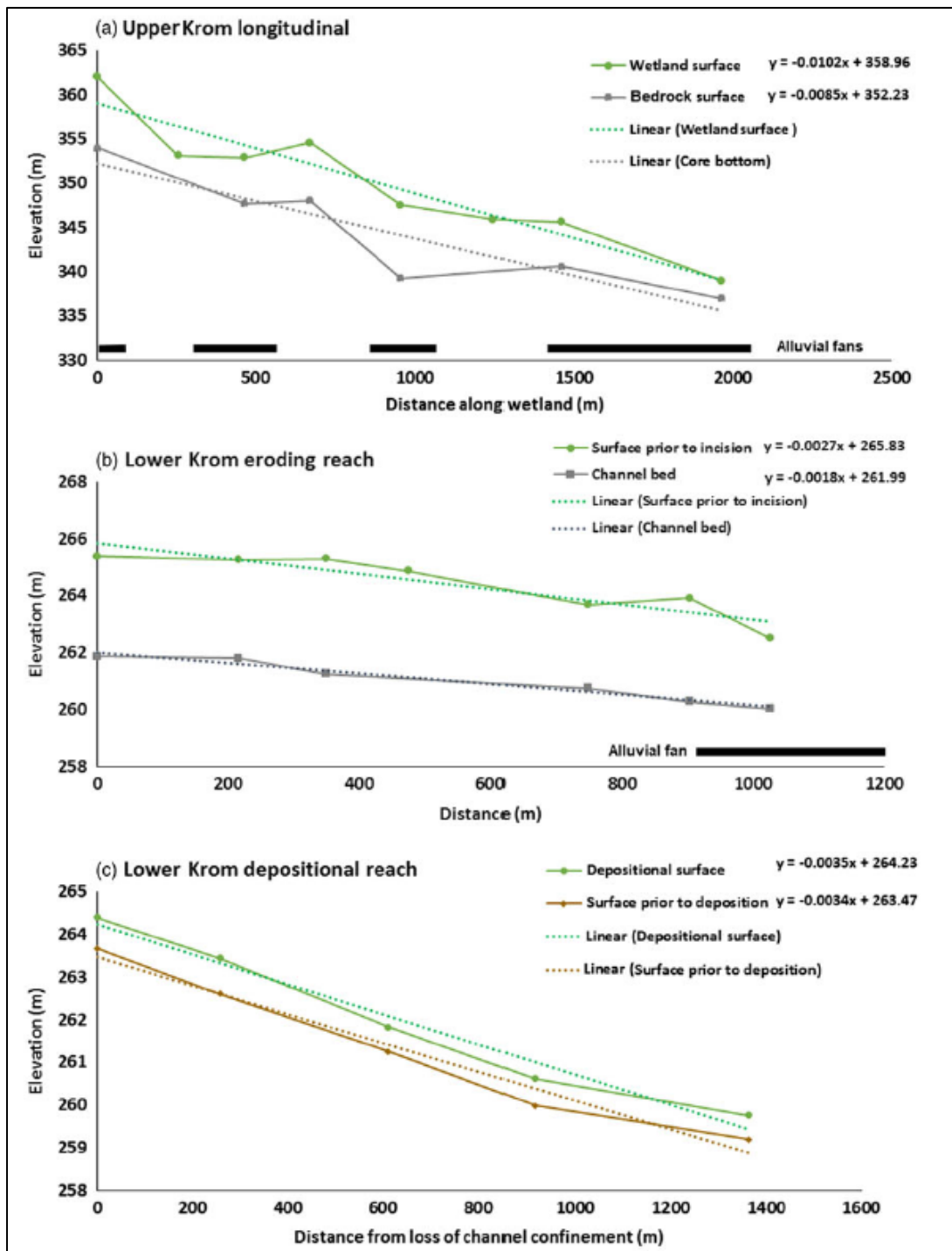
Figure 54: Change in slope along the Krom River with distance (Pulley et al., 2018)

Figure 55 illustrates the locations along the Krom River where the longitudinal slope of the wetland, the depositional reach and erosional reach were measured by Pulley et al. (2018). McNamara (2018:66) states that "*ongoing cut-and-fill cycles are the Krom Rivers' natural response to variation in water and sediment supply, and are therefore important longitudinal self-recovery processes within the system*". The structures in the Krom River are inhibiting the loss of existing palmiet wetlands, but are preventing periods of natural cutting (upstream of the structure) and filling (downstream of the structure) that cause reductions in longitudinal slope and valley widening; the conditions that are linked to the long-term re-establishment of palmiet wetlands in a more geomorphologically stable setting.

This continuous cycle of erosion and re-establishment results in little nett hydrological loss from the catchment. The local lowering of the water table in response to erosion gullies would not likely result in excessive drainage of water from the system in the longer term due to wetland re-establishment just downstream of the erosion. Rebelo, Emsens, Meire and Esler (2018) also investigated the effect of channel erosion on palmiet wetlands in the Eastern and Western Cape and found that there was no significant difference in relative groundwater depth between the degraded and pristine palmiet wetland sites.

Although this project proposes that gully erosion forms a natural part of palmiet system functioning, the loss of palmiet wetlands would have a significant impact on river systems. Palmiet wetlands provide essential sediment traps, hydrological attenuation and retention services that would impact local water users and downstream infrastructure. Restoration initiatives should therefore focus on ensuring downstream environments are kept suitable for the natural re-establishment of wetlands, and focus on softer protective infrastructures which do not completely inhibit the downstream movement of eroded sediment.

Figure 55: Locality map illustrating the locations of longitudinal slope measurements by Pulley et al. (2018)

6.3   Impacts of Erosion-control Structures and Gully Erosion on Groundwater Dynamics

De Haan (2016) mapped the water table in the vicinity of erosion-control structures (at the end of the Kompanjiesdrif wetland) and at planned erosion-control structure sites along the Krom River in order to investigate the effect that these structures as well as gully erosion have on groundwater dynamics of the Krom River. Water table elevations were measured at three sites along the Krom River using piezometers (Figure 56).

Figure 56: Sites of subsurface water level measurement through piezometers installed adjacent to erosion-control structures (at Site A) and potential structures (Site B and C)

The erosion-control structures at Site A (end of the Kompanjiesdrif wetland) caused a 7.76 m difference in surface water elevation above and below the structures. The structures elevated the water table upstream of them – increasing saturation of the wetland and promoting diffuse flow across the wetland. The flow is not concentrated into a channel but is rather spread out across the wetland. The structures also ensure flood retention – increasing the volume of water that can be retained by the palmiet wetland during high flows, cutting off-peak flows. The structures have a positive effect on water quality by decreasing the downstream sediment load. This capturing of sediment upstream, however, decreases bed load downstream. Since the implementation of the erosion-control structures at Site A in 2003 downstream of Kompanjiesdrif wetland, the main head cut has remained at the same location (has not migrated), but has widened significantly over a ten-year period.

De Haan (2016) found that the water table is significantly deeper along the eroded reaches than non-eroded reaches of the river. This is because gully erosion causes drainage of the intergully area resulting in a lowering of the water table as the gullies deepen. The water table also tends to slope towards the channel (recharging the channel). The water table along the non-eroded reaches appears to slope slightly away from the channel (groundwater discharge from the channel) (Figure 57 and Figure 58).

The investigation at Site A (described by De Haan, 2016) took place under impacted conditions where the structure resulted in upstream saturation and prevented downstream sediment deposition. The eroded section is just downstream of the structure and non-eroded section is just upstream of the structure. Without the structure, the water table is anticipated to behave differently and the eroded section is not expected to drain the water table as significantly.

De Haan (2016) also discovered old palmiet remnants at various locations and depths (up to 2.6 m below ground level) at Site C, which implies that palmiet has been present in the Krom River catchment (and has been re-establishing itself after erosion) for thousands of years. This also supports the theory of cutting and filling in the catchment put forward by Pulley et al. (2018).

De Haan (2016:35) stated that "*it could be argued that structures disrupt the natural long-term cycles to a certain extent. In this context, one could argue that the act of implementing structures implies trying to force a natural dynamic system to remain constant for as long as possible in order to benefit the needs of mankind*".

Figure 57: The locations of transects at Site A. Transect AT1 is along the non-eroded reach and AT6 is along the eroded reach downstream of the erosion-control structures
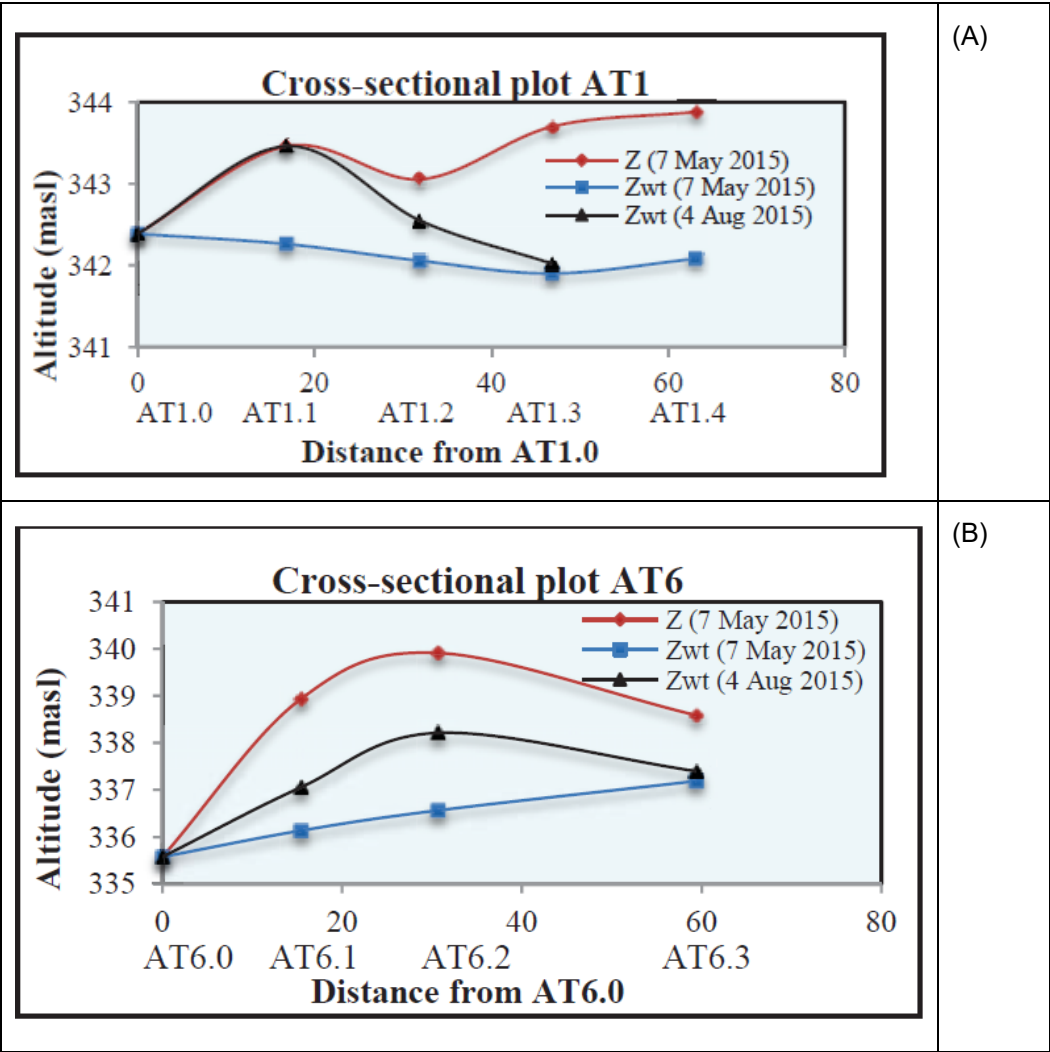
Figure 58: A) Cross-sectional profile along a non-eroded reach of the river channel. Z = surface elevation, Zwt = elevation of the water table; (B) Cross-sectional profile along the eroded reach illustrating the drop in water table elevation compared with surface elevation

7   CONCLUSIONS

The hydrological functioning of palmiet wetlands is closely linked to high subsurface discharges typically found within TMG aquifers. We propose that the palmiet wetlands are sustained by significant amounts of subsurface water (both groundwater and interflow) moving through preferential flow paths in the alluvial fans, which are in turn sustained by groundwater discharge from the surrounding sandstones and quartzites of the Nardouw Subgroup and Peninsula Formation. This conceptual model indicates that a consistent water supply is a palmiet system driver (Figure 59) and a key component of palmiet wetland formation. The wetlands clearly retain a significant amount of water, leading to the maintenance of prolonged flows and a larger baseflow. However, we suggest that the occurrence of palmiet as the dominant species in this wetland is due to the sustained low flows related to catchment geology and high hydrological connectivity between the catchment and the wetland that is enabled by flow paths that allow the free flow of water from the catchment to the wetland. The evidence presented indicates that the major pathway of subsurface water recharge to the wetlands is via preferential pathways in the alluvial fans; however, a more diffuse contribution through the surrounding fractured Bokkeveld shale cannot be discounted as another potential contributor.
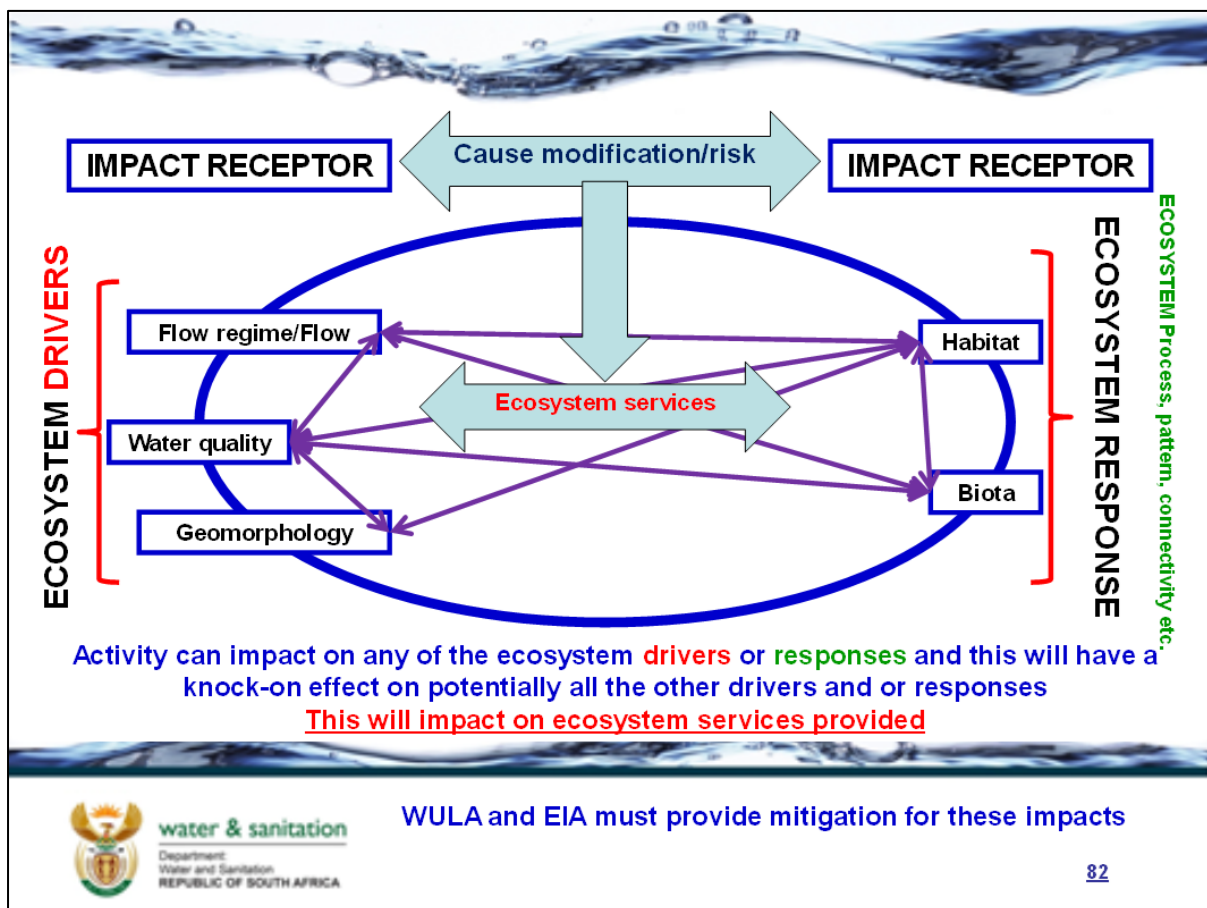
Figure 59: Ecosystem drivers and responses (WULA: Water use Licence Application, and EIA: Environmental Impact Assessment)

There is a strong relationship between the hydrological and geomorphological functioning of palmiet wetlands, and geomorphology is another clear system driver (Figure 59). The geomorphological aspect of the study has shown that gully erosion leads to longitudinal slope reduction and valley widening in ways that can lead to wetland formation. Extrinsic factors such as poor land management may accelerate natural gully formation, but erosion through gullying may also result from intrinsic factors.

The volume of sediment found within the wetlands (numerous sand lenses and filled gullies) indicate that palmiet traps sediment during high flow events, creating deposits of sediment that has freshly moved from the catchment and is protected from dissolution diagenesis within the wetland (Pulley et al., 2017).

The study demonstrated that stream power (modelled using Caesar-Lisflood), in addition to localised longitudinal slope increases (due to sediment deposition by numerous alluvial fans), can result in the initiation of natural erosion gullies. It is not known what the ratio of current erosion is in terms of being natural and anthropogenically influenced; however, it is certain that erosion would occur under natural conditions. Pulley et al. (2017; 2018) dated sediment from these gullies at between 470 YBP and 7060 YBP. This indicates that these gullies were a part of system that functioned prior to the introduction of European farming. Pulley et al. (2018) also identified that palmiet wetland erosion is key to re-establishing wetland habitats downstream of the eroded wetland reach by reducing the longitudinal slope of the river. A large portion of the eroded sediment is thus deposited just downstream of the original erosion knickpoint and does not travel far downstream. Therefore, it is unlikely to be a significant risk to infrastructure downstream, such as Churchill Dam. However, should all wetlands be removed, this sediment would be more likely to travel downstream in large flood events, eventually affecting downstream infrastructure.

Specific evidence for these conclusions and their links to the aims of this investigation include:

Aim 1: Determine the surface and groundwater dynamics of the Krom River upper catchment (K90A)

Specific deduction: Groundwater and interflow contribution from the TMG Peninsula and Nardouw aquifers to Krom River tributaries recharge the wetlands via preferential flow paths within the tributary alluvial fans:

- The larger catchment tributaries flowed continuously even in severe drought conditions (Section 4.2).

- The water quality within the tributaries is similar to that of groundwater sampled from boreholes located in the TMG Peninsula and Nardouw aquifers (although with evapotrans-pirational water losses) (Section 4.1.3).

- The wetland was largely unaffected by the severe drought in terms of size and health. It remained green throughout despite there being no visible inflow from the upstream river. Although no upstream inflow was visible and the water level in the wetland had dropped, there continued to be outflow from the wetland throughout the drought.

- The water quality analysis together with an MCM indicates a large groundwater baseflow contribution to the system (Section 5.2).

- Water level gradients within the wetland (measured along cross section transects) indicate that water is moving from the alluvial fans onto the wetlands (Section 4.2).

Specific deduction: The wetlands are located within a shale aquitard (Bokkeveld shale) with little diffuse recharge into the wetland from the surrounding shale geology, or from surrounding alluvium (similarly located within the shale aquitard):

- Low transmissivity of the alluvial fans (outside of the main preferential flow path of the fans) and valley-bottom material was found between the alluvial fans (Section 4.2).

- Water quality within the wetlands and river indicates little influence from the saline ground-water found within the Bokkeveld shale (demonstrated by water quality of groundwater in BH1) (Sections 4.2 and 5.2).

- The lower water level of the borehole (BH1) in comparison to the adjacent river channel (Section 4.1.1).

Specific deduction: The wetlands recharge the valley-bottom aquifers (Bokkeveld shale and alluvial deposits) outside of the recharge areas within the alluvial fans:

- Water level gradients within the wetland (measured along cross section transects) indicate that water is moving from the wetlands onto the surrounding valley-bottom/floodplain between the alluvial fans. There is essentially a repeated mounding of water within the wetland between the alluvial fans (Sections 4.2).
- Subsurface water levels on the valley bottom (measured in piezometers located between the alluvial fans) are lower than that of the wetland (Section 4.2.1).

Aim 2: Identify the relationship between wetlands and hydrological functioning of the catchment

Specific deduction: The wetlands regulate river flows, and maintain low flows:

- Water moves diffusely through the palmiet wetlands with very small channels forming along the perimeter of the wetlands (Section 2.3).
- Zero or very low flow rates measured between the wetlands (downstream of Krugersland wetland and upstream of Kompanjiesdrif wetland) even at significant water level depths of nearly 2 m.
- Continuous outflow from the wetland throughout the severe drought even with no visible upstream inflow.
- According to the hydrological model and wetland submodel (non-validated), the wetlands do play an important role in flood attenuation and the maintenance of low flows (Section 5.1).

Aim 3: Determine whether wetland degradation is affecting the hydrological integrity and water security of the river

Specific deduction: Gully erosion, although exacerbated by anthropogenic impacts, is a natural part of palmiet wetland functioning:

- Deposition of sediment due to the alluvial fans results in a reduction in cross-sectional width of the wetland resulting in increased water depth, leading to increased velocity for a given discharge in the confined section. Eventually, the retarding effects of vegetation are overwhelmed as the floodwaters flatten the vegetation, initiating erosion (Section 6.1).
- Gully erosion leads to longitudinal slope reduction and valley widening in ways that can lead to wetland formation (section 6.2).
- McNamara (2018) indicated that the erosion-control structures along the Krom River are in fact preventing the natural cutting-and-filling cycles that reduce longitudinal slope and valley widening; conditions that are linked to the long-term re-establishment of palmiet wetlands.
- Discovery of old palmiet remnants up to 2.6 m below the surface has shown that cycles of gully erosion followed by re-establishment of the palmiet has taken place in the Krom River for thousands of years (Section 6.3).
- The regional slope along the Krom River is 0.35%; however, the longitudinal slope of the Kompanjiesdrif wetland is 1.02% (Figure 54), thereby illustrating the steepness of this erosional reach compared with the regional slope.

- This continuous cycle of erosion and re-establishment results in little nett hydrological loss from the catchment. The local lowering of the water table in response to erosion gullies would not likely result in excessive drainage of water from the system in the longer term due to wetland re-establishment just downstream of the erosion. Rebelo, Emsens, Meire and Esler (2018) also investigated the effect of channel erosion on palmiet wetlands in the Eastern and Western Cape and found that there was no significant difference in relative groundwater depth between the degraded and pristine palmiet wetland sites.

Specific deduction: Gully erosion is not affecting the Churchill Dam significantly:

- Surveys of sediment deposition by McNamara (2018) and Pulley et al. (2018) indicate that eroded sediment is deposited immediately downstream of the eroded reach, which reduces longitudinal slope and creating conditions favourable for the re-establishment of wetlands downstream (Section 6.2).

Specific deduction: The erosion-control structures affect the subsurface water level dynamics.

- The erosion-control structures cause a significant difference in surface water elevation above and below the structures (Section 6.3).

- The structures have elevated the water table upstream of them – increasing saturation of the wetland.

- The structures decrease the downstream sediment load. This capturing of sediment upstream, however (causing a decreased bed load downstream), has destabilised the downstream stream bed. The Krom River erosion-control structure has controlled the main head cut at Kompanjiesdrif (it has remained at the same location) but has widened it significantly over a ten-year period.

- The water table is significantly deeper along the eroded reaches than non-eroded reaches of the river. This is because gully erosion causes drainage of the intergully area, resulting in a lowering of the water table as the gullies deepen.

- The water table along non-eroded reaches appears to slope slightly away from the channel (groundwater discharge from the channel) but this is reversed in eroded reaches (Section 6.3).

This project ultimately aimed to improve understanding around the hydrological functioning of palmiet wetlands and identify the primary reasons they are commonly found in the TMG geological region. The project has identified that a consistent water supply in the form of low flows in rivers is important for palmiet's establishment and survival. Palmiet has a thick system of fibrous roots that grow significantly deeper than other similar wetland plants (sometimes up to 5 m deep). Its deep rooting system appears to play an important role in the ecosystem functioning of the plant and its ability to withstand heavy floods that are characteristic of the TMG geology (Munro & Linder, 1997; Sieben, 2016).

Sieben (2012) and Barclay (2016) described palmiet as an ecosystem engineer since it alters its environment to support its own growth, which appears to play a significant role in the formation of valley-bottom wetlands. By extending across the valley floor, palmiet colonises the river, traps sediment and reduces flow. This process alters the flow in the river to a diffuse flow, allowing the accumulation of organic material and formation of a deep peat basin (Job, 2014). A similar process was also noted by Czegledi (2013) in a study of the Hudsonvale palmiet wetland on the Krom River and by Bekker (2016) in a study of the Tierkloof palmiet wetland along the Tierkloof River.

The Kompanjiesdrif wetland has been subjected to various episodes of gully formation and infilling. Barclay (2016) found that palmiet plays a role in naturally restoring eroded gullies. She indicated that

palmiet has an impact on these gullies by filling them (trapping sediment in the gullies), colonising gullies that have been filled by alluvial fan sediment, and encroaching into former gullies that are filled with water (dammed or ponded up) and are obstructed downstream by alluvial fan sediment. Palmiet forms a tangled mat over the open water surface of these former gullies.

There are regions outside of the TMG where limited palmiet stands are found, such as around the Natal Group sandstones in KwaZulu-Natal. But it seems that conditions within the TMG (acidic, nutrient-poor rivers and substrate) are particularly favourable to palmiet formation or dominance. Munyai (2013), however, investigated the soil nutritional levels of various sites across South Africa where palmiet is known to grow as well as sites (in the same geographic region) where it does not grow. It was found that soil nutritional values of the palmiet sites and non-palmiet sites were similar, indicating that the distribution of palmiet is not necessarily linked to edaphic factors but that other parameters (for example, hydrological regime) may, in fact, be responsible for its occurrence. Palmiet is thus possibly more reliant on a consistent water supply for its existence and survival than it is on acidic nutrient-poor soils and water as stated by other authors.

McNamara (2018:66) stated, "*ongoing cut-and-fill cycles are the Krom Rivers' natural response to variation in water and sediment supply, and are therefore important longitudinal self-recovery processes within the system*". The structures in the Krom River are inhibiting the loss of existing palmiet wetlands, but are preventing periods of natural cutting (upstream of the structure) and filling (downstream of the structure) that cause reductions in longitudinal slope and valley widening; the conditions that are linked to the long-term re-establishment of palmiet wetlands in a more geomorphologically stable setting.

This continuous cycle of erosion and re-establishment results in little nett hydrological loss from the catchment. The local lowering of the water table in response to erosion gullies would not likely result in excessive drainage of water from the system in the longer term due to wetland re-establishment just downstream of the erosion. Rebelo, Emsens, Meire and Esler (2018) also investigated the effect of channel erosion on palmiet wetlands in the Eastern and Western Cape and found that there was no significant difference in relative groundwater depth between the degraded and pristine palmiet wetland sites.

Although this project proposes that gully erosion forms a natural part of palmiet system functioning, the loss of palmiet wetlands would have a significant impact on river systems. Palmiet wetlands provide essential sediment traps, hydrological attenuation and retention services that would impact local water users, and downstream infrastructure. Restoration initiatives should therefore focus on ensuring downstream environments are kept suitable for the natural re-establishment of wetlands, and focus on softer protective infrastructures which do not completely inhibit the downstream movement of eroded sediment.

8   RECOMMENDATIONS

Although the hydrological model used in this investigation indicated that the wetland contributed significantly to the attenuation of high flows in the catchment, this could not be validated due to a lack of flow data. Continued monitoring of flow is recommended to ensure observed flow information is obtained during wetter periods with higher flow. This will contribute to a better understanding of palmiet wetland response under moderate and high flows.

The MCM shows good potential for tracing sources of water moving through the wetlands. More detailed water quality and isotope sampling under different catchment conditions (wet and dry) could improve the understanding of water moving through the system under different conditions.

An improved understanding of palmiet wetland ET will be valuable as this was a significant uncertainty. It is also recommended that a more detailed wetland model be applied to simulate palmiet behaviour under various flow conditions.

The installation of carefully sited boreholes in the catchment for monitoring purposes will provide extremely useful information regarding wetland hydrological functioning and assist in reducing current uncertainties in groundwater contributions. Similar studies of this type on other palmiet wetlands could confirm if characteristics identified in this study are common to other palmiet wetlands.

Finally, consultation with Working for Wetlands on alternative wetland protection mechanisms would be recommended.

LIST OF REFERENCES

Adar, E. (1984) Quantification of aquifer recharge distribution using environmental isotopes and regional hydrochemistry. PhD Thesis, University of Arizona, Tucson, AZ.

Adar, E. (1996) Quantitative evaluation of flow systems, groundwater recharge, and transmissivities using environmental tracers. In: Yurtsever, Y. (Ed.) *Manual on Mathematical Models in Isotope Hydrogeology*. International Atomic Energy Agency (IAEA).

Adar, E. and Kuells, C. (n.d.) *A short manual for the installation and operation of MCM$_{sf}$ using the MIG–mixing-cell input generator*.

Amaya, A.G., Dahlin, T., Barmen, G. and Rosberg, J-E. (2016) Electrical resistivity tomography and induced polarization for mapping the subsurface of alluvial fans: A case study in Punata (Bolivia). *Geosciences*, 6(51), 1–13.

Bailey, A.K. and Pitman, W.V. (2016) *Water resources of South Africa, 2012 STUDY: Book of maps*. WRC Report TT 382/08. Water Research Commission, Pretoria.

Barclay, A. (2016) Ecosystem engineering by the wetland plant palmiet: Does it control fluvial form and promote diffuse flow in steep-sided valleys of the Cape Fold Mountains. MSc Thesis, Rhodes University, Grahamstown.

Barrow, D. (2010) Ground water dependence of ecological sites located in the Table Mountain Group. MSc Thesis, University of the Free State, Bloemfontein.

Bates, P.D., Horritt, M.S. and Fewtrell, T.J. (2010) A simple inertial formulation of the shallow water equations for efficient two-dimensional flood inundation modelling. *Journal of Hydrology,* 387(1), 33–45.

Bekker, D. (2016) An investigation into the origin and evolution of the Tierkloof Wetland, a peatland dominated by Prionium serratum, in the Western Cape. MSc Thesis, Rhodes University, Grahamstown.

Boucher, C. and Withers, M. (2004) Prionium serratum, a Cape River Plant. *Veld and Flora*, 95(3), 153–155.

Brown, C., Colvin, C., Hartnady, C., Hay, R., Le Maitre, D. and Riemann, K. (2003) *Ecological and environmental impacts of large volume groundwater abstraction in the Table Mountain Group (TMG) aquifer system: Discussion document for scoping phase*. WRC Report K5/1327. Water Research Commission, Pretoria.

Campana, M.E. (1975) Finite state models of transport phenomena in hydrological systems. PhD Thesis, University of Arizona, Tucson, AZ.

Coulthard, T.J., Neal, J.C., Bates, P.D., Ramiraz, J., De Almeida, G.A.M. and Hancock, G.R. (2013) Integrating the LISFLOOD-FP 2D hydrodynamic model with the CAESAR model: Implications for modelling landscape evolution. *Earth Surface Processes and Landforms,* 38(15), 1897–1906.

Craig, H. (1961) Isotopic variations in meteoric waters. *Science*, 133 (3465), 1702–1703.

Colvin, C., Le Maitre, D. and Hughes, S. (2003) *Assessing terrestrial groundwater dependent ecosystems in South Africa*. WRC Report 1090-2/2/03. Water Research Commission, Pretoria.

Czegledi, N. (2013) Integrated assessment of human impacts on wetland services in the Upper Kromme River Catchment, South Africa. MSc Thesis, Wageningen University, Wageningen, Netherlands.

De Haan, V. (2016) The effects of erosion-control structures and gully erosion on groundwater dynamics along the Kromrivier, Eastern Cape, South Africa. MSc Thesis, Stockholm University, Stockholm, Sweden.

Dennis, I. and Pretorius, J. (2006) *Groundwater reserve determination for the Kromme/Seekoei catchments*. Final Report, Project No. 2005-18. Department of Water Affairs and Forestry, Pretoria.

Department of Water Affairs and Forestry (DWAF). (2006). *Groundwater resource assessment phase 2: Task 2C groundwater planning potential*. Department of Water Affairs, Pretoria.

Diamond, R.E. 2014. Stable isotope hydrology of the Table Mountain Group. PhD Thesis, University of Cape Town, Cape Town.

Ellery, W. Grenfell, M., Grenfell, S., Kotze, D., McCarthy, T., Tooth, S., … and Ramsay, L. (2009) *WET-Origins: Controls on the distribution and dynamics of wetlands in South Africa*. WRC Report TT 334/09. Water Research Commission, Pretoria.

Fretwell, J.D., Williams, J.S. and Redman, P.J. (1996) *National water summary on wetland resources, United States Geological Survey water-supply paper 2425*. United States Geological Survey, Washington, DC.

Giocoli, A., Magri, C., Vannoli, P., Piscitelli, S., Rizzo, E., Siniscalchi, A., … Di Nocera, S. (2008) Electrical resistivity tomography investigations in the Ufita Valley (Southern Italy). *Annals of Geophysics*, 51(1), 213–223.

Grundling, P-L., Grundling, A.T., Pretorius, L., Mulders, J. and Mitchell, S. (2017) *South African peatlands: Ecohydrological characteristics and socio-economic value*. WRC Report 2346/1/17. Water Research Commission, Pretoria.

Haigh, L., Illgner, P., Wilmot, J., Buckle, J., Kotze, D. and Ellery, F. (2009) The wetland rehabilitation project in the Kromme River Wetlands, Eastern Cape. In: Breen, C., Dini, J., Ellery, W., Mitchell, S. and Uys, M. (Eds). *WET-Outcome evaluate: An evaluation of the rehabilitation outcomes at six wetland sites in South Africa*. WRC Report TT343/09, 109–168. Water Research Commission, Pretoria.

Harrington, G.A., Walker, G.R., Love, A.J. and Narayan, K.A. (1999). A compartmental mixing-cell approach for the quantitative assessment of groundwater dynamics in the Otway Basin, South Australia. *Journal of Hydrology*, 214, 49–63.

Hughes, D.A. (2013) A review of 40 years of hydrological science and practice in southern Africa using the Pitman rainfall-runoff model. *Journal of Hydrology*, *501*, 111–124.

Hughes, D.A., Andersson, L., Wilk, J. and Savenije, H.H. (2006) Regional calibration of the Pitman model for the Okavango River. *Journal of Hydrology*, *331*(1), 30–42.

Hughes, D.A., Tshimanga, R.M., Tirivarombo, S. and Tanner, J. (2014) Simulating wetland impacts on stream flow in southern Africa using a monthly hydrological model. *Hydrological Processes*, 28(4), 1775–1786.

Jackson, C.R., Thompson, J.A. and Kolka, R.K. (2014) Wetland soils, hydrology and geomorphology. In: Batzer, D. and Sharitz, R. (Eds). *Ecology of Freshwater and Estuarine Wetlands*. Berkeley, CA: University of California Press, 23–60.

Jarmain, C., Singels, A., Bastidas-Obando, E., Paraskevopoulos, A., Olivier, F., Van der Laan, M., … Walker, S. (2014) *Water use efficiency of selected irrigated crops determined with satellite imagery*. WRC Report TT 602/14. Water Research Commission, Pretoria.

Job, N. (2014) Geomorphic origin and dynamics of deep, peat-filled, valley bottom wetlands dominated by palmiet (Prionium serratum): A case study based on the Goukou Wetland, Western Cape. MSc Thesis, Rhodes University, Grahamstown.

Jones, C.G., Lawton, J.H. and Shackak, M. (1994) Organisms as ecosystem engineers. *Oikos*, 69(3), 373–386.

Keen-Zebert, A., Tooth, S., Rodnight, H., Duller, G.A.T., Roberts, H.M. and Grenfell, M. (2013) Late quaternary floodplain reworking and the preservation of alluvial sedimentary archives in unconfined and confined river valleys in the eastern interior of South Africa. *Geomorphology*, 185, 54–66. https://doi.org/10.1016/j.geomorph.2012.12.004

Lagesse, J. (2017) Discontinuous gully erosion as a mechanism of wetland formation: A case study of the Kompanjiesdrif Basin, Kromrivier, Eastern Cape, South Africa. MSc Thesis, Rhodes University, Grahamstown.

Liu, F., Williams, M.W. and Caine, N. (2004) Source waters and flow paths in an alpine catchment, Colorado Front Range, United States. *Water Resources Research*, 40, 1–16.

Lyons, R., Tooth, S. and Duller, G.A.T. (2013) Chronology and controls of donga (gully) formation in the upper Blood River catchment, KwaZulu-Natal, South Africa: Evidence for a climatic driver of erosion. *The Holocene*, 23(12), 1875–1887. https://doi.org/10.1177/0959683613508157

Matthews, A.J. (2013) Application of the mixing cell model to the quantification of groundwater-surface water interaction. MSc Thesis, University of the Free State, Bloemfontein.

McCarthy, T. and Rubidge, B. (2005) *The Story of Earth and Life: A Southern African Perspective on a 4.6 Billion Year Journey*. Cape Town: Struik Nature.

McNamara, S. (2018) The influence of landscape disconnectivity on the structure and function of the Krom River, Eastern Cape, South Africa. MSc Thesis, Rhodes University, Grahamstown.

Mitsch, W.J. and Gosselink, J.G. (2007) *Wetlands*. 4th ed. Hoboken, NJ: John Wiley & Sons.

Mu, Q., Zhao, M. and Running, S.W. (2011) Improvements to a MODIS global terrestrial evapotranspiration algorithm. *Remote Sensing of Environment*, 115(8), 1781–1800.

Munro, S.L. and Linder, H.P. (1997) The Embryology and systematic relationships of Prionium serratum (Juncaceae: Juncales). *American Journal of Botany*, 84(6), 850–860.

Munro, S.L., Kirschner, J. and Linder, H.P. (2001) *Prioniaceae, Species Plantarum: Flora of the World, Part 5.* Canberra: Australian Biological Resources Study, 1–7.

Munyai, R. (2013) A systematic study of the South African genus Prionium (Thurniaceae). MSc Thesis, University of Cape Town, Cape Town.

Nel, J.L., Driver, A., Strydom, W.F., Maherry, A., Petersen, C., Hill, L., … Smith-Adao, L.B. (2011) *Atlas of freshwater ecosystem priority areas in South Africa: Maps to support sustainable development of water resources.* WRC Report TT55/11. Water Research Commission, Pretoria.

Nsor, C.A. and Gambiza, J. (2013) Land use changes and their impacts on the vegetation of the Krom River Peat Basin, South Africa. *Science Journal of Environmental Engineering Research*, 2013, 1–12.

Palacky, G.J. (1988) Resistivity characteristics of geological targets. In: Nabighian, M.N. and Corbett, J.D. (Eds). *Electromagnetic Methods in Applied Geophysics: Theory Volume 1*. Tulsa, OK: Society of Exploration Geophysicists, 52–129.

Parsons, R. (2009) Is Groenvlei really fed by groundwater discharged from the Table Mountain Group (TMG) Aquifer? *Water SA*, 35(5), 657–662.

Partington, D., Brunner, P., Simmons, C.T., Therrien, R., Werner, A.D., Dandy, G.C. and Maier, H.R. (2011) A hydraulic mixing-cell method to quantify the groundwater component of streamflow within spatially distributed fully integrated surface water groundwater flow models. *Environmental Modelling and Software*, 26(7), 886–898.

Pelgrum, H., Miltenburg, I.J., Cheema, M.J.M., Klaasse, A. and Bastiaanssen, W.G.M. (2012) ETLook: A novel continental evapotranspiration algorithm. *Remote Sensing and Hydrology: Proceedings of a symposium held at Jackson Hole, WY,* September 2010, 1–4.

Pulley, S., Ellery, W., Lagesse, J., Schlegel, P. and Mcnamara, S. (2018) Gully erosion as a mechanism for wetland formation: An examination of two contrasting landscapes. *Land Degradation and Development,* 29, 1756–1767.

Pulley, S., Lagesse, J. and Ellery, W. (2017) The mineral magnetic signatures of fire in the Kromrivier wetland, South Africa. *Journal of Soils and Sediments*, 17(4), 1170–1181.

Rebelo, A.G., Boucher, C., Helme, N., Mucina, L. and Rutherford, M.C. (2006) Fynbos biome. In: Mucina, L. and Rutherford, M.C. (Eds). *The Vegetation of South Africa, Lesotho, and Swaziland*. Pretoria: South African National Biodiversity Institute, 53–219.

Rebelo, A.J. (2012) An ecological and hydrological evaluation of the effects of restoration on ecosystem services in the Kromme River System, South Africa. MSc Thesis, Stellenbosch University, Stellenbosch.

Rebelo, A.J. and Cowling, R.M. (2013) Restoring the Kromme: Feature. *Veld and Flora*, 99(4), 202–203.

Rebelo, A.J., Emsens, W.-J., Esler, K.J. and Meire, P. (2018) Quantification of water purification in South African palmiet wetlands. *Water Science and Technology (in press).*

Rebelo, A.J., Emsens, W.-J., Meire, P. and Esler, K.J. (2018) The impact of anthropogenically induced degradation on the vegetation and biochemistry of South African palmiet wetlands. *Wetlands Ecology and Management*, 26(6), 1157–1171.

Rebelo, A.J., Le Maitre, D.C., Esler, K.J. and Cowling, R.M. (2015) Hydrological responses of a valley-bottom wetland to land-use/land-cover change in a South African catchment: Making a case for wetland restoration. *Restoration Ecology*, 23(6), 829–841.

Rebelo, A.J., Scheunders, P., Esler, K.J. and Meire, P. (2017) Detecting, mapping and classifying wetland fragments at a landscape scale. *Remote Sensing Applications: Society and Environment*, 8, 212–223.

Robson, A. and Neal, C. (1990) Hydrograph separation using chemical techniques: An application to catchments in Mid-Wales. *Journal of Hydrology*, 116, 345–363.

Roets, W., Xu, Y., Raitt, L. and Brendonck, L. (2008) Groundwater discharges to aquatic ecosystems associated with the Table Mountain Group (TMG) aquifer: A conceptual model. *Water SA*, 34(1), 77–88.

Rosewarne, P. (1981) *Geohydrology of the Hex River Valley*. Volume 1, Report No GH 3142. Department of Water Affairs, Forestry and Environmental Conservation, Pretoria.

Rosewarne, P. (2002) Hex River Valley. In: Pietersen, K. and Parsons, R. (Eds). *A Synthesis of the Hydrogeology of the Table Mountain Group: Formation of a Research Strategy*. WRC Report TT158/01. Water Research Commission, Pretoria, 178–182.

Schlegel, P. (2017) Spatial variation in modelled hydrodynamic characteristics associated with valley confinement in the Krom River Wetland: Implications for the initiation of erosional gullies. MSc Thesis, Rhodes University, Grahamstown.

Sieben, E. (2016) *Species in the spotlight, the habitat creator* (Internet). Available from: <http://cmsdata.iucn.org/downloads/species_spotlight_aquatic_plants.pdf> (Accessed 6 April 2016).

Sieben, J.J. (2012) Plant functional composition and ecosystem properties: The case of peatlands in South Africa. *Plant Ecology*, 213, 809–820.

Smart, M.C. and Tredoux, G. (2002) Groundwater quality and fitness for use. In: Pietersen, K. and Parsons, R. (Eds). *A synthesis of the hydrogeology of the Table Mountain Group: Formation of a Research Strategy*. WRC Report TT158/01. Water Research Commission, Pretoria, 118–123.

Smith, M.E., Clarke, S. and Cavé, L.C. (2002) Chemical evolution of Table Mountain Group groundwater and the sources of iron. *Proceedings of the Conference on Ground Water Division*. Somerset West, South Africa, 47–52.

Thamm, A.G. and Johnson, M.R. (2006) The Cape supergroup. In: Johnson, M.R, Anhaeusser, C.R. and Thomas, R.J. (Eds). *The Geology of South Africa*. Johannesburg: Geological Society of South Africa, 443–460.

Toerien, D.K. (n.d.) Legend for 1:50 000 sheets of area 3324 Port Elizabeth.

Toerien, D.K. (1972) 1:50 000 3323DD & 3423BB Joubertina field sheets.

Toerien, D.K. (1971–1972) 1:50 000 3324CC Wittelsbos field sheets.

Toerien, D.K. (1986) 1:250 000 3324 Port Elizabeth geological map.

Van Ginkel, C.E., Glen, R.P., Gordon-Gray, K.D., Cilliers, C.J., Muasya, M. and Van Deventer, P.P. (2011) *Easy identification of some South African wetland plants*. WRC Report TT 479/10. Water Research Commission, Pretoria.

Wilson, A.M. (2015) Hydrograph separation using hydrochemistry mixing models: An assessment of the Langtang River Basin. MA Thesis, University of Colorado, Boulder, CO.

Xu, Y., Lin, L. and Jia, H. (2009) *Groundwater flow conceptualization and storage determination of the Table Mountain Group (TMG) Aquifers*. WRC Report 1419/1/09. Water Research Commission, Pretoria.

APPENDIX A: OVERVIEW OF MODELS

Modified Pitman hydrological model

The model was set up in a semi-distributed manner with each subcatchment having its own rainfall and ET demand time series and its own parameter set used to represent the main hydrological processes. In this investigation, the model was applied in a semi-distributed manner by splitting the upper K90A catchment into linked subcatchments based on the direction of surface water and groundwater flow. The full details of the model are available in recent publications (Hughes et al., 2006; Hughes, 2013) and are not repeated here. However, the important components relevant to this investigation are summarised below. The full model also includes interception, infiltration, surface run-off and routing components. A wetland submodel (Hughes et al., 2014) was used to represent the wetlands.

Although the groundwater components of the model are based on relatively simple geometry, simulations are done at a larger scale to reflect the effects of wetter or drier periods on the catchment in the recharge and discharge. Differing delays or attenuation effects can be represented by differences in the storativity (volume of storage within the aquifer) and transmissivity (rate of water movement through the aquifer) parameters. The main groundwater balance components in the model are shown in Figure 60.
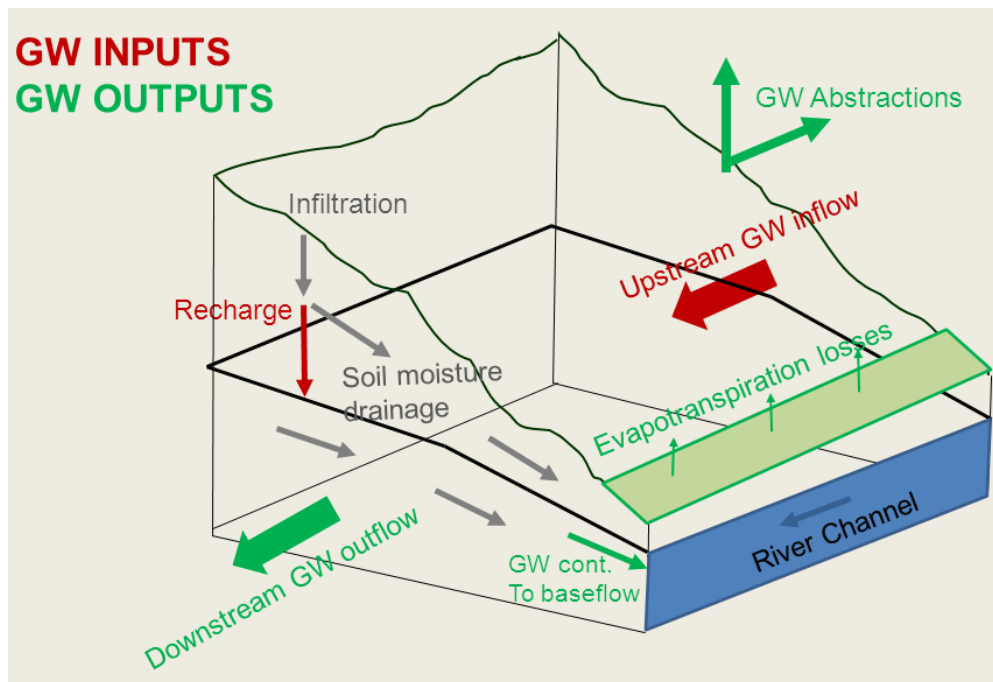
Figure 60: Diagrammatic summary of the main interaction processes (where groundwater is contributing to surface water)

Pitman wetland submodel

The wetland submodel was originally designed to be used with large wetlands. It was assumed that the dynamics of the larger wetlands and lakes would be dominated by seasonal patterns of upstream inflow, the available wetland/lake storage, and the balance between rainfall and ET. The wetland model seemed to run appropriately; however, validation with more flow data would confirm this. Details of the wetland submodel are given in Hughes et al. (2014). The parameters are described in Table 15 and a brief summary is outlined below:

- The lake/wetland area is calculated from the volume using a power function with two parameters.

- Evaporative losses are calculated using nett PET after accounting for rainfall inputs.

- Wetland inflow is assumed to occur as a proportion of upstream channel flow above a specified threshold.

- Outflow from the lake/wetland occurs when the storage volume is above a nominal value.

- Local run-off directly onto the lake/wetland.

- Artificial abstractions from the lake/wetland.

Table 15: Modified Pitman Model wetland parameters

Wetland and lake submodel parameters

MaxWA	km^2	Maximum wetland area.
RWV	$m^3 \times 10^6$	Residual wetland storage volume below which there are no return flows to the river channel.
IWV	$m^3 \times 10^6$	Initial wetland storage volume at the start of the simulation.
AVC	m^{-1}	Constant in the $WA = AVC \times WV^{AVP}$ relationship, where WA (m^2) and WV (m^3) are the current wetland area (limited to MaxWA) and volume, respectively.
AVP		Power in the $WA = AVC \times WV^{AVP}$ relationship.
QCap	$m^3 \times 10^6$	Channel capacity below which there is no spill from the channel to the wetland.
Parameters	**Units**	**Description**
QSF		Channel spill factor in $SPILL = QSF \times (Q - QCAP)$, where Q is the upstream flow and SPILL is the volume added to wetland storage.
RFC		Return flow constant in the $RFF = RFC \times (WV/RWV)^{RFP}$ relationship.
		RFF is a fraction limited to a maximum of 0.95 and then adjusted when Q is greater than QCap ($RFF = RFF \times QCap/Q$).
		The return flow volume is calculated from $RFLOW = RFF \times (WV - RWV)$.
RFP		Return flow power in the $RFF = RFC \times (WV/RWV)^{RFP}$ relationship.
EVAP	mm	Annual evaporation from the wetland (distributed into monthly values using a table of calendar month percentages).
ABS	$m^3 \times 10^6$	Annual water abstractions from the wetland (distributed into monthly values using a table of calendar month percentages).

Pitman model parameters

Table 16 lists the Pitman model natural surface and groundwater parameters. Additional compulsory data requirements include basin area, a time series of basin average rainfall, seasonal distributions of evaporation (fraction), and monthly parameter distribution factors.

Table 16: The modified Pitman Model surface and groundwater parameters

Parameters	Units	Description
Surface water parameters		
RDF		Rainfall distribution factor. Controls the distribution of total monthly rainfall over four model iterations.
AI	fraction	Impervious fraction of subbasin.
PI1s	mm	Summer interception storage for vegetation type 1.
PI1w	mm	Winter interception storage for vegetation type 1.
PI2s	mm	Summer interception storage for vegetation type 2.
PI2w	mm	Winter interception storage for vegetation type 2.
AFOR	%	% area of subbasin under vegetation type 2.
FF		Ratio of PET rate for Veg2 relative to Veg1.
PEVAP	mm	Annual basin PET.
ZMINs	mm·month^{-1}	Summer minimum basin absorption rate.
ZMINw	mm·month^{-1}	Winter minimum basin absorption rate.
ZAVE	mm·month^{-1}	Mean basin absorption rate.
ZMAX	mm·month^{-1}	Maximum basin absorption rate.
ST	mm	Maximum moisture storage capacity.
SL	mm	Soil moisture below which there is no recharge.
POW		Power of the moisture storage run-off equation.
FT	mm·month^{-1}	Run-off from moisture storage at full capacity.
R		Evaporation-moisture storage relationship parameter.
TL	months	Lag of surface run-off.
Groundwater parameters		
GW	mm·month^{-1}	Maximum recharge depth at maximum moisture capacity.
TLGMax	mm	Maximum channel loss.
GPOW		Power of the moisture storage recharge equation.
DD	km km^{-2}	Effective drainage density.
T	m^2 day^{-1}	Transmissivity.
S		Storativity.
RG		Regional groundwater drainage slope.
Rest RWL	m below surface	Aquifer depth.
RSF	% slope width	Riparian strip factor.

The essential assumptions of the model are that the groundwater storage water balance is determined by inputs of recharge and upstream groundwater flow, and outputs of flow to the river, riparian losses in the channel margins, drainage to a downstream subcatchment and abstractions from boreholes. A further input component of channel transmission loss is added if the groundwater level is below the channel and there is flow in the channel generated from the surface water components of the model. The groundwater storage variations are therefore translated, through simple geometry calculations and the storativity parameter, into variations in the gradients of the two groundwater segments.

The wetland model does not include groundwater inputs to the wetland, however, this was not considered significant as most of the groundwater contribution seems to be from the tributaries entering the wetland.

Mixing cell model

Methodology and brief mathematical description

Adar and Kuells (n.d.) developed software for running an MCM for a steady flow system in Excel™. The model uses a mixing input generator that runs within Excel™. The software is downloadable for free from http://www.uhydro.de/hywa/en/models/compartmentmodels?s[]=mixing&s[]=cell&s[]=model. Examples and a short manual are also provided on the website.

An updated MCM code and manual were provided by Prof. Adar (of Ben-Gurion University of the Negev) for the purposes of this study. The brief description of one of the typical mass balance equations used provided below was taken from this manual as well as from Adar (1996). For a more detailed description and further mass balance equations used in the model, refer to the abovementioned manual.

A set of mass balance equations for the water and solute is written for each cell over a given period. For a simple flow model of water (constant density), the mass balance equation for a cell *n* is written as:

$$Q_n - W_n + \sum_{i=1}^{I_n} q_{in} - \sum_{j=1}^{J_n} q_{ni} = S_n^* \frac{dh_n}{dt}$$

Where,

Q_n = Flow sources into cell *n*,

q_{in} = Flow from the upstream i^{th} into the nth cell,

q_{nj} = Outflow from the nth cell into the jth cell,

W_n = Abstraction from cell n,

S_n = Storage capacity in cell n,

h_n = Hydraulic head associated with that compartment,

I_n and J_n = Number of sources and cells from which flow enters and leaves the nth cell.

Figure 61 illustrates these flow parameters in a compartmental system.
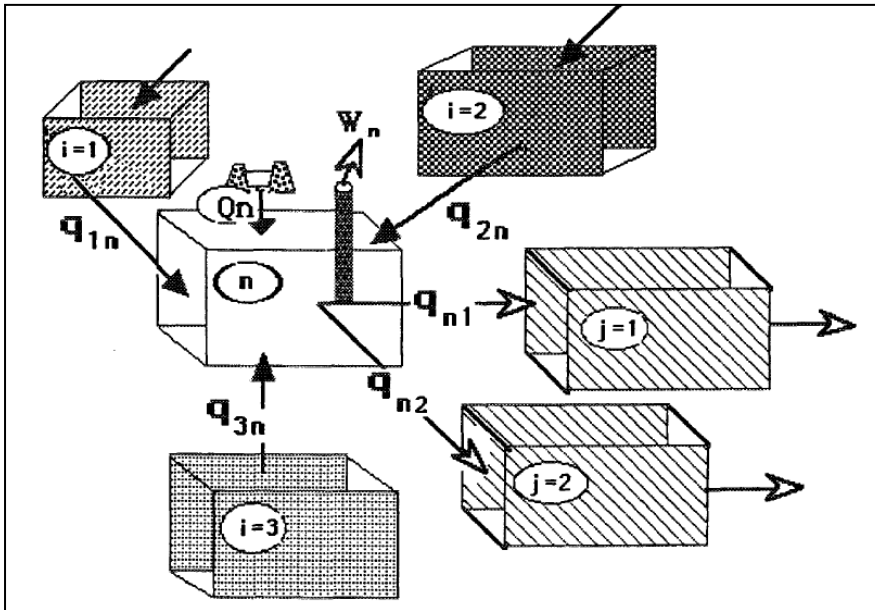
Figure 61: Illustration of the various flow parameters used in the MCM (Adar, 1996). (q = unknown flows; i and j = direction of flow; Qn = known inflow into the cell; and W= known outflow from the cell)

The output files created during the model run are illustrated as follows:

Single-cell MCM output file:

```
   There are   6 potential inputs.
   There are  10 tracers to be considered.
   There are   2 cells in this model.
   There are   1 flows between the cells.

   N =  6  NN =  8  NOC =  2  NOP = 10


   Number of inflows to each cell:
     Num.cell  1  2
     Inflows   6  0

   Number of internal flows from and into each cell:
     Num.cell  1  2
     Interfl.  1  1

   The internal flows are:
     From cell  1
     To cell    2

   The outflow out of the last cell is [volume/year]:
     QOUT =   107100.00


   The rate of output (pumpage) and/or evapotranspiration
   from each cell is [volume/time]:
     PM( 1) =      .00
     PM( 2) = 13500.00
      Constant for Flows =   13500.000
     PM( 1) =      .00
     PM( 2) =     1.00
 *****************************


   The weighting parameters are:
    1.000   1.000   1.000   1.000   1.000   1.000   1.000   1.000   1.000   1.000

   There are  22 mass balance equations.
     Number of iterations:  15

     The rest of the variables are equal to zero.


 The unknown inflows are:
          Name of       Rate of      Perc. of     Perc. of
          inflow        inflow       tot. inflow  cell inflow  flux
   Cell 1
        1  BH1      =      .04          .4 %         .4 %       496.25
        2  Trib     =      .00          .0 %         .0 %          .00
        3  Wet1     =     5.83        67.0 %       67.0 %     78658.97
        4  PZA      =      .00          .0 %         .0 %          .00
        5  BH2      =      .72          8.3 %        8.3 %      9765.43
        6  BH3      =     2.11        24.3 %       24.3 %     28535.33
   Cell 2
```

```
The intermediate flows are:
  From   To    Rate of      Real
  cell   cell   flow       number
   1      2     8.768    118370.02

                          ----------      ----------
                 Total:   117455.98        100.00  %
          QOUT + PPP =    120600.00
                          ----------
       Absolute diff.:      3144.02

       Percentage diff.:      2.61 %




   **** Ion balance over the entire basin ***

   Id      SUMIN          SUMOUT         Abs.        Perc.
                                         error:      error:

pH          54.331          65.928       -11.60      -17.6%
Ec        1700.468        1896.547      -196.08      -10.3%
Mg          52.766          62.533        -9.77      -15.6%
Ca           7.698           7.147          .55        7.7%
K            8.370           8.933         -.56       -6.3%
Cl         490.723         700.373      -209.65      -29.9%
Si          55.939          50.281         5.66       11.3%
Al            .177            .179          .00       -1.1%
D         -220.385        -189.907       -30.48       16.0%
O-18       -47.011         -43.594        -3.42        7.8%


   Total salt transport:

   Observed output  ( mass/time ):   13807.8
   Estimated input  ( mass/time ):   11350.3



      End of MCM.
```

Two-cell MCM output file:

```
There are   9 potential inputs.
There are  10 tracers to be considered.
There are   2 cells in this model.
There are   1 flows between the cells.

N =  9  NN = 11  NOC =  2  NOP = 10


Number of inflows to each cell:
   Num.cell  1  2
   Inflows   5  4

Number of internal flows from and into each cell:
   Num.cell  1  2
   Interfl.  1  1

The internal flows are:
   From cell  1
   To cell    2

The outflow out of the last cell is [volume/year]:
   QOUT =   107100.00


The rate of output (pumpage) and/or evapotranspiration
from each cell is [volume/time]:
   PM( 1) = 28500.00
   PM( 2) = 13500.00
    Constant for Flows =   13500.000
   PM( 1) =      2.11
   PM( 2) =      1.00
*****************************


The weighting parameters are:
 1.000   1.000   1.000   1.000   1.000   1.000   1.000   1.000   1.000   1.000

There are  22 mass balance equations.
   Number of iterations:  14

   The rest of the variables are equal to zero.


The unknown inflows are:
            Name of         Rate of       Perc. of       Perc. of
            inflow          inflow        tot. inflow    cell inflow  flux
 Cell 1
         1  SS2in    =        1.82          19.1 %         46.8 %     24531.34
         2  BH1      =         .10           1.1 %          2.7 %      1399.18
         3  Trib     =         .34           3.6 %          8.7 %      4562.39
         4  BH2      =        1.49          15.6 %         38.3 %     20067.56
         5  BH3      =         .14           1.4 %          3.5 %      1850.44
 Cell 2
         6  BH1      =         .09           1.0 %          1.6 %      1239.31
         7  Trib     =         .27           2.8 %          4.7 %      3582.78
         8  BH2      =        2.72          28.6 %         48.3 %     36707.40
         9  BH3      =        2.55          26.8 %         45.3 %     34447.96

The intermediate flows are:
   From   To    Rate of      Real
   cell   cell   flow       number
    1      2     2.387     32224.13

                          ----------     ----------
                 Total:    128388.36      100.00  %
            QOUT + PPP =   149100.00
                          ----------
         Absolute diff.:    20711.64

         Percentage diff.:     13.89 %



   **** Ion balance over the entire basin ***

   Id      SUMIN          SUMOUT         Abs.         Perc.
                                         error:       error:

pH          55.458         79.566        -24.11       -30.3%
Ec        2128.161       2254.169       -126.01        -5.6%
Mg          61.989         73.089        -11.10       -15.2%
Ca           9.505          8.836          .67         7.6%
K           10.350          9.778          .57         5.9%
Cl         681.840        799.807       -117.97       -14.7%
Si          51.475         62.164        -10.69       -17.2%
Al            .239           .242          .00         -1.2%
D         -309.863       -231.926        -77.94        33.6%
O-18       -61.349        -53.501         -7.85        14.7%

   Total salt transport:

   Observed output  ( mass/time ):   16203.0
   Estimated input  ( mass/time ):   14182.3


      End of MCM.
```

Caesar-Lisflood hydrodynamic model

Hydrological modelling was also undertaken using two-dimensional modelling software, namely, Caesar-Lisflood 1.9b. The Caesar-Lisflood is a reduced complexity model, which means that the two-dimensional depth-averaged form of the shallow water equation is not solved (it is not purely physics based). Caesar-Lisflood features conservation of mass but only partial conservation of momentum.

The Caesar-Lisflood model is the product of the integration of the Caesar landscape evolution model created by Coulthard et al. (2013), with the latest model version of Lisflood-FP, which is a one-dimensional hydrodynamic flow model that is applied in the x and y directions to simulate two-dimensional flow as created by Bates, Horritt and Fewtrell (2010). The Caesar-Lisflood model couples a landscape evolution model with a simplified two-dimensional hydrodynamic model. This coupling produces faster results because it is based on a simple but stronger physical basis than the ones usually governing ordinary landscape evolution models (Coulthard et al., 2013). Caesar-Lisflood 1.9b can be downloaded from: http://code.google.com/p/CAESAR-Lisflood

Caesar-Lisflood is a storage cell model, where a digital terrain model (DTM) represents the landscape and water is stored at the raster cell locations. Water is routed over the landscape in the x and y directions (two-dimensional) from raster cell to cell using a simplification of the shallow water equations (Bates et al., 2010). To calculate the flow (Q) between cells, the model uses the equation:

$$Q = \frac{q - gh_{flow}\Delta t \frac{\Delta(h+z)}{\Delta x}}{\left(1 + gh_{flow}\Delta t n^2 \backslash q / h_{flow}^{10/3}\right)}$$

where *q* is the flux between cells from the previous iteration ($m^2.s^{-1}$),

g is acceleration due to gravity ($m.s^{-1}$),

n is Manning's roughness coefficient,

h is depth in metres,

z is elevation (m),

h_{flow} is the maximum depth of flow between cells, and

x is grid cell width in metres and *t* is time in seconds.

This equation establishes the discharge (Q) across all four boundaries of a cell. Thereafter, the cell water depth *(h)* is updated using the equation:

$$\frac{\Delta h^{i,j}}{\Delta t} = \frac{Q_x^{i-1,j} - Q_x^{i,j} + Q_y^{i,j-1} - Q_y^{i,j}}{\Delta x^2}$$

where *i* and *j* are cell coordinates.

The last part of the formulation is the time step *(t)* that is controlled by the shallow water Courant–Freidrichs–Lewy condition, which requires that the wave does not spread across more than one cell per time step. This is represented by the equation:

$$\Delta t_{max} = a \frac{\Delta x}{\sqrt{g h}}$$

where *d* is a coefficient typically defined between 0.3 and 0.7 (Bates et al.*,* 2010).

The coefficient enhances the model's strength because the Courant–Freidrichs–Lewy condition is a necessary but (importantly) not a sufficient condition for stability in nonlinear systems.

Parameters

The input parameters for Caesar-Lisflood at the reach scale are:

- A DTM data file, which was derived from topographical surveys carried out in the field combined with 10 m contour data of slopes adjacent to the wetland. This resulted in a suitable resolution DTM of the wetland. Different cell sizes of the DTM were explored to understand the effect of varying cell sizes on the results of the model.

- Under the *Numerical* tab within the software: max number of iterations, the minimum time step, the maximum time step, and maximum run duration were specified.

- Under the *Hydrology* tab, the discharge data file was specified. The inputs from this file were spread across several cells within the DTM to represent the input of flow to the wetland more accurately.

- In the *Flow Model* tab, the input/output difference and minimum discharge for depth calculation were indicated following the advice from the manual.

It must be noted that there are many input parameters within Caesar-Lisflood that can be defined/ modified according to the users' needs or to suit different circumstances. All the parameters explained above are inputs that were adjusted for this research. The remaining input parameters were set up according to the user manual and were not varied for this study.

Hydrological Engineering Center River Analysis System

HEC-RAS is a one-dimensional hydraulic modelling software developed by the Hydrologic Engineering Center of the US Army Corps of Engineers. HEC-RAS is a one-dimensional hydraulic analysis program and can be run in four modes: steady flow, unsteady flow analysis, and simulations can be done for sediment transport and water quality analysis.

For this study, the hydraulic analysis was used, which is explained in more detail below. The software is capable of modelling subcritical, supercritical, and mixed-flow regimes for streams consisting of a network of channels, a dendritic system, or a single river reach. The program output can be used in a multitude of ways to answer a host of questions related to river analysis. The HEC-RAS program results are usually employed in floodplain management and flood insurance studies in order to evaluate the effects of floodway encroachments. The HEC-RAS program can be downloaded at: www.hec.usace. army.mil/software/hec-ras/hecras-hecras.html.

In a HEC-RAS steady-state simulation, water surface profiles are computed from one cross section to the next by solving a standard step iterative procedure to solve the energy equation. The energy equation is intended to calculate water surface profiles for steady gradually varied flow. The energy equation is shown below for two adjacent cross sections XS1 and XS2.

$$y_2 + z_2 + \frac{a_2 V_2^2}{2g} = y_1 + z_1 + \frac{a_1 V_1^2}{2g} + h_e$$

where $y1$ and $y2$ are depths of water at adjacent cross sections,

XS1 and XS2, $Z1$ and $Z2$ are the elevations of the main channel inverts,

$V1$ and $V2$ are average velocities (total discharge/ total flow area),

$a1$ and $a2$ are velocity weighting coefficients,

g is the gravitational acceleration, and h_e is the energy head loss.

The energy head loss is defined in the equation:

$$h_e = L S_f + C \left| \frac{a_2 V_2^2}{2g} - \frac{a_1 V_1^2}{2g} \right|$$

where L is discharge-weighted reach length,

Sf is representative friction slope between XS1 and XS2, and

C is an expansion or contraction loss coefficient.

In order to calculate the representative friction slope, HEC-RAS uses the average conveyance equation and the distance weighted reach length defined in the equations:

$$S_f = \left(\frac{Q_1 + Q_2}{K_1 + K_2} \right)^2$$

$$L = \frac{L_{lob} Q_{lob} + L_{ch} Q_{ch} + L_{rob} Q_{rob}}{Q_{lob} + Q_{ch} + Q_{rob}}$$

where K is conveyance for the subdivision,

n is Manning's roughness coefficient for the subdivision,

A is flow area for the subdivision, and

R is hydraulic radius for each subdivision.

The total conveyance for each subdivision is calculated as the sum of the conveyance from the left component of overbank flow, flow in the main channel, and the right component of overbank flow. Flow in the main channel is subdivided only when the Manning's roughness coefficient changes within the channel area. The composite main channel Manning's roughness coefficient is defined in the equation:

$$n_c = \left[\frac{\sum_{i=1}^{N} \left(\mathcal{P}_i n_i^{1.5} \right)}{\mathcal{P}} \right]^{2/3}$$

where n_c is the composite or equivalent coefficient of roughness,

P is the wetted perimeter of the whole main channel,

Pi is the wetted perimeter of subdivision, and

i and n_i is the coefficient of roughness for subdivision i.

The limitations to running a simulation of steady flow calculations within HEC-RAS software is that the software assumes that the flow is steady, the flow is gradually varied, the flow is one-dimensional, and the slope of the channel is small. This can create erroneous results if one is modelling a very complex system.

Parameters

HEC-RAS uses a number of input parameters for hydraulic analysis of the stream channel geometry and water flow. These parameters are used to establish a series of cross sections along the stream. In each cross section, the locations of the stream banks are identified and used to divide into segments, the left floodplain, main channel, and right floodplain (Figure 19). HEC-RAS subdivides the cross sections in this manner, to account for variances in hydraulic parameters. This subdivision allows control over parameters of the channel and floodplain, such as roughness values.

At each cross section, HEC-RAS uses several input parameters to describe channel and floodplain geometry, elevation, and relative location along the stream:

- River station (cross section) number, starting at the most upstream section.
- Lateral and elevation coordinates for each (dry, unflooded) terrain point.
- Left and right bank station locations.
- Reach lengths between the left floodplain, stream centreline, and right floodplain of adjacent cross sections. The three reach lengths represent the average flow path through each segment of the cross section pair. The three reach lengths between adjacent cross sections may differ in magnitude due to bends in the stream.
- Manning's roughness coefficients.
- Channel contraction and expansion coefficients.
- Geometric description of any hydraulic structures, such as bridges, culverts, and weirs.
- Geographic coordinates can be entered for the topographic points and stream line.

After defining the stream geometry, flow values for each reach within the river system are entered. One can choose from either a steady flow or unsteady flow analysis. In this research, steady flow analysis was used. Steady flow describes conditions in which, if the discharge is constant, depth and velocity at a given channel location do not change with time. Gradually varied flow is characterised by minor changes in water depth and velocity from cross section to cross section. The primary procedure used by HEC-RAS to compute water surface profiles assumes a steady, gradually varied flow scenario, and is called the direct step method. The channel geometric description and flow rate values are the primary model inputs for the hydraulic simulations.